

Ruthenium Carboxylate Complexes as Probes to Metal Ligand Interactions

Oliver J.S. Pickup

MSc By Research

University of York

Chemistry

January 2012

Abstract

A synthetic route to $[\text{Ru}(\kappa^2\text{-O}_2\text{CC}_6\text{H}_4\text{-R})_2(\text{PPh}_3)_2]$ complexes (where R= 4-F, 4-CH₃, 4-OMe, 4-NMe₂, 3-F, 3-CH₃, 3-OMe, 3-NMe₂) has been developed. From these species, novel ruthenium-carbonyl $[\text{Ru}(\kappa^2\text{-O}_2\text{CC}_6\text{H}_4\text{-R})(\kappa^1\text{-O}_2\text{CC}_6\text{H}_4\text{-R})(\text{CO})(\text{PPh}_3)_2]$ (where R= 4-F, 4-CH₃, 4-OMe, 4-NMe₂, 3-F, 3-CH₃, 3-NMe₂), and vinylidene complexes $[\text{Ru}(\kappa^2\text{-O}_2\text{CC}_6\text{H}_4\text{-R})(\kappa^1\text{-O}_2\text{CC}_6\text{H}_4\text{-R})(=\text{C}=\text{HPh})(\text{PPh}_3)_2]$ (where R= 4-F, 4-CH₃, 4-OMe, 4-NMe₂, 3-F, 3-CH₃, 3-NMe₂), have been synthesised.

Hammett studies have shown the effect of changing the substituent on the carboxylate ligand on the M-C π -back bonding for the complexes of the general type $[\text{Ru}(\kappa^2\text{-O}_2\text{CC}_6\text{H}_4\text{-R})(\kappa^1\text{-O}_2\text{CC}_6\text{H}_4\text{-R})(\text{CO})(\text{PPh}_3)_2]$ and $[\text{Ru}(\kappa^2\text{-O}_2\text{CC}_6\text{H}_4\text{-R})(\kappa^1\text{-O}_2\text{CC}_6\text{H}_4\text{-R})(=\text{C}=\text{HPh})(\text{PPh}_3)_2]$. The CO stretching frequencies in the IR spectra of the complexes $[\text{Ru}(\kappa^2\text{-O}_2\text{CC}_6\text{H}_4\text{-R})(\kappa^1\text{-O}_2\text{CC}_6\text{H}_4\text{-R})(\text{CO})(\text{PPh}_3)_2]$ demonstrate the more electron-donating substituents strengthen the bonding between the metal and the carbonyl ligand. A similar trend is observed in the case of the vinylidene-containing ruthenium complexes, demonstrating that the electronic properties of the ancillary ligands may profoundly affect the metal-vinylidene interaction.

Table of Contents

1. Introduction	8
1.1 Introduction to Transition Metal vinylidene complexes.	8
1.1.2 Transition Metal Vinylidenes and their Chemistry.....	9
1.1.3 Interconversion between a coordinated alkyne and vinylidene	12
1.2 Why Ruthenium? Background to Ruthenium and its use in catalysis.....	14
1.3 The development of the chemistry of the complex $[\text{Ru}(\kappa^2\text{-OAc})_2(\text{PPh}_3)_2]$	15
1.3.1. The reaction of $[\text{Ru}(\kappa^2\text{-OAc})_2(\text{PPh}_3)_2]$ with terminal alkynes	15
1.3.2 Ligand Assisted Proton Shuttle (LAPS)	16
1.3.3 The reaction of $[\text{Ru}(\text{OAc})_2(\text{PPh}_3)_2]$ with propargylic alcohols	21
1.4 Principles that govern metal-carbon bond strength in the complex $[\text{Ru}(\kappa^2\text{-OAc})(\kappa^1\text{-OAc})(=\text{C}=\text{CHR})(\text{PPh}_3)_2]$	26
1.4.1 Transition metal complexes and π -back bonding	26
1.4.2 Competing ligands for π back-bonding such as phosphines.....	31
1.5 Further work on $[\text{Ru}(\kappa^2\text{-OAc})_2(\text{PPh}_3)_2]$	33
1.6 Aims and Objectives	35
2. Results and discussion	36
2.1 Background for the characterisation of the complexes $[\text{Ru}(\kappa^2\text{-O}_2\text{CR})_2(\text{PPh}_3)_2]$	36
2.2 The development of a synthetic route to complexes of the type $[\text{Ru}(\kappa^2\text{-O}_2\text{CR})_2(\text{PPh}_3)_2]$	38
2.2.1 Starting material.....	38
2.2.2 Reaction with KOBU^t as the K counter ion donor to make KO_2CR	38
2.2.3 Reactions with sodium <i>bis</i> (trimethylsilyl)amide	42
2.2.4 Reaction with NaOBU^t as the Na counter ion donor to make NaO_2CR	43
2.3 Discussion for the series of complexes $[\text{Ru}(\kappa_2\text{-O}_2\text{CC}_6\text{H}_4\text{-R})_2(\text{PPh}_3)_2]$	48
2.3.1 Crystal structure for the complexes $\text{Ru}(\kappa_2\text{-O}_2\text{CC}_6\text{H}_4\text{-R})_2(\text{PPh}_3)_2$	52
2.3.2 Other crystal structures of interest	54
3.1 Transition metal carbonyl complexes and π -back bonding.....	57
3.2 Preparation of $[\text{Ru}(\kappa^1\text{-OAc})(\kappa^2\text{-OAc})(\text{CO})(\text{PPh}_3)_2]$	57
3.3 The preparation of complexes of the general type $[\text{Ru}(\kappa^1\text{-O}_2\text{CC}_6\text{H}_4\text{-R})(\kappa^2\text{-O}_2\text{CC}_6\text{H}_4\text{-R})(\text{CO})(\text{PPh}_3)_2]$	59
4.1 Synthesis of complexes of the general type $[\text{Ru}(\kappa^1\text{-O}_2\text{CC}_6\text{H}_4\text{-R})(\kappa^2\text{-O}_2\text{CC}_6\text{H}_4\text{-R})(=\text{C}=\text{HPh})(\text{PPh}_3)_2]$	65
5. Conclusions	74

5.1 Synthesis of precursors 2a-5a and 2b-5b	74
5.2 Synthesis of carbonyl complexes 7a-10a and 7b-9b	75
5.3 Synthesis of the vinylidene complexes 11a-14a and 11b-13b	76
5.4 Further work	76
6 .Experimental	78
6.1 Synthesis of RuCl ₂ (PPh ₃) ₃ . 1	79
6.2 Synthesis and characterisation of 2a-5a and 2b-5b	79
6.2.1 General procedure for the synthesis of Ru(κ ² -O ₂ C ₆ H ₄ -R) ₂ (PPh ₃) ₂ 2a-5a and 2b-5b	79
6.2.2 Synthesis of [Ru(κ ² -O ₂ CPh) ₂ (PPh ₃) ₂]. 2	81
6.2.3 Synthesis of [Ru(κ ² -O ₂ CC ₆ H ₄ -4-F) ₂ (PPh ₃) ₂]. 2a	82
6.2.4 Synthesis of [Ru(κ ² -O ₂ CC ₆ H ₄ -4-CH ₃) ₂ (PPh ₃) ₂]. 3a	85
6.2.5 Synthesis of [Ru(κ ² -O ₂ CC ₆ H ₄ -4-NMe ₂) ₂ (PPh ₃) ₂]. 4a	86
6.2.6 Synthesis of [Ru(κ ² -O ₂ CC ₆ H ₄ -4-OMe) ₂ (PPh ₃) ₂]. 5a	88
6.2.7 Synthesis of [Ru(κ ² -O ₂ CC ₆ H ₄ -3-F) ₂ (PPh ₃) ₂]. 2b	89
6.2.8 Synthesis of [Ru(κ ² -O ₂ CC ₆ H ₄ -3-CH ₃) ₂ (PPh ₃) ₂]. 3b	90
6.2.9 Synthesis of [Ru(κ ² -O ₂ CC ₆ H ₄ -3-NMe ₂) ₂ (PPh ₃) ₂]. 4b	92
6.2.10 Synthesis of [Ru(κ ² -O ₂ CC ₆ H ₄ -3-OMe) ₂ (PPh ₃) ₂]. 5b	93
6.3 Synthesis and characterisation of 7a-10a and 7b-9b	95
6.3.1 General procedure for the synthesis of [Ru(κ ² -O ₂ CC ₆ H ₄ -R)(κ ¹ -O ₂ CC ₆ H ₄ -R)(CO) (PPh ₃) ₂] 7a-10a and 7b-9b	95
6.3.2 Synthesis of [Ru(κ ² -O ₂ CC ₆ H ₄ -4-F)(κ ¹ -O ₂ CC ₆ H ₄ -4-F)(CO)(PPh ₃) ₂]. 7a	95
6.3.3 Synthesis of [Ru(κ ² -O ₂ CC ₆ H ₄ -4-CH ₃)(κ ¹ -O ₂ CC ₆ H ₄ -4-CH ₃)(CO)(PPh ₃) ₂]. 8a	97
6.3.4 Synthesis of [Ru(κ ² -O ₂ CC ₆ H ₄ -4-NMe ₂)(κ ¹ -O ₂ CC ₆ H ₄ -4-NMe ₂)(CO)(PPh ₃) ₂]. 9a	98
6.3.5 Synthesis of [Ru(κ ² -O ₂ CC ₆ H ₄ -4-OMe)(κ ¹ -O ₂ CC ₆ H ₄ -4-OMe)(CO)(PPh ₃) ₂]. 10a	99
6.3.6 Synthesis of [Ru(κ ² -O ₂ CC ₆ H ₄ -3-F)(κ ¹ -O ₂ CC ₆ H ₄ -3-F)(CO)(PPh ₃) ₂]. 7b	100
6.3.7 Synthesis of [Ru(κ ² -O ₂ CC ₆ H ₄ -3-CH ₃)(κ ¹ -O ₂ CC ₆ H ₄ -3-CH ₃)(CO)(PPh ₃) ₂]. 8b	101
6.3.8 Synthesis of [Ru(κ ² -O ₂ CC ₆ H ₄ -3-NMe ₂)(κ ¹ -O ₂ CC ₆ H ₄ -3-NMe ₂)(CO)(PPh ₃) ₂]. 9b	103
6.4 Synthesis and characterisation of 11a-14a and 11b-13b	105
6.4.1 General procedure for the synthesis of [Ru(κ ² -O ₂ CC ₆ H ₄ -R)(κ ¹ -O ₂ CC ₆ H ₄ -R)(=C=HPh)(PPh ₃) ₂] 11a-14a and 11b-13b	105
6.4.2 Synthesis of [Ru(κ ² -O ₂ CC ₆ H ₄ -4-F)(κ ¹ -O ₂ CC ₆ H ₄ -4-F)(=C=HPh)(PPh ₃) ₂]. 11a	105
6.4.3 Synthesis of [Ru(κ ² -O ₂ CC ₆ H ₄ -4-CH ₃)(κ ¹ -O ₂ CC ₆ H ₄ -4-CH ₃)(=C=HPh)(PPh ₃) ₂]. 12a	107

6.4.4.Synthesis of $[\text{Ru}(\kappa^2\text{-O}_2\text{CC}_6\text{H}_4\text{-4-NMe}_2)(\kappa^1\text{-O}_2\text{CC}_6\text{H}_4\text{-4-NMe}_2)(=\text{C}=\text{HPh})(\text{PPh}_3)_2]$. 13a	109
6.4.5 Synthesis of $[\text{Ru}(\kappa^2\text{-O}_2\text{CC}_6\text{H}_4\text{-4-OMe})(\kappa^1\text{-O}_2\text{CC}_6\text{H}_4\text{-4-OMe})(=\text{C}=\text{HPh})(\text{PPh}_3)_2]$. 14a	110
6.4.6 Synthesis of $[\text{Ru}(\kappa^2\text{-O}_2\text{CC}_6\text{H}_4\text{-3-F})(\kappa^1\text{-O}_2\text{CC}_6\text{H}_4\text{-3-F})(=\text{C}=\text{HPh})(\text{PPh}_3)_2]$. 11b ..	111
6.4.7 Synthesis of $[\text{Ru}(\kappa^2\text{-O}_2\text{CC}_6\text{H}_4\text{-3-CH}_3)(\kappa^1\text{-O}_2\text{CC}_6\text{H}_4\text{-3-CH}_3)(=\text{C}=\text{HPh})(\text{PPh}_3)_2]$. 12b	114
6.4.8 Synthesis of $[\text{Ru}(\kappa^2\text{-O}_2\text{CC}_6\text{H}_4\text{-3-NMe}_2)(\kappa^1\text{-O}_2\text{CC}_6\text{H}_4\text{-3-NMe}_2)(=\text{C}=\text{HPh})(\text{PPh}_3)_2]$. 13b	115
7. Abbreviations	1197
8. References	1179

Acknowledgements

I would like to thank all those who have helped me through this year, especially my supervisor Dr. Jason Lynam for his support and encouragement and helping me to become a better chemist. I would like to thank the whole SLUGS group for their friendship and help throughout this year. I would also like to thank my whole family for their love and support especially my grandmother Petra for believing in me and helping greatly with the financing throughout my whole MSc, which without, this would not have been possible.

Authors Declaration

I hereby declare that the work described in this thesis was conducted in the Department of Chemistry at the University of York between October 2010 and January 2012 under the supervision of Dr. Jason M. Lynam. The work described was conducted by myself, original except where due credit has been given to other authors or my collaborators.

Oliver J.S. Pickup

1. Introduction

1.1 Introduction to Transition Metal vinylidene complexes.

Vinylidene, :C=CH_2 , is the simplest unsaturated carbene and is a high-energy tautomer of acetylene: in the gas phase vinylidene is 188 kJ mol^{-1} higher in energy than acetylene,¹ but can be stabilised upon coordination to a transition metal fragment giving rise to transition metal vinylidene species. Over the last 30 years a large number of catalytic reactions have been found to involve transition metal vinylidene intermediates, which readily form from the addition of terminal alkynes to a suitable transition metal precursor.²⁻⁴

The involvement of a metal vinylidene species for metal catalytic processes was proposed for the first time in 1986 to explain the regioselective formation of vinyl carbamates directly from terminal alkynes, carbon dioxide and amines.⁵ The reaction involved $[\text{Ru}_3(\text{CO})_{12}]$ as a catalytic precursor to this process. It was soon found that the reaction was better promoted by mononuclear ruthenium species such as $[\text{RuCl}_2(\text{pyridine})_2(\text{norbornadiene})]$.⁶

Since this initial report, various metal vinylidenes, which are key activation intermediates, have proved extremely useful for many alkyne transformations and have contributed to the rational design of new catalytic reactions.² After the first mononuclear vinylidene complex was reported in 1972⁷ the most straightforward route to vinylidene complexes is through the direct activation of terminal alkynes and propargylic alcohols. At present there are many transition metal complexes that can facilitate the conversion of alkynes into their vinylidene tautomers. Typically these are electron rich species from Groups 7, 8 and 9 such as Mn,⁸ Ru,⁹⁻¹² Rh,¹³⁻¹⁶ Co,¹⁷ Re,¹⁸ Os,^{19,20} Fe,²¹ and Ir.²² There have been Group 6

vinylidene species reported for Mo,^{23,24} W,^{23,25} and Cr²⁶ but not as many as the other Group 7, 8 and 9. Also some dinuclear species combining Re-M (M=Pt, Pd)²⁷ and Mn-Fe.²⁸

The stabilization of vinylidene upon co-ordination to a transition metal is now a common feature encountered with many transition metals. The ability of transition metal complexes to facilitate the conversion of alkynes into their vinylidene tautomers is also a current area of experimental^{2,4,10,18,29,30} and theoretical interest.^{1,3,4,11,19,30-32} The synthesis and stoichiometric reactivity of these unsaturated ligands have been broadly developed but are still under investigation and have led to many reviews.^{3,4,15,19,30,31,33}

1.1.2 Transition Metal Vinylidenes and their Chemistry

A contributing factor to this interest in transition metal vinylidene complexes are the differences observed in the chemistry of these complexes compared to the organic (free) vinylidene and their parent alkyne forms. Trost and McColry, published a review article addressing the differences between organic vinylidenes and transition metal vinylidenes stated “Organic vinylidene species have found limited use in organic synthesis due to their inaccessibility. In contrast, metal vinylidenes are much more stable, and may be readily accessed through transition metal activation of terminal alkynes.”³⁴ This inaccessibility is due to the fact that the vinylidene tautomer’s are thermodynamically less stable than their parent alkynes and thus there is a high energy barrier; temperatures in excess of 500 °C,³⁵ are required for the interconversion of the two species.

One advantage of a metal-catalysed process is the change in the polarity of the substrates when they are coordinated to the metal. The polarity of the alkyne α -carbon and β -carbon is reversed such that the α -carbon of the vinylidene ligand which is bonded to the metal is electrophilic and is thus extremely susceptible to nucleophilic attack by relatively weak oxygen nucleophiles,³⁶ whereas the β -carbon is nucleophilic and exhibits reactivity towards

electrophiles.^{37, 38} This was reported by Davison and Selegue, who succeeded in reducing an alkynyliron complex to an alkyliron complex in 1980,³⁸ the same tendency is evident in the reactions reported by Bruce and his co-workers⁴ and by other groups.² Once a metal vinylidene species is formed the reactivity of these species is usually governed by this nucleophilic attack to C_α . The origin of this reactivity becomes apparent on examination of a general molecular orbital diagram of the metal-vinylidene interaction (Figure 1.1).³⁹ Wakatsuki, carried out a study of some d^6 and d^8 -electron complexes via molecular orbital calculations and compared them to that of a similar study by Kirchner and co-workers;⁴⁰ he found that they were essentially similar.

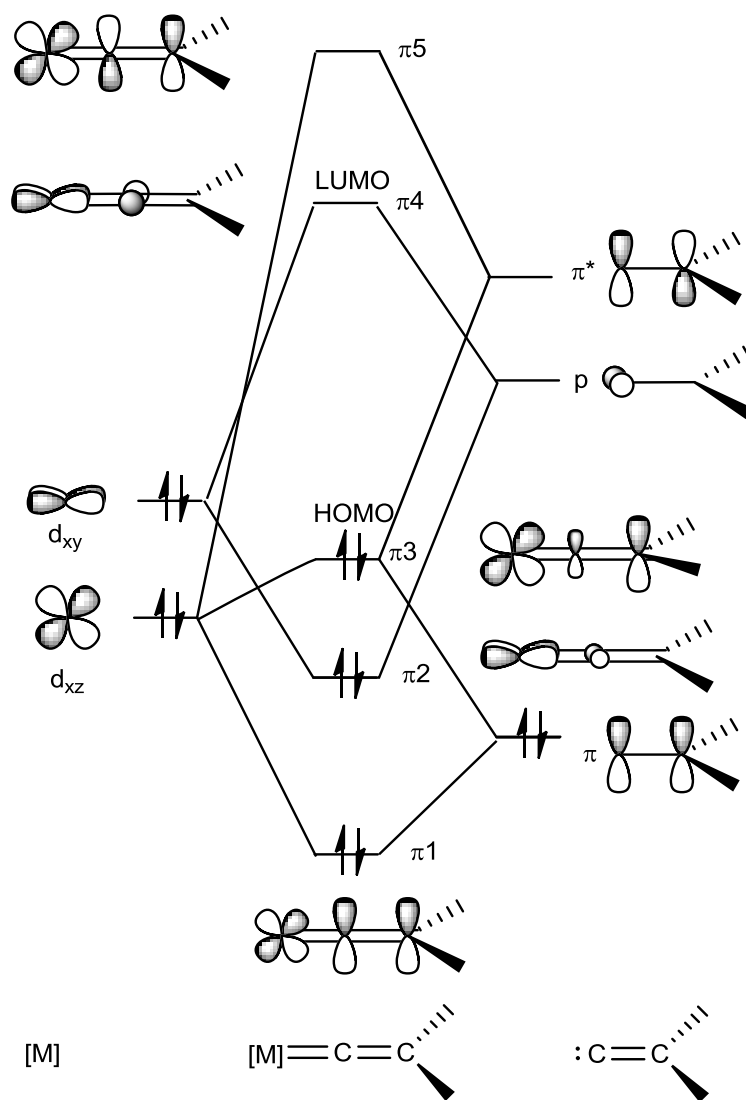


Figure 1.1: Simplified molecular orbital diagram for a transition-metal vinylidene complex.

These studies showed that the LUMO has an exclusively larger contribution from the empty p-orbital of the vinylidene C_α with some portion of the metal d_π-orbital, interacting with each other in an anti-bonding manner as a counterpart to the back-donation interaction. Together with the low-lying σ-donative interaction of the lone pair electrons at the C_α with the metal dσ-orbital, giving rises to the metal-C_α being similar to those of CO and metal-carbene bonds.³⁹ The HOMO is in most cases derived from four-electron interaction between a filled metal dπ-orbital and the π orbital of the C=C of the vinylidene fragment.

This enhanced reactivity observed by transition metal vinylidene complexes has been exploited for the catalytic transformation of terminal alkynes.^{41,42} Given this current catalytic interest in transition metal vinylidene complexes attention has been given to understanding the precise mechanism by which these compounds facilitate the conversion of alkynes into vinylidenes.^{11,13,14,30,43}

1.1.3 Interconversion between a coordinated alkyne and vinylidene

There are three main pathways by which the transformation between an alkyne and a vinylidene may be considered to occur (Figure 1.2). All the pathways start off with the initial formation of a complex which contains an alkyne in a η^2 -binding mode such as **A**.

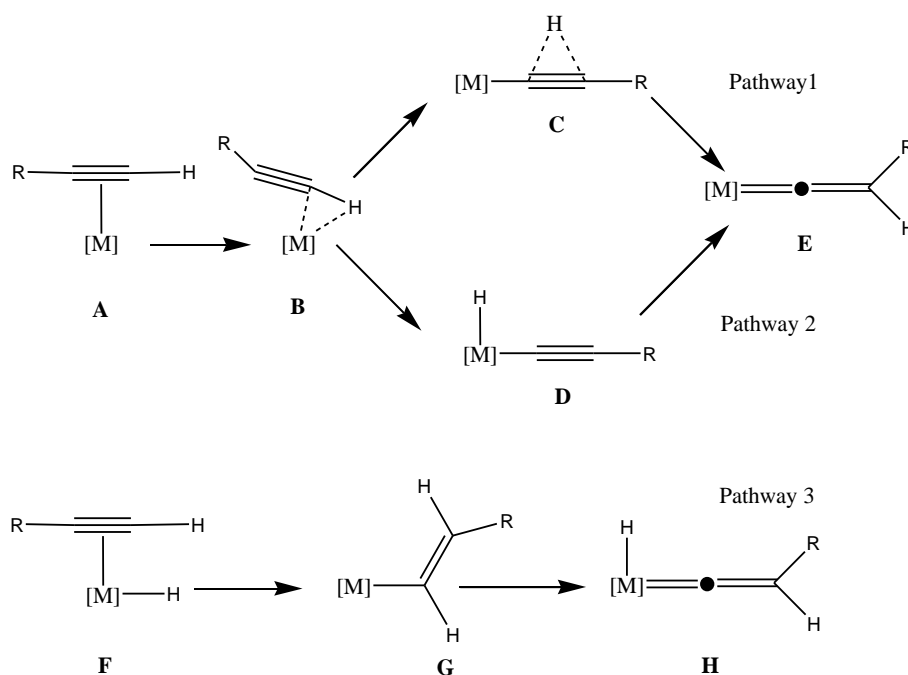


Figure 1.2 Pathways for alkyne to vinylidene transformation.

Therefore any metal precursor must possess a vacant co-ordination site that maybe generated by dissociation of a labile group or (in the case of the complexes that were examined during this project) the switch in the binding mode of the acetate ligand from the κ^1 binding mode to the κ^2 binding mode.¹² The next stage of the reaction is dependent on the nature of both the ligands and the metal complex employed. In the case of both pathways 1 and 2 the next step is the formation of an σ -complex, **B**, in which the alkyne is bonded in an η^2 (C-H) sigma fashion.

For pathway 1 the vinylidene ligand is formed by a 1,2-hydrogen atom migration *via* a transition state such as **C**.^{8,11,14} Alternatively in pathway 2 the formation of the vinylidene occurs *via* a well-defined intermediate, **D**, in which formal oxidative addition of the C-H bond has occurred to give an alkynyl ruthenium hydride complex, that will undergo a 1,3-hydride migration to result in the formation of the vinylidene.^{13,44,45}

In general, pathway 1 is preferred for electron-deficient metal complexes, whereas the formation of a vinylidene *via* pathway 2 is preferred for electron rich metal species, although it is possible by subtle variation of the ligands within the co-ordination sphere of the metal complex to switch between the two mechanistic pathways.³

The third mechanistic pathway by which vinylidene ligands can be formed, pathway 3, involves the intermediary of a metal alkenyl ligand which may be obtained through the insertion of an alkyne into a metal hydride bond.^{20,46}

No matter the mechanism by which the 1,2-hydrogen shift occurs, the requirement that the metal possesses a vacant co-ordination site for the alkyne bonding is a common feature. This can be achieved in a number of ways, for instance the use of a halide scavenger. One example of this is for the reaction of complexes of the type $[\text{RuCl}(\eta^5\text{-L})(\text{L}')_2]$ with terminal alkenes in the presence of a suitable halide scavenger, such as an appropriate sodium salt, which results in the formation of vinylidene cations $[\text{Ru}(\text{=C=CHR})(\eta^5\text{-L})(\text{L}')_2]^+$ ($\text{L} = \text{C}_5\text{H}_5, \text{C}_9\text{H}_7$; $\text{L}' =$ phosphorus-based ligand).^{35,47,48} Another method utilised to generate a vacant site at the metal is the loss of a neutral ligand, for example the reaction reported by Bruce *et al.*, of $[\text{RuCl}(\eta^5\text{-C}_5\text{Me}_5)(\text{PPh}_3)_2]$ with $\text{HC}\equiv\text{CPh}$ which results in the loss of a bulky PPh_3 ligand and the formation of the neutral complex $[\text{RuCl}(\eta^5\text{-C}_5\text{Me}_5)(\text{=C=CHR})(\text{PPh}_3)]$; the phosphine loss is enhanced by using benzene as a solvent to reduce the tendency of the Cl to ionise.⁴⁹ A further example of utilizing phosphine loss to prepare metal vinylidene

complexes has been reported by Wakatsuki, in this case the reaction of $[\text{RuCl}_2(\text{PPh}_3)_3]$ with $\text{HC}\equiv\text{C}^t\text{Bu}$ results in the formation of $[\text{RuCl}_2(=\text{C}=\text{CH}^t\text{Bu})(\text{PPh}_3)_2]$.⁵⁰ One strategy that was important to this work is the use of labile groups which dissociate or switch bonding mode, to create a vacant coordination site at a formally saturated metal centre, examples of ligands able to achieve this are NO^{51} or acetate.^{12,52} Werner demonstrated that reaction of the complex $[\text{Ru}(\kappa^2\text{-OAc})_2(\text{PR}_3)_2]$ ($\text{R} = ^i\text{Pr}, \text{Cy}$) with $\text{HC}\equiv\text{CPh}$ results in the formation of $[\text{Ru}(\kappa^2\text{-OAc})(\kappa^1\text{-OAc})(\text{PR}_3)_2(=\text{C}=\text{CHPh})]$. A further example of this has been reported by Lynam *et al* where the complex $[\text{Ru}(\kappa^2\text{-OAc})_2(\text{PPh}_3)_2]$ utilizes the same pathway to make the vinylidene derivative. This work by Lynam and co-workers will be discussed in more detail later in this chapter.

1.2 Why Ruthenium? Background to Ruthenium and its use in catalysis.

Organoruthenium complexes have been the subject of much study over the past 50 years.^{3, 4, 15,19,31} This is due not only to the fact that ruthenium is the cheapest of the platinum group metals, but also to its versatile synthetic and reactive chemistry. With its high tolerance towards a variety of functional groups and the highly variable oxidation state of ruthenium, with oxidation states ranging from +1 to +8 and with the -2 oxidation state being observed within the complex $[\text{Ru}(\text{CO})_4]^{2-}$, there is a plethora of ruthenium-based complexes containing numerous ligand combinations. The most famous of all the ruthenium-based catalysts are those in the Grubbs series which are very effective for alkene and olefin metathesis.⁵³

1.3 The development of the chemistry of the complex $[\text{Ru}(\kappa^2\text{-OAc})_2(\text{PPh}_3)_2]$

1.3.1. The reaction of $[\text{Ru}(\kappa^2\text{-OAc})_2(\text{PPh}_3)_2]$ with terminal alkynes

The ruthenium *bis*-acetate complex $[\text{Ru}(\kappa^2\text{-OAc})_2(\text{PPh}_3)_2]$, **1**, developed by Wilkinson,⁵⁴ was used in York by Welby as a precursor for vinylidene complexes. Reaction with a range of terminal alkynes $\text{HC}\equiv\text{CR}$ ($\text{R}=\text{Ph}, \text{CO}_2\text{Me}, \text{C}(\text{OH})\text{Ph}_2, \text{C}(\text{OH})\text{Me}_2$), resulted in the formation of the vinylidene complexes $[\text{Ru}(\kappa^2\text{-OAc})(\kappa^1\text{-OAc})(=\text{C}=\text{CHR})(\text{PPh}_3)_2]$ **2**. They found that in these species the acetate ligands were fluxional and in the case where $\text{R}=\text{Ph}$, they undergo fast exchange on the NMR time scale even at 195 K, and no intermediates could be observed.¹² This was in stark contrast to the corresponding reaction between $[\text{RuCl}_2(\text{PPh}_3)_3]$ and $\text{HC}\equiv\text{C}^t\text{Bu}$ that was reported by Wakatsuki and co-workers for the formation of the complex $[\text{RuCl}_2(=\text{C}=\text{CH}^t\text{Bu})(\text{PPh}_3)_2]$. The same group reported that the reaction of $[\text{RuCl}_2(\text{PPh}_3)_3]$ and $\text{HC}\equiv\text{CR}$, proceeded *via* intermediates **5a** and **5b** (Figure 1.3). The reaction was also considerably slower requiring a 24 hour period to generate the vinylidene complex.⁵⁵

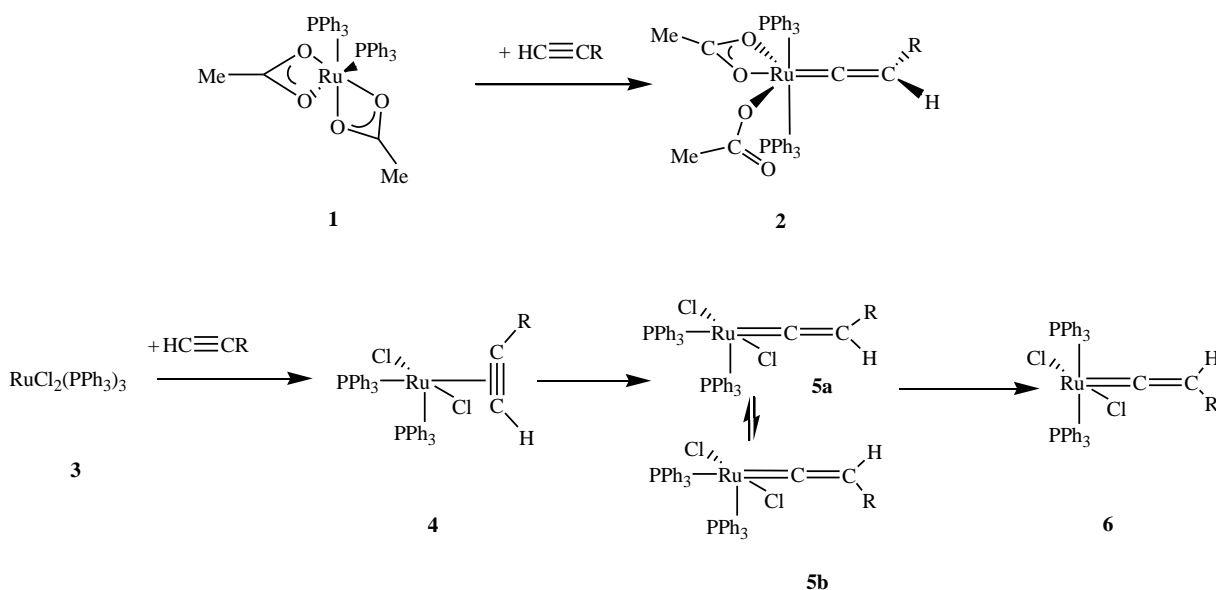


Figure 1.3 Reaction scheme of $\text{RuCl}_2(\text{PPh}_3)_3$ and $[\text{Ru}(\kappa^2\text{-OAc})_2(\text{PPh}_3)_2]$ with phenyl acetylene.

In other published work Zhang and co-workers showed that $[\text{Ru}(\kappa^2\text{-OAc})_2(\text{PPh}_3)_2]$ catalysed a coupling reaction between terminal alkynes with azides to give triazoles, whereas $\text{RuCl}_2(\text{PPh}_3)_3$ was rather ineffective.⁵⁶

With no detectable intermediates observed for the acetate substituted system it was therefore evident that the acetate ligand significantly enhances the rate of formation to the vinylidene ligand. This work by Lynam and co-workers led to a joint study by the Lynam and Slaterry groups, at York, to probe into the reasons why this enhancement occurred.

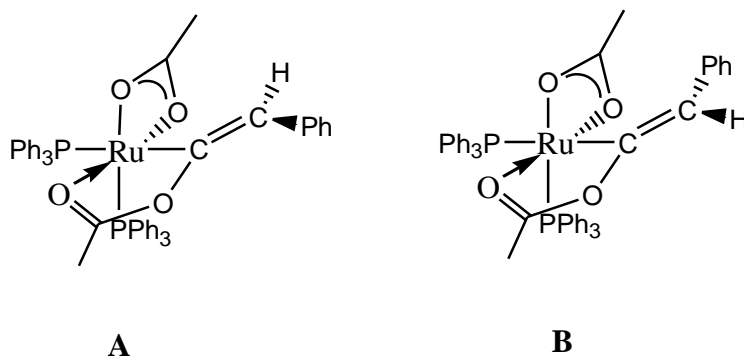
1.3.2 Ligand Assisted Proton Shuttle (LAPS)

Through experimental and theoretical studies Lynam *et al* showed the reasons that reaction of complex **1** with terminal alkynes proceeded rapidly to form complex **2**; Their studies showed that initially one of the co-ordinated acetate changes from a κ^2 to a κ^1 binding mode, to allow the co-ordination of the terminal alkyne in a η^2 fashion as described in section 1.1.3. After the co-ordination of the alkyne the acetate deprotonates the C-H bond of the alkyne. The subsequently formed acetic acid then reprotonates the formed alkynyl ligand in an intramolecular fashion. In the system described here the acetate acts as a proton shuttle that facilitates the migration of a proton from the 1- to the 2- position of the alkyne, hence the term Ligand Assisted Proton Shuttle (LAPS).¹

The evidence for this came firstly from the experimental study. A series of different NMR spectroscopic experiments were run to shed light on the mechanism. The first piece of evidence came from a ^{13}C labelling study. The reaction of $[\text{Ru}(\kappa^2\text{-OAc})_2(\text{PPh}_3)_2]$ with $\text{H}^{13}\text{C}\equiv\text{CPh}$ was shown to result in the formation of $[\text{Ru}(\kappa^2\text{-OAc})(\kappa^1\text{-OAc})(=^{13}\text{C}=\text{CHR})(\text{PPh}_3)_2]$. The $^{31}\text{P}\{^1\text{H}\}$ NMR spectrum of the complex showed a single doublet resonance at δ_{p} 34.2 ppm ($^2J_{\text{PC}} = 16.7$ Hz),¹ and in the ^{13}C NMR spectrum the corresponding resonance of the triplet for the α carbon at δ_{c} 355.6 ($^2J_{\text{PC}} = 16.7$ Hz), which

indicated the formation of the vinylidene complex occurred exclusively *via* hydrogen, rather than phenyl migration.⁵⁷

As stated before the reaction of $[\text{Ru}(\kappa^2\text{-OAc})_2(\text{PPh}_3)_2]$ with $\text{HC}\equiv\text{CPh}$ shows no evidence of intermediates at room temperature but when the reaction was repeated at low temperature and the reaction was monitored by NMR spectroscopy, Lynam and co-workers found evidence for a new complex, **A**, at 245 K; two new doublet resonances in the proton decoupled ^{31}P NMR spectrum at δ 66.7 and δ 30.8 ppm ($^2J_{\text{PP}} = 16.8$ Hz) indicated that the new species contained in equivalent and mutually *cis* phosphine ligands. This was consistent with the appearance of a broad new resonance in the ^1H NMR spectrum at δ 5.94 which was also due to the new species.



On warming the reaction mixture to 255 K they reported that the resonance in both the ^1H and the proton decoupled ^{31}P NMR spectrum for **A** rapidly decreased in intensity whereas the singlet for $[\text{Ru}(\kappa^2\text{-OAc})(\kappa^1\text{-OAc})(=\text{C}=\text{CHR})(\text{PPh}_3)_2]$ increased and on further warming they reported that there was only the resonance for $[\text{Ru}(\kappa^2\text{-OAc})(\kappa^1\text{-OAc})(=\text{C}=\text{CHR})(\text{PPh}_3)_2]$. The low temperature ^{13}C NMR spectroscopy labelling studies shed further light on the nature of **A**. Reaction of $[\text{Ru}(\kappa^2\text{-OAc})_2(\text{PPh}_3)_2]$ with $\text{H}^{13}\text{C}\equiv\text{CPh}$ at 245 K afforded resonances consistent with complex **A**, with the ^{13}C at the α position on the vinylidene. The ^1H NMR spectrum at δ 5.94 ppm now showed additional doublet coupling of 10.9 Hz. This data showed that as well as possessing two mutually *cis*-phosphine

ligands, the ^{13}C -labeled α -carbon of the vinylidene were now *trans* to the phosphorus atom. The hydrogen resonance at δ 5.94 ppm was inconsistent with the presence of an alkyne and thus indicated that the migration of the hydrogen had already occurred. In addition to this the chemical shift and the size of the coupling in complex **A** were inconsistent with the presence of a vinylidene ligand. The resonance for the proton in the vinylidene complex $[\text{Ru}(\kappa^2\text{-OAc})(\kappa^1\text{-OAc})(=^{13}\text{C}=\text{CHR})(\text{PPh}_3)_2]$ was observed at δ 5.20 ppm with a carbon coupling constant of just 3.11 Hz.

Further insight into the nature of the organic ligand came when they reacted $[\text{Ru}(\kappa^2\text{-OAc})(\kappa^1\text{-OAc})(=^{13}\text{C}=\text{CHR})(\text{PPh}_3)_2]$ with CO. They demonstrated that this reaction resulted in formal nucleophilic attack by an acetate group onto the vinylidene ligand of $[\text{Ru}(\kappa^1\text{-OAc})(\text{CO})(\text{CO}\{\text{Me}\}\text{O}-^{13}\text{C}=\text{CHR})(\text{PPh}_2)_3]$, **C**, Figure 1.4.

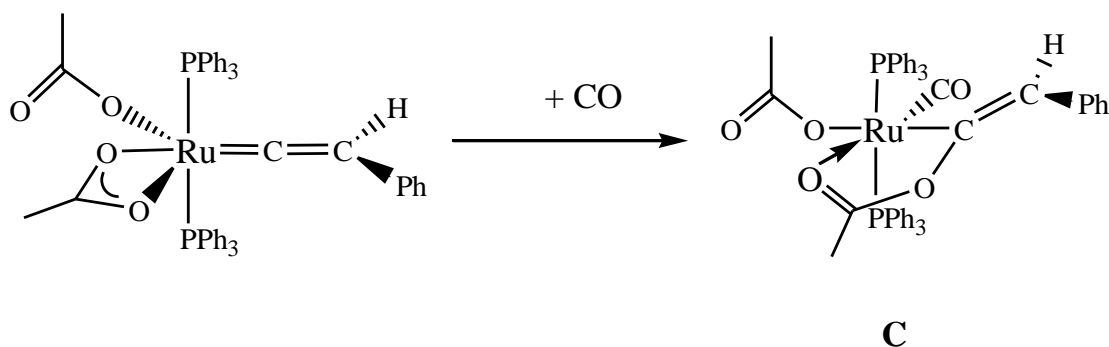


Figure 1.4 Reaction scheme of $\text{Ru}(\kappa^2\text{-OAc})(\kappa^1\text{OAc})(=\text{C}=\text{CHR})(\text{PPh}_3)_2$ with CO.

Because of the low energy barriers of the reaction of the *bis*-acetate complex to the vinylidene, attempts to observe any further intermediates were viewed as futile. So in order to explore the mechanism of this reaction further a Density Functional Theory (DFT) study was performed to map the potential energy surfaces for the alkyne to vinylidene isomerisation. They studied three potential pathways the first being a direct 1,2 hydrogen migration, the second being oxidative addition of the alkynes to ruthenium to form an

alkynyl hydride intermediate followed by a 1,3-hydride shift to form the vinylidene. The final pathway considered was an acetate-mediated mechanism where the acetate acts as a proton shuttle deprotonating the alkyne to form an intermediate alkynyl complex that is then protonated at the β -carbon by the coordinated acetic acid.

From calculations based on a number of isomers of the model system $[\text{Ru}(\kappa^2\text{-OAc})(\kappa^1\text{-OAc})(=\text{C}=\text{CHMe})(\text{PPh}_3)_2]$ it was demonstrated that both the η^2 (CC) alkyne complex $[\text{Ru}(\kappa^2\text{-OAc})(\kappa^1\text{-OAc})(\eta^2\text{-HC}\equiv\text{CMe})(\text{PPh}_3)_2]$ and the agostic σ -complex $[\text{Ru}(\kappa^2\text{-OAc})(\kappa^1\text{-OAc})(\eta^2\text{-}\{\text{CH}\}\text{-HC}\equiv\text{CMe})(\text{PPh}_3)_2]$ are minima on the potential energy surface. The lowest energy pathway for the formation of the vinylidene complex involves the intramolecular deprotonation of the σ -complex by an acetate ligand followed by the reprotonation of the subsequently formed alkynyl ligand. Thus as mentioned earlier this process is termed a Ligand-Assisted Proton Shuttle or LAPS. Calculations on the full experimental system reinforced the notion that the presence of the acetate ligand within the coordination sphere of ruthenium significantly enhances the rate of formation of the vinylidene ligand as it offers a lower energy pathway for the alkyne to vinylidene tautomerisation (Figure 1.5).

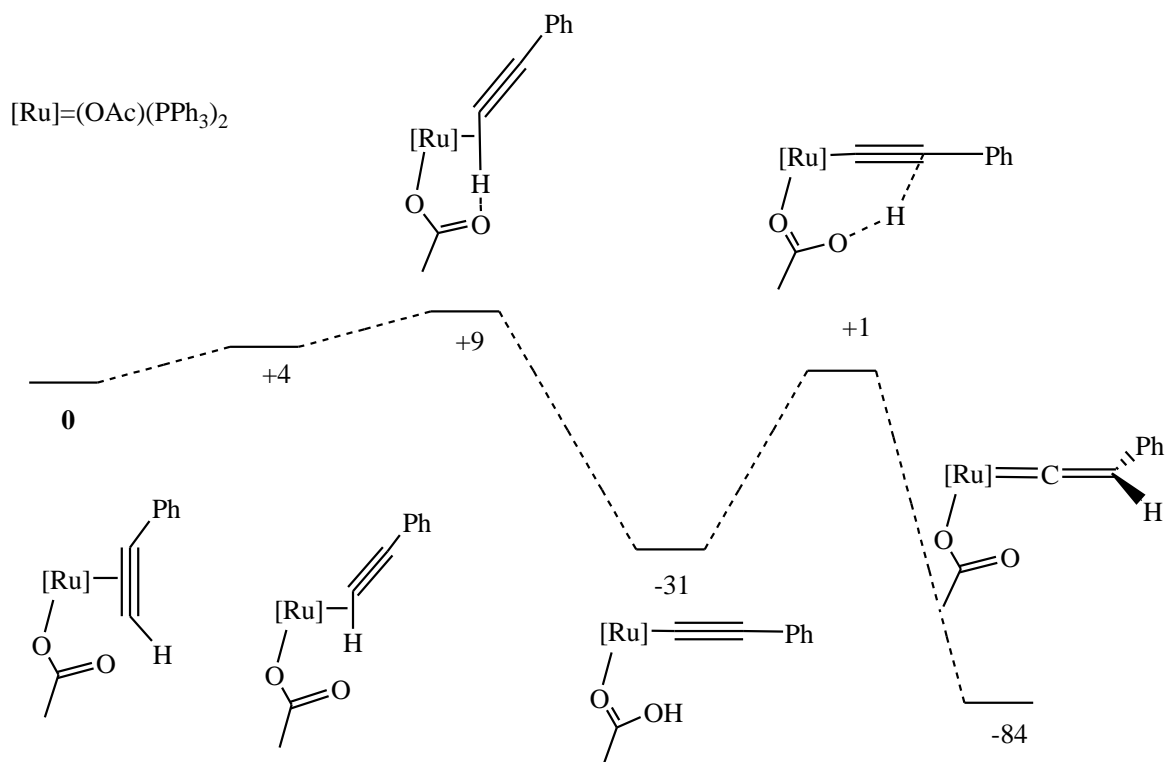


Figure 1.5 Potential energy surfaces for (LAPS) in Gibbs energy.

It is believed that the LAPS mechanism is widespread in alkyne to vinylidene tautomerisations involving complexes where Lewis-basic groups are present in the primary co-ordination sphere of the metal^{36,45,58} and as such should be considered an independent pathway for hydrogen transfer in these species from those mentioned in section 1.1.3. The LAPS mechanism is very similar to the Ambiphilic Metal-Ligand Activation (AMLA) process describe by Davies and Macgregor⁵⁹ which had been implicated extensively in the application of various metal/carboxylate systems in catalytic C-H activation processes.⁶⁰ They have shown in a number of studies that the combination of an electrophilic metal and a lone pair on an internal base, either metal bound AMLA-4,(4-membered) or pendant, AMLA-6, (6-membered) can lead to the concerted ambiphilic activation of C-H bonds.⁵⁹⁻⁶¹ This was first shown for the complex $\text{Pd}(\text{OAc})_2$, Figure 1.6; the authors first proposed the transfer of a proton from a metal acyliumintermediate to a bound acetate *via* a highly

ordered six membered (i) or four membered species (ii) transition state.⁵⁹ The reaction was shown by DFT studies to proceed *via* an agostic C-H complex followed by the facile intramolecular H-transfer *via* the AMLA-6 species. This was due to the activation barrier for AMLA-6 species being much lower than the AMLA-4, as the six-membered transition state allowed deprotonation to occur with very little distortion.⁵⁹

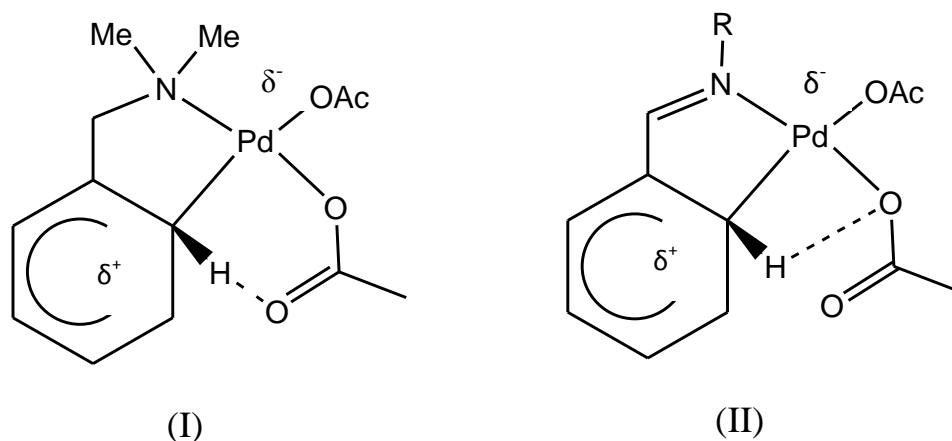


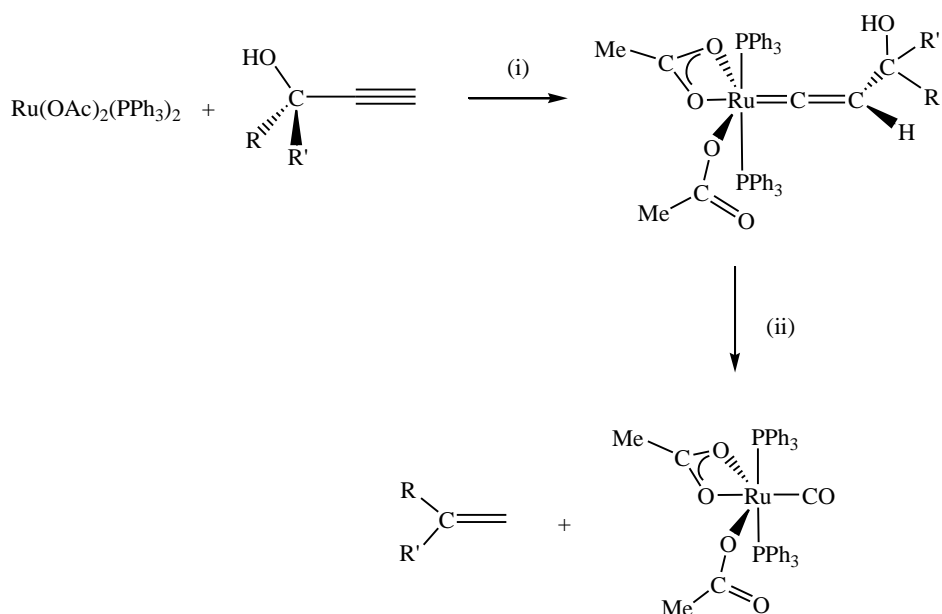
Figure 1.6 Showing AMLA-6 and AMLA-4 intermediates

The AMLA-6 mechanism is viewed to be essentially identical to the CMD (concerted metalation-deprotonation) mechanism for carbon-hydrogen activation.⁶² But more importantly can be viewed as being similar to the LAPS mechanism but in the case of LAPS vs AMLA/CMD the former deprotonates and reprotonates whereas the later mechanisms only deprotonates, thus making these mechanisms variations of each other.

1.3.3 The reaction of $[\text{Ru}(\text{OAc})_2(\text{PPh}_3)_2]$ with propargylic alcohols

The reaction of suitable metal complexes with propargylic alcohols ($\text{HC}\equiv\text{C}-\text{C}(\text{OH})\text{R}_2$) has been shown to be a versatile route to allenylidene species $\text{M}=\text{C}=\text{C}=\text{CR}_2$,⁶³ as well as vinylidenes as mentioned earlier in section 1.1. On reaction of the ruthenium acetate complex with propargyl alcohols, the complex $\text{Ru}(\kappa^2\text{-OAc})(\kappa^1\text{-}$

$\text{OAc})(=\text{C}=\text{CH}(\text{OH})\text{R}_2)(\text{PPh}_3)_2$ was formed. A crystal structure of the complex showed there was a strong hydrogen bond between the OH group of the vinylidene ligand and the κ^1 -acetate ligand. The strength of this bond was verified by the short distance between the O-H...O of just 2.69 Å.¹² Attempts to try and induce elimination of water from the complex were unsuccessful which directly contrasted that of the corresponding interaction of $\text{RuCl}_2(\text{PPh}_3)_3$ with $(\text{HC}\equiv\text{C}-\text{C}(\text{OH})\text{Ph}_2)$.



Key (i) CH_2Cl_2 ; (ii) 1 hour

Figure 1.7. Reaction scheme for $[\text{Ru}(\kappa^2\text{-OAc})_2(\text{PPh}_3)_2]$ with propargyl alcohols.

Further interest came from the fact that on storage in CD_2Cl_2 for several weeks these complexes underwent a further reaction forming the carbonyl complex and alkene¹², as shown in Fig1.7. Although Wilkinson had previously reported the synthesis of $\text{Ru}(\kappa^2\text{-OAc})(\kappa^1\text{-OAc})(\text{CO})(\text{PPh}_3)_2$,⁶⁴ and the conversion of vinylidene ligands to carbonyls *via* hydrolysis⁶⁵ or oxidation^{10, 48, 66} is a well-established phenomenon, Lynam and co-workers proposed that this reaction occurred by a different route. They showed by ^1H NMR spectroscopy that as the decomposition of $\text{Ru}(\kappa^2\text{-OAc})(\kappa^1\text{-OAc})(=\text{C}=\text{CH}(\text{OH})\text{R}_2)(\text{PPh}_3)_2$

proceeded identical quantities of $\text{Ru}(\kappa^2\text{-OAc})(\kappa^1\text{-OAc})(\text{CO})(\text{PPh}_3)_2$ and an alkene were formed. Datta *et al* have also shown that the transformation of propargylic alcohols into CO and alkenes can be catalyzed by $[\text{RuTp}(\text{NCMe})_2(\text{PPh}_3)][\text{PF}_6]$ (Tp = tris(1-pyrazolyl)borate) with LiOTf as a cocatalyst.⁶⁷ In this case the reaction was thought to proceed via an intermediate formed by nucleophilic attack by LiOH at the α -carbon of the allenylidene ligand. As this reaction described by Datta required a catalyst to drive this process, it was proposed that the reaction of $[\text{Ru}(\kappa^2\text{-OAc})_2(\text{PPh}_3)_2]$ with propargyl alcohols occurred by a different route.

The original proposed mechanism was that the alkynes were formed via intramolecular attack of the OH group at the α carbon of the vinylidene to give a complex containing a four-membered ring as shown in Figure 1.8.

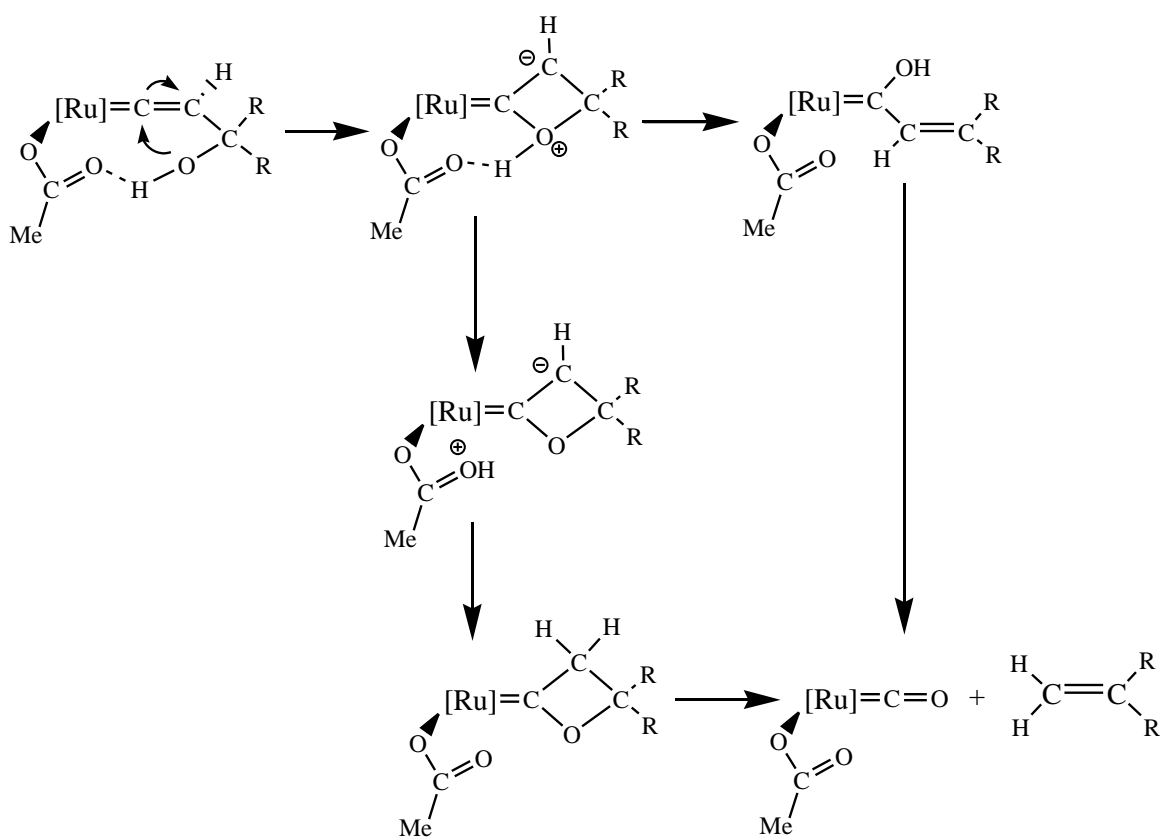


Figure 1.8 .Original proposed mechanism for the reaction of $[\text{Ru}(\kappa^2\text{-OAc})_2(\text{PPh}_3)_2]$ with propargyl alcohols.

In unpublished work by Lynam and Slattery *et al*, they propose a similar mechanism to LAPS for the decarbonylation of propargyl alcohols; it has been shown that the key step to this reaction pathway is intramolecular attack by a coordinated ligand onto the α carbon of the vinylidene but as yet the final mechanism is yet to be fully elucidated.

Even though the mechanism is not fully understood, this represents an unprecedented mechanism for the decarbonylation of propargyl alcohols and given that these compounds may be easily prepared from ketones and aldehydes, this represents an alternative to the Wittig reaction. The Wittig reaction, is the reaction of an aldehyde or ketone with triphenylphosphoniumylide to give an alkene and triphenylphosphine oxide as a side product. Though very effective the fact that there is a side product doesn't make it very atom efficient whereas the reaction of $[\text{Ru}(\kappa^2\text{-OAc})_2(\text{PPh}_3)_2]$ with propargylic alcohols to produce an alkene does not give any side products.

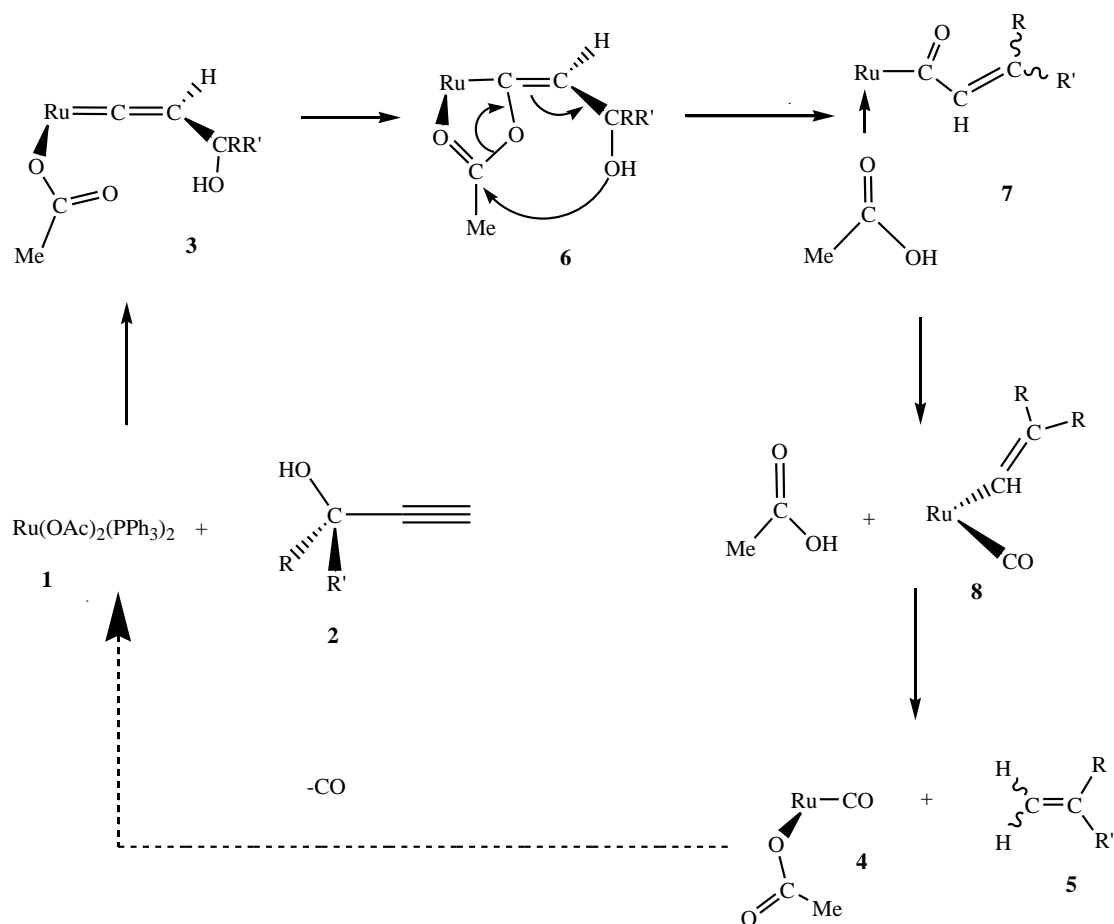


Figure 1.9. Original proposed reaction scheme for decarbonylation of propargyl alcohols.

For this reaction to be an effective alternative to the Wittig reaction the reaction needs to become catalytic, as the starting complex is not regenerated but instead a carbonyl complex is formed.

The aim of this project was to prepare new ruthenium-based complexes containing a range of ligands capable of adjusting the electronic and steric environment of the metal, to see how this affects the chemistry of the compounds.

To make the system catalytic the new ligands must facilitate the reaction with terminal alkynes to make the vinylidene tautomer of the complex, and have reduced the extent of

the back bonding in the carbonyl derivative so that the M-C bond is weaker and thus can be broken and the starting carboxylate complex regenerated.

1.4 Principles that govern metal-carbon bond strength in the complex $[\text{Ru}(\kappa^2\text{-OAc})(\kappa^1\text{-OAc})(=\text{C}=\text{CHR})(\text{PPh}_3)_2]$.

1.4.1 Transition metal complexes and π -back bonding

To be able to adjust the M-C bond length for these species we first have to understand the chemistry that governs this process as π -back bonding is one of the important interactions that govern the strength of a vinylidene bond.

When a ligand interacts with a metal the amount of ligand-to-metal donation and the metal to ligand back-donation determine many properties of both the metal centre (e.g. reduction or oxidation potential) and the ligand (e.g. lability).⁶⁸ Commonly bonding of a ligand to a metal is treated as a purely σ -donor interaction. However in many cases the bonding of a ligand to a metal involves π -interactions. Ligands capable of accepting an appreciable amount of π -electron density, from the metal atoms into empty π or π^* -orbitals of their own are referred to as π -acceptor or π -acid ligands. The vacant orbitals are of the correct symmetry to interact with certain filled d orbitals. Carbon monoxide (CO) is a prime example of a π -acceptor; in the case of the CO it is the carbonyl π^* -orbitals which have the correct symmetry to interact with the metal. A molecular orbital description of CO shows the existence of a carbon centred lone pair (HOMO) and of the degenerate π^* -levels (LUMOs). There are two interactions with the metal to consider, firstly the σ -donor interaction from the CO lone pair into the empty metal orbital and in an octahedral ML_6 complex these would be the e_g , $d\sigma$ set ($d_{x^2-y^2}$ and d_{z^2}). If the metals t_{2g} orbitals, d_{xy} , d_{xz} and d_{yz} , are filled, then the vacant π^* -orbitals of the CO ligand are of the correct symmetry and

energy to overlap with the metal t_{2g} orbitals.⁶⁹ This type of interaction effectively means there is a flow of electron density from the metal to the ligand, as shown in Figure 1.10.

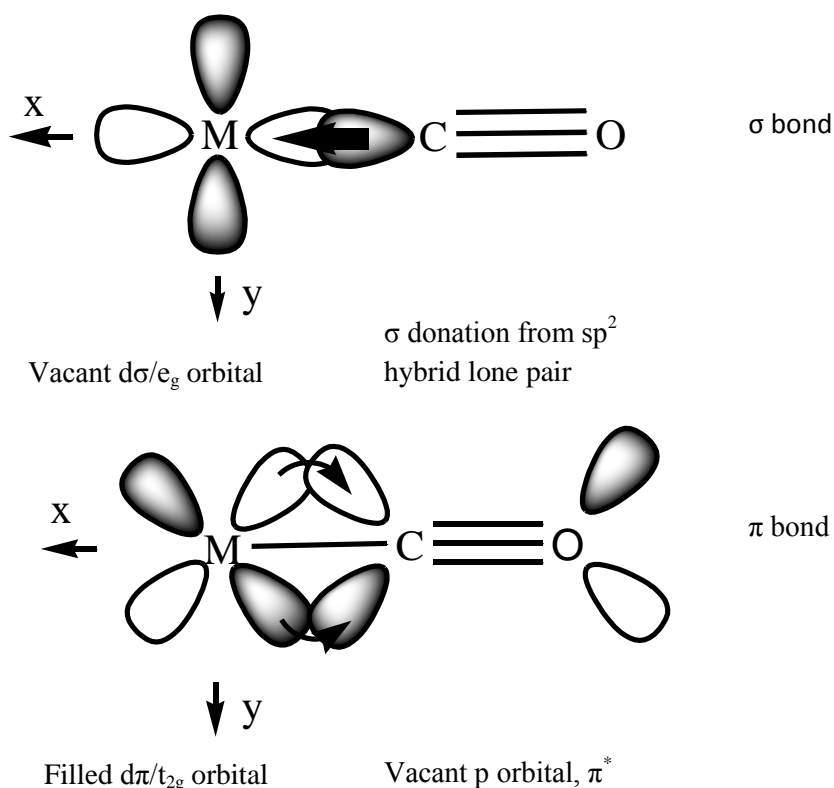


Figure 1.10: Diagram of the bonding interaction between a metal centre and a CO ligand.

The donation of electrons from the metal to the ligand is referred to as back-bonding, since the direction of the electron transfer from the metal to the ligand is the reverse of the usual direction of electron transfer from ligand to metal. In carbonyls because this happens in the π orbitals, it is referred to as π -back-bonding.

The CO bonding to a transition metal is said to be synergistic π^* back-bonding, due to the way that CO acts as a σ -donor and π -acceptor. The effect of the orbital interactions is to produce a set of bonding orbitals, which are predominately metal t_{2g} but lower in energy. In the d^6 situation these orbitals are filled and since the energy of these electrons drop, the overall effect is to increase the total bonding of the system. This π -interaction has no effect

on the e_g orbitals but leads to a stabilisation of the t_{2g} orbitals and an increase in ligand-field splitting (Δ_o). This interaction is shown in the diagram (Figure 1.11).

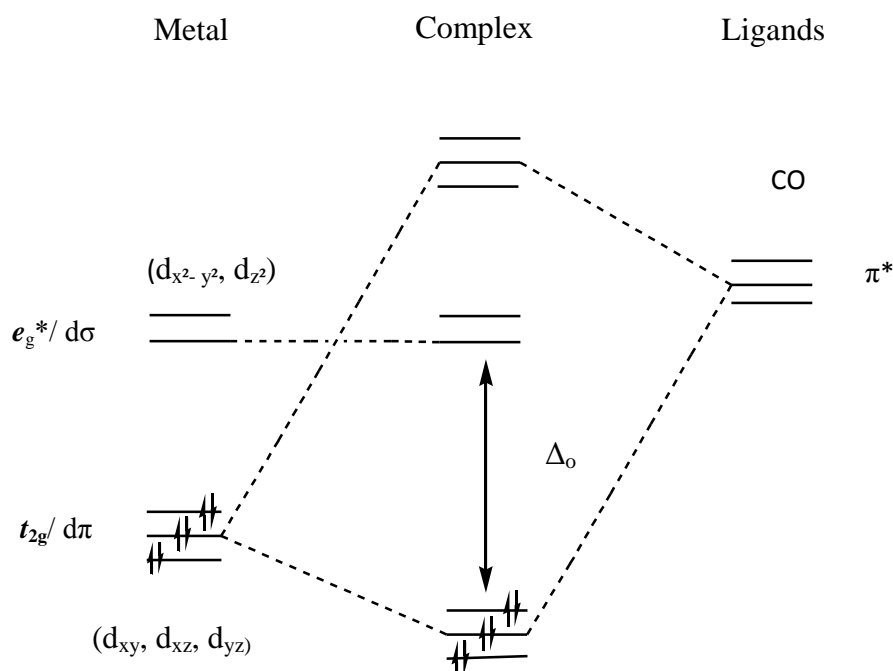


Figure 1.11: Effect of π -back-bonding on the t_{2g}/e_g , $d_{\pi}/d_{\sigma}(\Delta_o)$ separation with π -acceptor ligands.

This π -bonding is an important source of stabilisation in the metal complexes of such ligands and has enormous significance in the bonding interactions present within organometallic compounds. Where there is a large Δ_o gap, low spin 18-electron complexes are favoured, which are kinetically inert to ligand substitution. The more σ -donation by the carbonyl (or other σ -donors on the metal centre), the stronger the back bonding interaction. The back-bonding also depends on the electron density of the metal centre; electron rich complexes lead to extensive back-bonding which increase the $M-CO$ bond order to >1 and lowers the $MC-O$ bond order to <3 . As the extent of the back donation from the M to the CO increases, one would expect the M-C to bond becomes stronger and the C-O bond becomes weaker. Thus, the changes in bond order should be demonstrated by shorter M-C and longer C-O bonds compared to M-C single bonds and $C\equiv O$ triple bonds, respectively.

However this is a simplistic and classical view of metal carbonyl bonding and Hocking and Hambley have given new insight into the effects electronic structure has on the M-C≡O moiety. By plotting C≡O bond length against M-C bond length for over 20,000 crystal structures, they observed that complexes fall into three distinct classes; the longest C≡O bonds and shortest M-C bonds occupy class 1, where π bonding dominates over σ . Class 2 have intermediate C≡O and M-C bond lengths, where the σ and π bonding are more in balance and class 3 where the shortest C≡O and longest M-C bonds occur, this is due to σ and ionic contributions being more dominant. Second and third row transition elements overlap into class 3 but increasingly diverge through classes 1 and 2. Most of the observed compounds fall into class 2 (90%).⁷⁰

Wilkinson and Cotton state that the bond length in CO itself is 1.128 Å, while the bond lengths in metal carbonyl species are ~1.15 Å. For M-C distances, the sensitivity to bond order in the range concerned (1-2) is relatively high, ~0.3 to 0.4 Å per unit of bond order, and good evidence for multiple bonding can therefore be expected from such data.⁷¹

To do this, the length of the M-CO bond is measured in the same molecule in which some other bond, M-X exists, which must be single. Then, using the known covalent radius for X, estimating the single bond radius for C to be 0.70 Å when a sp hybrid orbital is used (the greater s character makes this ~0.07 Å shorter than that for sp^3 carbon), the length for a single M-CO bond in the said molecule can be estimated and compared with the observed value.⁷¹ These observed values can be obtained from the X-ray crystal structure data of the carbonyl complexes.

On the other hand Hocking and Hambley found factors that affected these bond lengths were numerous. Fragment with the shortest M-C bond lengths and longest C≡O bond lengths had the highest electron density and those with the longest M-C bond and shortest C≡O bonds had the lowest electron density. They observed that the bonding of M-C≡O

fragments, that they don't add electrons equally to the metal and to the carbonyl due to the fact that they added electrons in the most energetically favourable distribution. Also the effect of the d orbitals plays a role in the case of that for 4d and 5d orbitals, this is because M-C bond strength is determined by how far apart in energy the orbitals are (ΔE). For equivalent interactions the difference in energy between the 5d orbitals and the π acceptor orbitals of the carbonyl is less than that between 4d and the same set of orbitals, which favours stronger π back bonding. Thus the reverse is true when you consider σ donation as the lowering of the 4d orbitals decreases the energy difference between the carbonyl σ donor orbitals thus making σ overlap more favourable. Also the position of the M in the periodic table and an effect on the M-C bond length with the decreasing as you go across the period and increasing as you go down, thus giving the opposite effect for the C \equiv O bond length.⁷⁰

Infrared spectroscopy (IR) can be used to provide evidence concerning metal carbonyl complexes, and also to infer the extent of the back-bonding of the CO to the metal. This is most easily done by studying the CO stretching frequency rather than the MC stretching frequencies, since the former gives rise to strong sharp bands, well separated from all other vibrational modes of the molecules. The value of $\nu(\text{CO})$ is a measure of the strength of the C-O bond. Gaseous CO vibrates at 2143 cm^{-1} .⁷¹ The additional electron density in a carbonyl anti-bonding orbital weakens the C-O bond and, consequently, the vibrational frequency is lowered compared to that of free CO. The vibrational frequency range observed for metal carbonyl ligands is $1850\text{-}2125 \text{ cm}^{-1}$.⁶⁹ The lower the value of the CO stretching frequency, the greater the back-bonding and thus the stronger the M-C bond.

One important observation by Hocking and Hambley was that the change of ligand in the coordination sphere could have a similar effect on the C \equiv O bond length to a change in oxidation state⁷⁰ and this is one of the central themes that will come through the thesis.

1.4.2 Competing ligands for π back-bonding such as phosphines

The bonding in phosphine ligands (PX_3), like that of carbonyls, can be thought of as having two important components. The primary component is σ donation of the phosphine lone pair to an empty orbital on the metal. The second component is back donation from a filled metal orbital to an empty orbital on the phosphine ligand. This empty phosphorous orbital has been described as being either a d-orbital or an anti-bonding sigma orbital. Phosphine ligands can also form π -acceptor complexes with transition metals because these orbitals are suitable for overlap. Figure 1.12 shows how a molecular orbital can be formed between a metal $3d_{xz}$ orbital and a σ^* anti-bonding orbital on phosphorus.

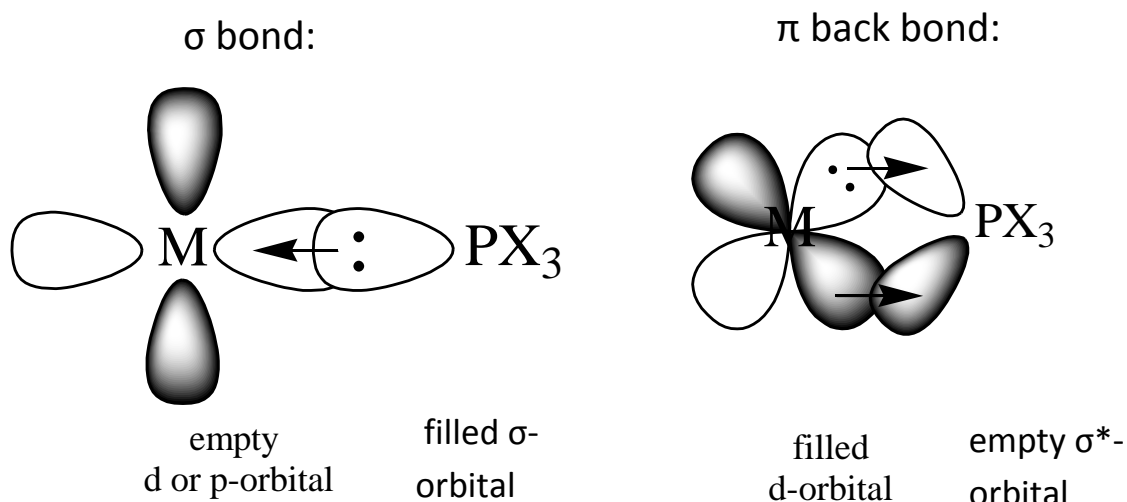


Figure 1.12: Diagram of the bonding interaction between phosphine ligands and a metal centre.

Therefore phosphines can exhibit a range of σ -donor and π -acceptor capabilities, and the electronic properties of a metal centre can be tuned by the substitution of electronically different but isosteric phosphines. The extent of the σ -donation from phosphorus and the back-bonding from the metal depends (in part) on the nature of the groups attached to the phosphorus. As electron-withdrawing groups are placed on the phosphorus, the σ -donating capacity of the phosphine ligand tends to decrease. At the same time, the π -acceptor

properties of the phosphorus are increased, providing an enhanced back-bonding ability. This is due to the fact that it lowers the energy of the σ^* -orbital therefore σ^* -orbital is more localised on the phosphorus and thus the size of the σ^* -lobe on the phosphorus increases, giving better overlap with the metal d-orbital. Also the σ^* -orbital is nearer in energy to the metal orbital giving rise to a stronger bonding interaction.

1.5 Further work on $[\text{Ru}(\kappa^2\text{-OAc})_2(\text{PPh}_3)_2]$

In other work by Lynam *et al*, Hiatt showed that one can replace the methyl on the acetate group with a phenyl group to make the complex $[\text{Ru}(\kappa^2\text{-O}_2\text{CPh})_2(\text{PPh}_3)_2]$: it exhibited similar chemistry to $[\text{Ru}(\kappa^2\text{-OAc})_2(\text{PPh}_3)_2]$ and was able to facilitate the reaction with terminal alkenes and propargyl alcohols.⁴² This showed that the R group on the carboxylates could be adjusted and that the reaction was not specific for acetate only.

In some recent unpublished work by Lynam *et al*, Shilling showed that the ruthenium complexes $[\text{Ru}(\kappa^1\text{-OAc})(\kappa^2\text{-OAc})(\text{PPh}_3)_2(\text{CO})]$ and $[\text{Ru}(\kappa^1\text{-OAc})(\kappa^2\text{-OAc})(\text{PPh}_3)_2(\text{NO})]^+$ are highly effective catalysts for the coupling reaction of carboxylic acids to alkynes, to give synthetically useful enol ester products. A range of catalytic reactions were carried out, using substituted phenylacetylenes and benzoic acids. The study showed that the electronic effects of substituents have a strong effect in directing the regio- and stereochemistry in the resulting enol esters. When using $p\text{-X-C}_6\text{H}_4\text{C}\equiv\text{CH}$ with benzoic acid, electron withdrawing groups (F, CF_3) in the *para*-position favour the anti-Markovnikov addition products, whilst using electron donating groups (NMe_2 , OMe, Me) in the *para*-position favours the Markovnikov addition product. Further experiments were carried out using $p\text{-R-C}_6\text{H}_4\text{COOH}$ and phenylacetylene, in this case the trend observed when using substituted phenylacetylenes was reversed, with electron withdrawing groups (F, CF_3) favouring the Markovnikov addition product, whilst electron donating groups (NMe_2 , OMe, Me) favoured the anti-Markovnikov addition products, at this moment in time the exact reason for this phenomena is still under investigation.⁷²

As Hiatt showed that a benzoate group can be incorporated in the R position of the carboxylate and that this would not affect the reaction with propargyl alcohols, and Shilling had shown interesting chemistry when reacting $p\text{-R-C}_6\text{H}_4\text{COOH}$ and

phenylacetylene with $[\text{Ru}(\kappa^1\text{-OAc})(\kappa^2\text{-OAc})(\text{PPh}_3)_2(\text{CO})]$ and $[\text{Ru}(\kappa^1\text{-OAc})(\kappa^2\text{-OAc})(\text{PPh}_3)_2(\text{NO})]^+$ (where in this reaction the acetate groups inter-change with the substituted carboxylic acid), it had been demonstrated that there was a large scope of different groups that could be incorporate in the R position on the carboxylate ligand, and the effects investigated.

1.6 Aims and Objectives

Aims

The aim of this project was to see what effect changing the substituent groups on the carboxylate ligand would have and in particular how this would affect the reaction of the complexes of general type $[\text{Ru}(\kappa^2\text{-O}_2\text{CR})_2(\text{PPh}_3)_2]$ with terminal alkynes, and specifically if they would facilitate the conversion of the terminal alkynes to vinylidene as reported for $[\text{Ru}(\kappa^2\text{-OAc})_2(\text{PPh}_3)_2]$.¹²

Objectives

- 1) To synthesise the precursor $[\text{RuCl}_2(\text{PPh}_3)_3]$ from $[\text{RuCl}_3 \cdot x\text{H}_2\text{O}]$.
- 2) To develop a synthetic method allowing the preparation of a series of different $[\text{Ru}(\kappa^2\text{-R-C}_6\text{H}_4\text{CO}_2)_2(\text{PPh}_3)_2]$ complexes with R being different substituents.
- 3) To test $[\text{Ru}(\kappa^2\text{-R-C}_6\text{H}_4\text{CO}_2)_2(\text{PPh}_3)_2]$ complexes to assess whether they exhibit similar reactivity to $[\text{Ru}(\kappa^2\text{-OAc})_2(\text{PPh}_3)_2]$, and produce the vinylidene derivatives $[\text{Ru}(\kappa^2\text{-R-C}_6\text{H}_4\text{CO}_2)(\kappa^1\text{-R-C}_6\text{H}_4\text{CO}_2)(=\text{C}=\text{CHPh})(\text{PPh}_3)_2]$.
- 4) To prepare and characterise the carbonyl derivatives, $[\text{Ru}(\kappa^2\text{-R-C}_6\text{H}_4\text{CO}_2)(\kappa^1\text{-R-C}_6\text{H}_4\text{CO}_2)(\text{CO})(\text{PPh}_3)_2]$.
- 5) Investigate the effects of altering the substituent on the carboxylate group has on complexes of the general type $[\text{Ru}(\kappa^2\text{-R-C}_6\text{H}_4\text{CO}_2)(\kappa^1\text{-R-C}_6\text{H}_4\text{CO}_2)(\text{CO})(\text{PPh}_3)_2]$ and $[\text{Ru}(\kappa^2\text{-R-C}_6\text{H}_4\text{CO}_2)(\kappa^1\text{-R-C}_6\text{H}_4\text{CO}_2)(=\text{C}=\text{CHPh})(\text{PPh}_3)_2]$.
- 6) Assess the effects this causes on the electronic properties of the ruthenium complexes, by spectroscopic methods.

2. Results and discussion

The aim of this project was to see what effect changing the substituent groups on the carboxylate ligand would have and in particular how this would affect the reaction of the complexes of general type $[\text{Ru}(\kappa^2\text{-O}_2\text{CR})_2(\text{PPh}_3)_2]$ with terminal alkynes, and specifically if they would facilitate the conversion of the terminal alkynes to vinylidene as reported for $[\text{Ru}(\kappa^2\text{-OAc})_2(\text{PPh}_3)_2]$.¹²

To show what affect changing the R group had on these subsequently produced vinylidene species, a catalogue of different carboxylate complexes first had to be synthesised. So the first objective of the project was to find a synthetic route by which the complexes of the general type of $[\text{Ru}(\kappa^2\text{-O}_2\text{CR})_2(\text{PPh}_3)_2]$ could be prepared.

This chapter will deal with the development of a synthetic route to these complexes and the characterisation of the novel compounds that were synthesised.

2.1 Background for the characterisation of the complexes $[\text{Ru}(\kappa^2\text{-O}_2\text{CR})_2(\text{PPh}_3)_2]$

To show if the following methods produced the desired complexes there are a certain analytical techniques that we can employ to show that the product has been successfully synthesized. The main evidence comes from NMR spectroscopy; the ³¹P spectra should show a singlet at around δ_{p} 60 ppm which corresponds to the phosphorus ligands being in the *cis* position.

The group that is most interesting for this study are the carboxylate; a carboxylate is a salt or ester of a carboxylic acid with the general formula, $[\text{M}(\text{RCOO})_n]$. The carboxylic acid is deprotonated to form the carboxylate anion and a free proton. This dissociation can occur more readily than with an alcohol group, as the carboxylate anion is stabilised by the delocalization of the negative charge that is left after deprotonation between the two

electronegative oxygen atoms. The delocalization of the electron cloud means that either of the oxygen atoms is less strongly negatively charged, thus the proton is therefore less strongly attracted back to the carboxylate group once it has left.

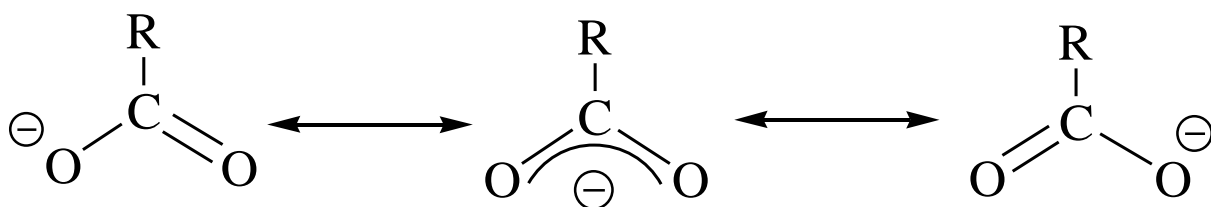


Figure 2.1: Diagram of the delocalisation of the electron cloud and charge in a carboxylate ligand.

The acetate ligand can be bound in two fashions either κ^2 where it is bound through both oxygens to the metal centre or κ^1 where it is only bound through one of the oxygens to the metal centre.

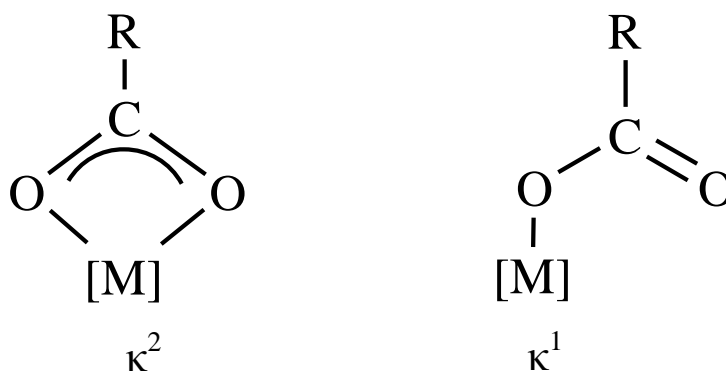


Figure 2.2: Diagram of the delocalisation of the modes of coordination for a carboxylate ligand.

Evidence for the type of bonding mode exhibited by an acetate group in a organometallic complex is gained through IR spectroscopy. The $\nu(\text{OCO})_{\text{sym}}$ and $\nu(\text{OCO})_{\text{asym}}$ bands occur at different frequencies depending upon the mode of coordination and the difference in their frequencies, $\Delta\nu$, is also indicative of their coordination mode.⁷³ The $\Delta\nu$ of the

symmetric and asymmetric stretches of a unidentate carboxylate is generally larger than that of a chelated ligand; typically in the region of 210 – 270 cm^{-1} for monodentate coordination and 40–120 cm^{-1} for chelate. Monodentate coordination of a carboxylate ligand involves two inequivalent CO moieties with different bond orders; one single and one double as in an ester. This results in an increase in the ν_{asym} and a decrease in ν_{sym} with a net increase in $\Delta\nu$ relative to the ionic value. When the carboxylate ligand is chelated, no change in the bond orders should occur so the $\Delta\nu$ should be similar to the ionic value, although experimental investigations have suggested that a $\Delta\nu$ smaller than the ionic value is indicative of a κ^2 -coordinated carboxylate.⁷³

2.2 The development of a synthetic route to complexes of the type $[\text{Ru}(\kappa^2\text{-O}_2\text{CR})_2(\text{PPh}_3)_2]$

2.2.1 Starting material

The complex $[\text{RuCl}_2(\text{PPh}_3)_3]$ **1** was successfully synthesised following the literature procedure, which requires the reaction of $[\text{RuCl}_3 \cdot x\text{H}_2\text{O}]$ with triphenylphosphine in ethanol at reflux for 3 hours to produce a black crystalline product, complex **1**.⁷⁴ This was employed as the starting material for making the complexes of the general type $[\text{Ru}(\kappa^2\text{-O}_2\text{CR})_2(\text{PPh}_3)_2]$.

2.2.2 Reaction with KOBU^t as the K counter ion donor to make KO_2CR

The first route tested employed KOBU^t , in $^t\text{BuOH}$, which was reacted with a carboxylic acid of the general formula $[\text{RCO}_2\text{H}]$ to make $[\text{KO}_2\text{CR}]$ *in situ*. It was hoped that the subsequent reaction with **1** would afford the desired product. This was an adjusted approach to that used by Welby,¹² in the synthesis of $[\text{Ru}(\kappa^2\text{-OAc})_2(\text{PPh}_3)_2]$, the proposed reaction scheme is shown in Figure 2.3.

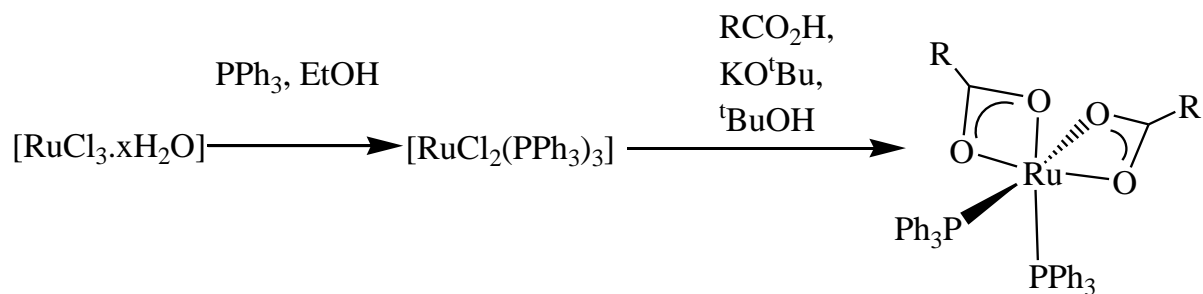


Figure 2.3: Original proposed reaction scheme to make complexes of the general type $[\text{Ru}(\kappa^2\text{-O}_2\text{CR})_2(\text{PPh}_3)_2]$.

The first complex that was attempted to be synthesised was $[\text{Ru}(\kappa^2\text{-O}_2\text{CEt})_2(\text{PPh}_3)_2]$. The reaction yielded the desired product which was analysed MS and NMR spectroscopic analysis, the mass spectrometry (MS) showed a peak at 740.14 m/z which corresponded to $[\text{Ru}(\kappa^2\text{-O}_2\text{CEt})(\text{PPh}_3)_2(\text{NCCH}_3)]^+$ but nothing for the intact complex; this is often seen for species of these types as they are susceptible to attack by acetonitrile which replaces one of the labile carboxylate ligands, this phenomena is present in much of the work of the Lynam group as acetonitrile is present in the ESI Mass Spectrometer (it is used by many other groups in the department as a solvent). The ^1H NMR spectrum showed aromatic peaks in the region δ_{H} 7.35-7.65 ppm. A quartet at δ_{H} 3.21 ppm and a triplet at δ_{H} 2.19, corresponding to the protons on the O_2CEt ligand. The ^{31}P NMR spectrum showed a broad peak at δ_{P} 61.9 ppm indicating that the triphenylphosphine ligands were in the desired *cis* position. The product proved hard to isolate from the reaction mixture as it was soluble in diethyl ether which is used to remove any free triphenylphosphine. A recrystallization was attempted to try and precipitate the product using a mixture of DCM and pentane. This was left for few days to see if the complex would crash out; when this did not work the DCM/pentane mixture was cooled to see if this would entice the product out of solution. All attempts to isolate the complex proved unsuccessful.

Further reactions with the carboxylic acids being pivalic acid $[(\text{CH}_3)_3\text{CCO}_2\text{H}]$ and *p*-toluic acid $[\textit{p}\text{-CH}_3\text{C}_6\text{H}_4\text{CO}_2\text{H}]$ allowed for a solid to be isolated, MS and NMR spectroscopic analysis indicated a mixture of ruthenium complexes were present, some of which could be assigned to the desired product. For the complex $[\text{Ru}(\kappa^2\text{-O}_2\text{CC}\{\text{CH}_3\}_3)_2(\text{PPh}_3)_2]$, the MS spectrometry data showed a peak at 727.14 *m/z* for $[\text{Ru}(\kappa^2\text{-O}_2\text{CC}(\text{CH}_3)_3)(\text{PPh}_3)_2]^+$, but peaks were also observed at 889.17 *m/z* $[\text{Ru}(\text{PPh}_3)_3]^+$, which corresponds to a complex with three PPh_3 ligands. Peaks were also observed at 557.17 *m/z*, 579.16 *m/z*, 857.24 *m/z* and 919.21 *m/z* which did not have a ruthenium splitting pattern which indicated that we had multiple products in the reaction mixture.

In the case of the attempted preparation of complex $[\text{Ru}(\kappa^2\text{-O}_2\text{CC}_6\text{H}_4\text{-4-CH}_3)_2(\text{PPh}_3)_2]$ the MS data showed evidence for the desired complex, 761.14 *m/z* for $[\text{Ru}(\kappa^2\text{-O}_2\text{CC}_6\text{H}_4\text{-4-CH}_3)(\text{PPh}_3)_2]^+$, and the acetonitrile complex 802.16 *m/z* for $[\text{Ru}(\kappa^2\text{-O}_2\text{CC}_6\text{H}_4\text{-4-CH}_3)(\text{PPh}_3)_2(\text{CNMe})]^+$ but also some starting material 889.17 *m/z* for $[\text{Ru}(\text{PPh}_3)_3]^+$, and some of the unusual peaks mentioned above. The ^{31}P NMR spectroscopic data showed multiple phosphorus environments δ_{P} at 44.1, 53.1, 63.5 and 77.7 ppm.

From the evidence gained by MS of peaks being observed for complexes that did not show a ruthenium splitting pattern it was deduced that there could be a competing reaction taking place. To test this hypothesis an experiment was carried reacting KOBU^\dagger and complex **1**, to see if complex **1** was reacting preferably with KOBU^\dagger instead of the carboxylic acid as desired. The reaction produced a similar yellow solid to that seen with the reactions above, but it was found to be very air sensitive and difficult to keep the resulting product from decomposing so it was not analysed.

To test further what was occurring in the reaction mixture, the reaction was repeated again but this time KOBU^\dagger and a carboxylic acid were reacted with complex **1** in a different

solvent, to see whether it was the solvent ^tBuOH that was reacting and producing the unknown product. Such a process was observed by Wilkinson and co-workers; they reported that the complex [RuCl₂(PPh₃)₄], which is a similar species to starting material **1**, would react with the solvent (acetone) to produce the complex [RuCl₂(PPh₃)₂(solvent)₂].⁷⁴ The resulting reaction only yielded starting material. This showed that there was no reaction taking place between the solvent and complex **1**, and that the side reaction must be a result of the KOBu^t reacting with complex **1**.

To test further the effect of using KOBu^t as an *in situ* base, the proposed method was used to try and synthesise the complex [Ru(O₂CPh)₂(PPh₃)₂],⁴² **2**: It was decided to prepare this complex as the proposed reaction scheme could be compared to that of the literature preparation of complex **2**. KOBu^t was added to a ^tBuOH solution of benzoic acid followed by **1**. The ³¹P NMR spectrum showed a single resonance at δ_P 44.4 ppm indicating that the desired complex had not formed.

To show that it was not any steric effect or lack of space around the metal centre, the literature procedure for complex **2** was modified to make some substituted benzoate complexes of the general type [Ru(κ²-O₂CC₆H₄ R)₂(PPh₃)₂], from their sodium carboxylate derivatives. This proved to be successful, and the complex [Ru(κ²-O₂CC₆H₄-4-OH)₂(PPh₃)₂] was successfully synthesised and verified by MS and ¹H and ³¹P NMR spectroscopy. The reaction was repeated to try and synthesise the complex [Ru(κ²-O₂CC₆H₄-4-NH₂)₂(PPh₃)₂]; this proved to be interesting because instead of affording the desired complex a *dimer* was produced instead, which was subsequently verified by a single X-ray Crystallographic study (Figure 2.12).

Because the use of potassium as an *in situ* base had been unsuccessful, whereas the reactions that had utilised sodium had proven successful for producing complexes of the

general type $[\text{Ru}(\kappa^2\text{-O}_2\text{CR})_2(\text{PPh}_3)_2]$, it was determined that sodium salts worked much better as a counter-ion in this reaction series than potassium. The next part of this chapter deals with identifying a method for incorporating sodium as the *in situ* base for the synthesis of complexes of this type.

2.2.3 Reactions with sodium *bis*(trimethylsilyl)amide

Initially this was attempted by using sodium *bis*(trimethylsilyl)amide to deprotonate the desired carboxylic acid to create its sodium salt. The reaction scheme is shown in Figure 2.4.

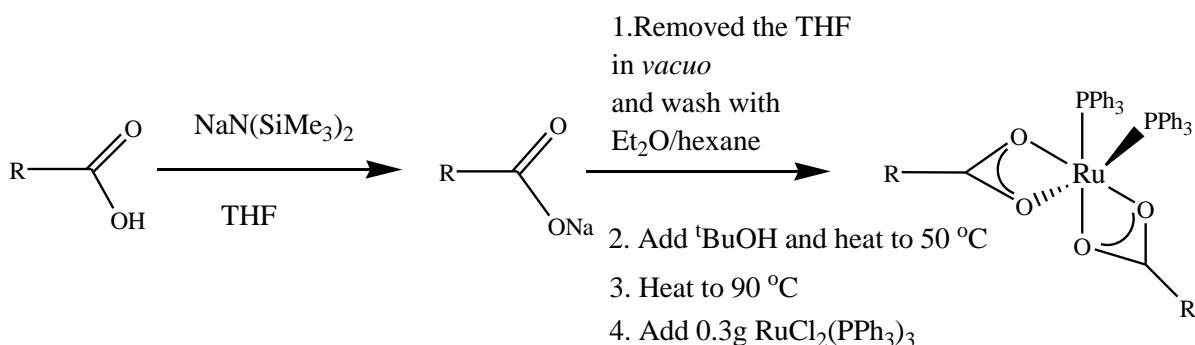


Figure 2.4: Reaction with sodium *bis*(trimethylsilyl)amide to synthesise complexes of the general type $[\text{Ru}(\kappa^2\text{-O}_2\text{CR})_2(\text{PPh}_3)_2]$.

The reaction proved to be successful and the complex $[\text{Ru}(\kappa^2\text{-O}_2\text{CC}_6\text{H}_4\text{-4-F})_2(\text{PPh}_3)_2]$ **2a**, was synthesised using 4-fluorobenzoic acid as the starting carboxylic acid. The synthesis was verified by MS which gave peaks at 806.13 m/z ($[\text{Ru}(\kappa^2\text{-O}_2\text{CC}_6\text{H}_4\text{-4-F})(\text{PPh}_3)_2(\text{CNCH}_3)]^+$), 765.1 m/z ($[\text{Ru}(\kappa^2\text{-O}_2\text{CC}_6\text{H}_4\text{-4-F})(\text{PPh}_3)_2]^+$) and NMR spectroscopic analysis with the characteristic singlet in the ^{31}P NMR spectrum at δ_{P} 63.4 ppm corresponding to the phosphorus being in the *cis*-position, as previously reported for complexes of this type.^{12, 42}

The same method was used in an attempt to prepare $[\text{Ru}(\kappa_2\text{-O}_2\text{CC}_6\text{H}_4\text{-4-CH}_3)_2(\text{PPh}_3)_2]$ **3a**, but it proved unsuccessful. The reaction was tried numerous times as it was thought that some of the reactants had decomposed in the case of the sodium *bis*(trimethylsilyl)amide or that the THF solvent was not degassed enough or had too much water content. New batches of the reactants were prepared and the reaction re-run but it still did not yield the desired product. The synthesis of complex **2a** was repeated with the newly prepared reactants to test the repeatability of the reaction method. It was attempted three times but complex **2a** was unable to be re-synthesised due its decomposition. An alternative synthetic approach was therefore required.

2.2.4 Reaction with NaOBu^t as the Na counter ion donor to make NaO_2CR

Learning from all the previous experiments carried out it seemed plausible that sodium was important as a counter-ion to the carboxylic acid. So a method was developed similar to the original reaction scheme proposed. The method proposed started with the reaction of NaOBu^t (which was prepared by reacting sodium with $^t\text{BuOH}$ at $90\text{ }^\circ\text{C}$), with the carboxylic acid to make the sodium salt derivative, and subsequent reaction with complex **1** to prepare the desired product (Figure 2.5.)

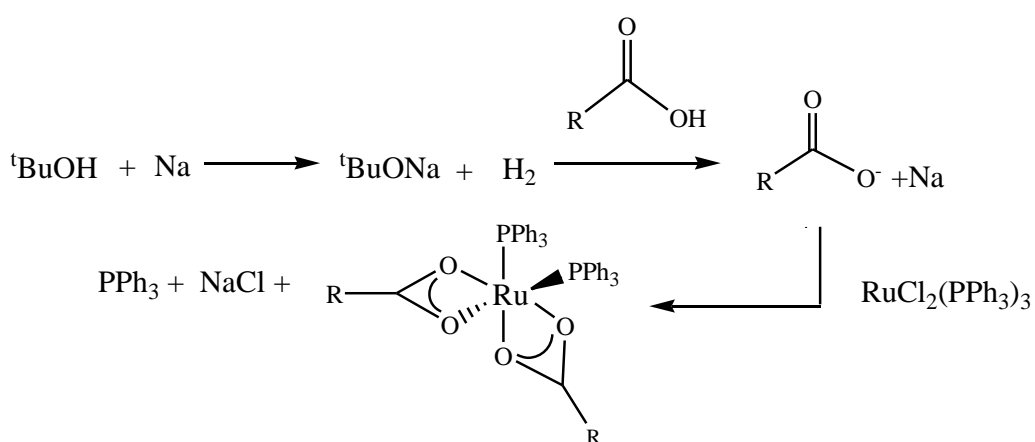


Figure2.5: Reaction with NaOBu^t to synthesise complexes of the general type $[\text{Ru}(\text{O}_2\text{CR})_2(\text{PPh}_3)_2]$.

Because complex **2a** had already been prepared, this was the first complex attempted to be synthesised by this method. Complex **2a** was successfully prepared by this method and this was verified by MS; 927.11, m/z ($[M]^+Na$): 806.13, m/z ($[Ru(O_2CC_6H_4-4-F)(PPh_3)_2(CNCH_3)]^+$): 765.1, m/z ($[Ru(O_2CC_6H_4-4-F)PPh_3)_2]^+$). The complex was also verified by 1H , ^{13}C , ^{31}P , ^{19}F NMR spectroscopy, with the characteristic peaks for this complex being the singlet in the ^{31}P NMR spectra at δ_P 63.4 ppm and the singlet in the ^{19}F NMR spectra at δ_F -108.7 ppm. The IR spectrum support the proposed structure, with stretching frequencies for the κ^2 binding mode at 1427 cm^{-1} ($\kappa^2\text{-OCO}_{sym}$) and 1482 cm^{-1} ($\kappa^2\text{-OCO}_{asym}$), $\Delta\nu$ (chelate) 68 cm^{-1} .

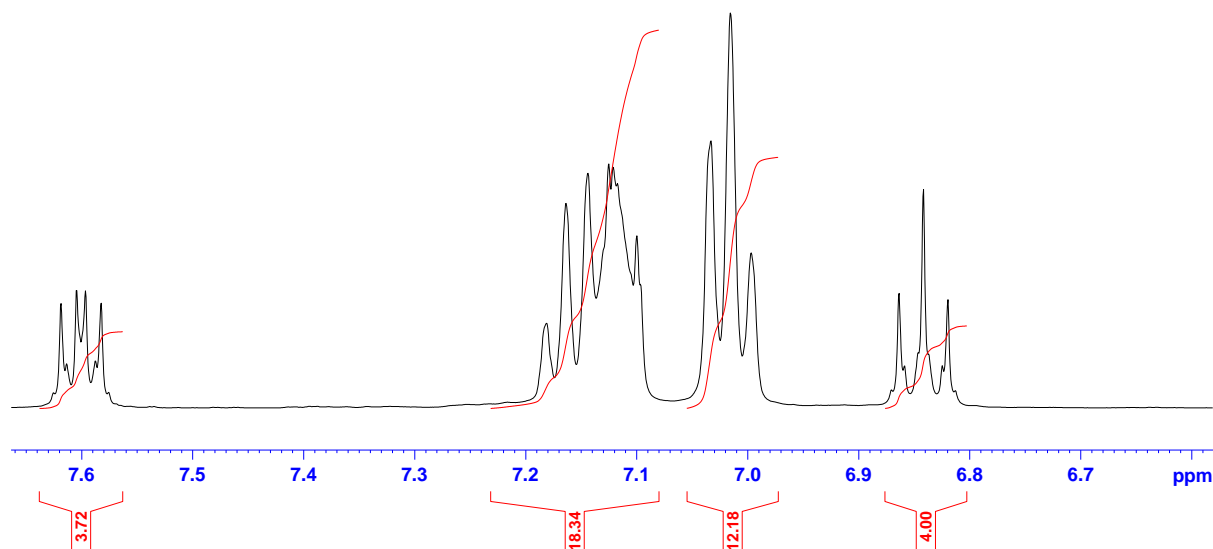


Figure 2.6. ^1H NMR spectrum of **2a**

The peaks in the ^1H NMR spectrum were first integrated to find out how many protons each peak corresponded to. The peak at δ_{H} 6.84 which was an apparent triplet, with an integration value of 4H. Because it was an apparent triplet this meant it must be being split by two different environments, one was assigned to $^3J_{\text{HH}}$ splitting, and the other to the $^3J_{\text{HF}}$. The apparent triplet was due to an AA'BB'F spin system, this peak was assigned to *m*-C₆H₄F. The next peak was at δ_{H} 7.01, the integration of this peak corresponded to a value of 12H, this was also an apparent triplet, the splitting this time was due to $^3J_{\text{HH}}$ and $^3J_{\text{HF}}$ giving a value of 7.5 Hz, this was assigned to the *ortho* protons on the triphenylphosphine not because of the splitting, but mainly because of the integration value. The large multiplet at δ_{H} 7.18-7.11 ppm integrated to 18H so was assigned to the rest of the protons on the triphenylphosphine ligand. The last peak in the proton spectrum was at δ_{H} 7.60 ppm; this was a doublet of doublets, which meant there must be two different environments again causing the splitting; the coupling was thus due to $^3J_{\text{HH}} = 8.8$ Hz and $^4J_{\text{HF}} = 5.66$ Hz, and thus the last remaining 4H can be assigned to *o*-C₆H₄F.

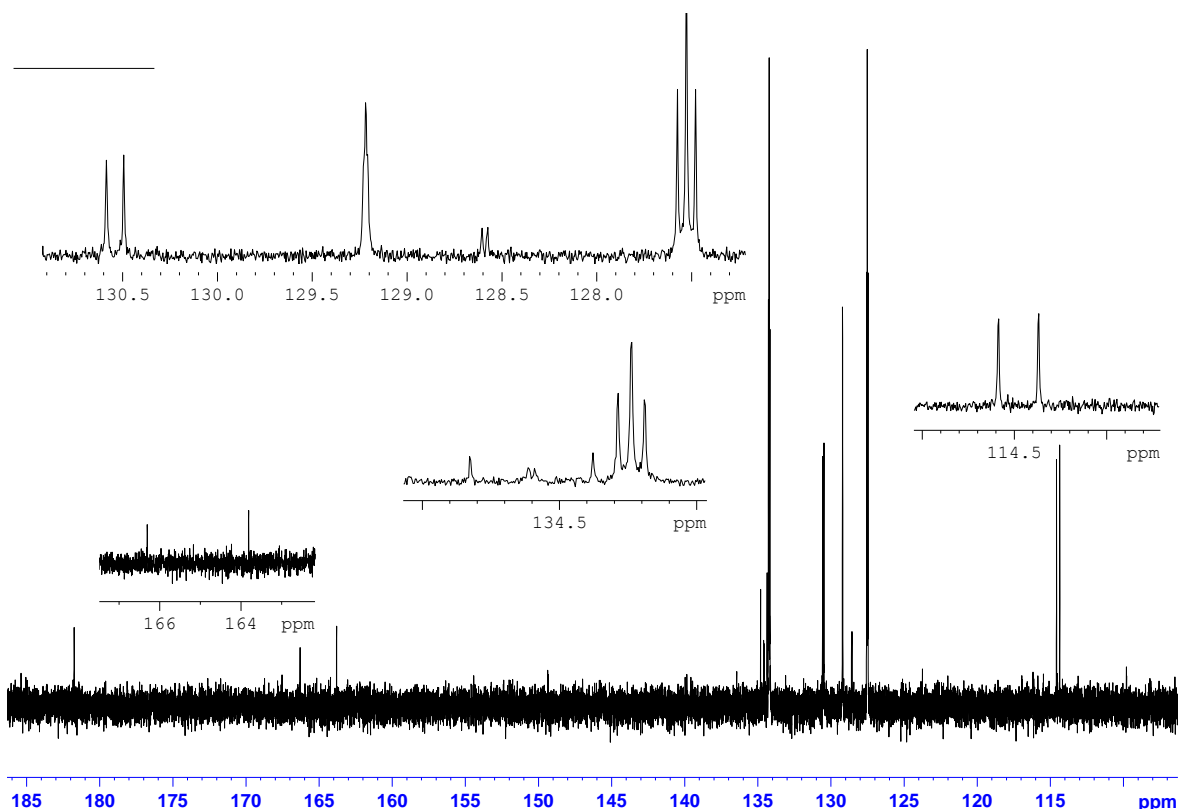


Figure 2.7. ^{13}C NMR spectrum of **2a**

The ^{13}C NMR spectrum contained four different sets of doublets at δ_{C} 114.4, 128.5, 130.5 and 165.0 ppm, with splitting values of $^2J_{\text{CF}} = 22.7$ Hz, $m\text{-C}_6\text{H}_4\text{F}$, $^4J_{\text{CF}} = 3.0$ Hz, $i\text{-C}_6\text{H}_4\text{F}$; $^3J_{\text{CF}} = 9.07$ Hz, $o\text{-C}_6\text{H}_4\text{F}$ and $^1J_{\text{CF}} = 251$ Hz $p\text{-C}_6\text{H}_4\text{F}$ respectively. The closer the carbon was to the fluorine atom the larger the J coupling value. The spectrum also contained three sets of multiplets the first two being at δ_{C} 127.5 and 134.2 ppm. They were assigned to the carbons on the triphenylphosphine ligand; the splitting was due to the coupling between the carbons and the phosphorus and a small amount of splitting due to the phosphorus-phosphorus coupling. With the J couplings being of different strengths, the smallest was thus due to the distance between the carbon and phosphorus being further thus the peak at δ_{C} 127.5 was assigned as $^3J_{\text{PC}} = 4.8$ Hz corresponding to the $m\text{-PPh}_3$. Therefore the peak at δ_{C} 134.2 $^2J_{\text{PC}} = 5.0$ Hz was assigned to $o\text{-PPh}$. The last triplet, at δ_{C} 134.8, was a virtual triplet this is cause because the carbons is being split by two different phosphorus

environments which makes it look like a triplet, but the middle peak has a further very small splitting due to the interaction between the two phosphorus coupling to each other. This gave a J coupling values $^1J_{PC} + ^3J_{PC} = 45.3$ Hz. For this splitting to occur the carbon must be close to the environments so the peak was assigned to the *p-PPh*. The last two peaks in the spectra were both singlets the first being δ_C 181.7. This peak was in the region that usually corresponds to quaternary carbons occur so was assigned to $\text{CO}_2\text{C}_6\text{H}_4\text{F}$, also this peak had a very low intensity which is often the case for quaternary carbons. The last remaining peak at δ_C 129.2 was thus assigned to the last remaining carbon *p-PPh*.

The method also proved successful for the synthesis of complex **3a**. As this complex had not been synthesised successfully by the other preparation methods, this was a very encouraging result. The synthesis of the complex was verified by MS giving peaks at m/z : 919.16 ($[\text{M}]^+\text{Na}$), 897.18 ($[\text{M}]\text{H}^+$), 802.15 ($[\text{Ru}(\kappa^2\text{-O}_2\text{CC}_6\text{H}_4\text{-4-CH}_3)(\text{PPh}_3)_2(\text{CNCH}_3)]^+$) and 761.13 ($[\text{Ru}(\kappa^2\text{-O}_2\text{CC}_6\text{H}_4\text{-4-CH}_3)(\text{PPh}_3)_2]^+$). Further evidence was gained through ^1H , ^{13}C and ^{31}P NMR spectroscopy, with the ^{31}P NMR spectrum showing a singlet at δ_P 63.5 ppm. The IR spectrum also showed that the acetates were bound in the desired κ^2 binding mode; 1423cm^{-1} ($\kappa^2\text{-OCO}_{\text{sym}}$), 1505cm^{-1} ($\kappa^2\text{-OCO}_{\text{asym}}$), $\Delta\nu$ (chelate) 82 cm^{-1} .

Not only had these results demonstrated that the synthetic route worked for different carboxylic acids but it was also reproducible. Also in most cases the reaction could be scaled up from 0.3 g to 1 g with very little adjustment to the method.

2.3 Discussion for the series of complexes $[\text{Ru}(\kappa^2\text{-O}_2\text{CC}_6\text{H}_4\text{-R})_2(\text{PPh}_3)_2]$

A series of complexes were prepared of the general type $[\text{Ru}(\kappa^2\text{-O}_2\text{CC}_6\text{H}_4\text{-R})_2(\text{PPh}_3)_2]$. It was decided to make these series of complexes because the type and position of the R-group on the phenyl ring could be altered. Hammett relationships can potentially be used to explain the effects of these substituents. All the compounds of the general type $[\text{Ru}(\kappa^2\text{-O}_2\text{CC}_6\text{H}_4\text{-R})_2(\text{PPh}_3)_2]$ that have been synthesised for this study are shown in Figure 2.8.

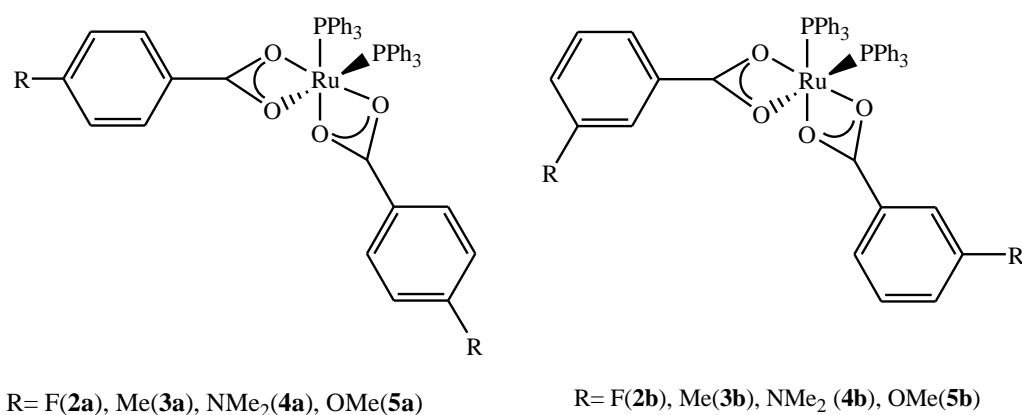


Figure 2.8: Complexes that were successfully synthesised and their R group and compound reference.

The compounds that were synthesised have been characterised by ¹H, ³¹P and ¹³C NMR spectroscopic analysis, IR spectroscopy (KBr), ESI-MS and, where possible, elemental analysis.

As for **2a** and **3a**, the $\Delta\nu$ values calculated for the $\kappa^2\text{-O}_2\text{CC}_6\text{H}_4\text{R}$ ligands of **4a**, **5a**, **2b**, **3b**, **4b** and **5b** obey the limits proposed by Robinson.⁷³ This indicates that all the complexes synthesised had the carboxylates bound in the desired κ^2 position. There also appeared to be a trend in the values for $\kappa^2\text{-}\Delta\nu$ with the more electron withdrawing groups (EWG) displaying the lowest frequency range for the bidentate carboxylate ligand.

Table 2.2: Selected IR spectral data for complexes **2a-5a** and **2b, 3b** and **5b**.

	Vibration (cm ⁻¹)						
	2a	3a	4a	5a	2b	3b	4b
P-Ph	1482	1480	1480	1480	1482	1480	1482
κ^2 - OCO _{sym}	1427	1423	1422	1414	1434	1432	1419
κ^2 - OCO _{asym}	1495	1505	1506	1506	1503	1505	1508
κ^2 - $\Delta\nu$	68	82	84	92	69	73	89

This was further investigated by plotting the Hammett parameter against κ^2 - $\Delta\nu$. Hammett plots utilise the Hammett equation which explains that for any reaction where the only difference is (i) the substituent's on the phenyl ring being either in the *meta* or the *para* position or (ii) a different R group, then the change in free energy of activation is proportional to the change in Gibbs free energy. Complexes containing groups in the *ortho* position cannot be analysed like this as they would introduce steric effects. Hammett published a series of substituent constants, σ , relating to the R groups and their position on the phenyl ring relative to H (H, $\sigma = 0$).⁷⁵ They are commonly used to plot graphs of substituent's constants, σ , against either bond length, IR stretching frequencies or reaction rates to show the relationship between the different groups and their position and how they affect different aspects of either a reaction or a complex's properties. A large positive σ -value implies high electron withdrawing power by inductive and/or resonance effect, relative to H; a large negative σ -value implies high electron donating power relative to H.

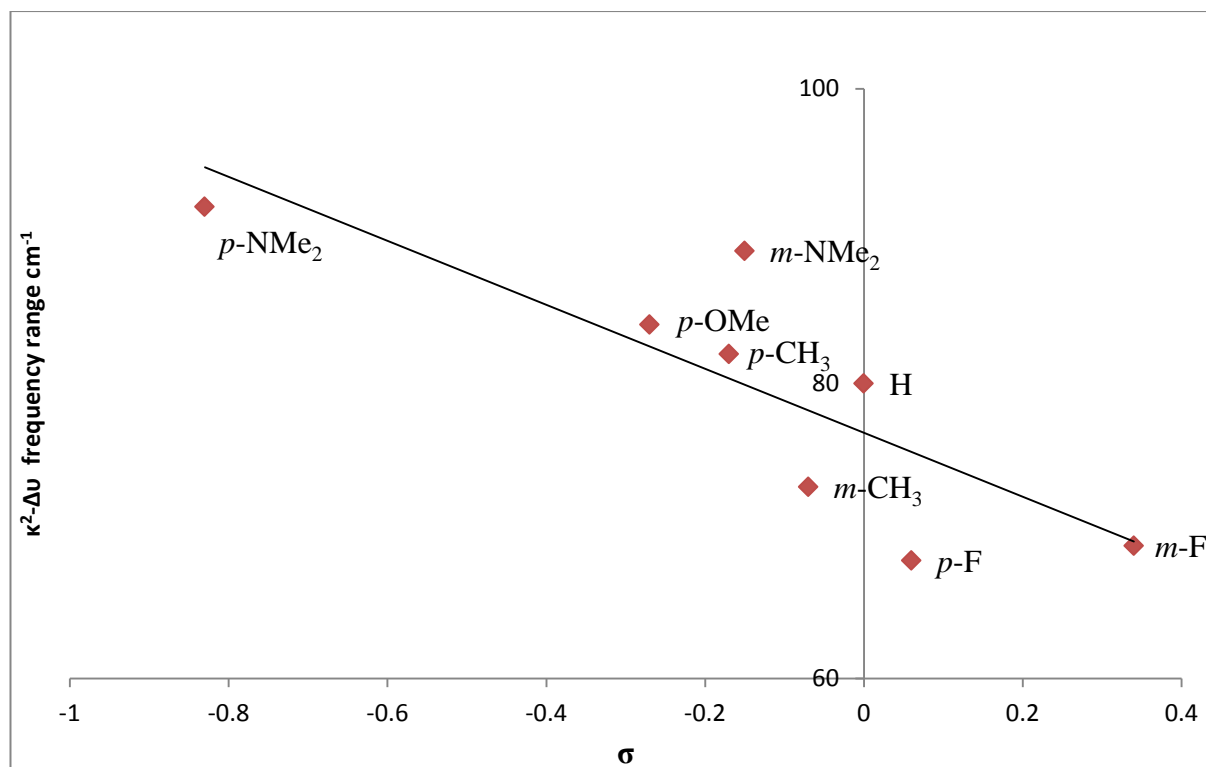


Figure 2.9: Plot of Hammett σ constants vs $\kappa^2-\Delta\nu$.

A Hammett plot of the Hammett parameters for the different R groups synthesised against $\kappa^2-\Delta\nu$ is shown above (Figure 2.9). It shows a poor correlation, which indicates that changing the substituent groups on the carboxylate group has little effect.

Even though using the original Hammett parameters did not show a correlation between the changing of the substituent on the carboxylate and the change in $\kappa^2 \Delta\nu$ they do not take into account the resonance effect that occurs between the substituent and the metal centre. It is possible by introducing a second sigma constant that takes into account the resonance effect that you can get a better correlation. The second constants are designated as σ^- or σ^+ , σ^- indicates that the *p*-substituent group is capable of resonance electron withdrawing effect and σ^+ indicates that the *p*-substituent groups is capable of resonance electron donating effect. If using σ^- or σ^+ constants give a better correlation for the Hammett plot then this indicate that resonance has an effect.

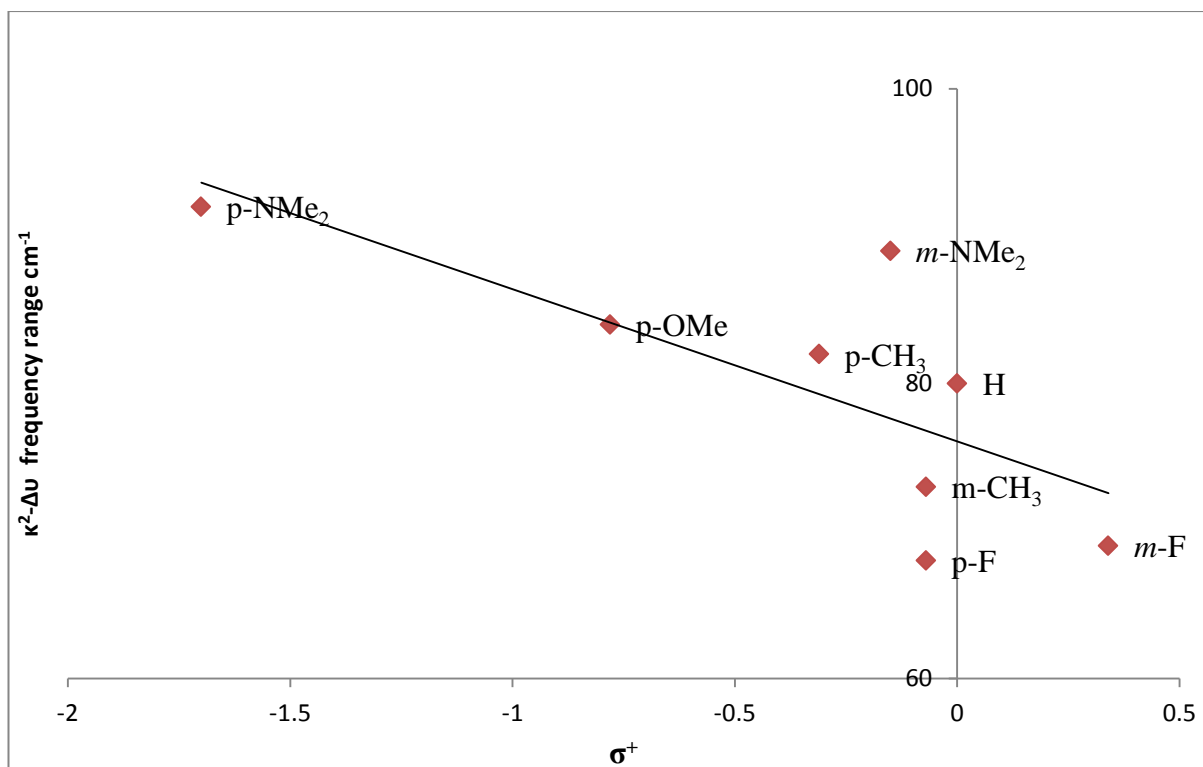


Figure 2.10: Plot of Hammett σ^+ constants vs $\kappa^2-\Delta\nu$.

Figure 2.10 shows that when you take into account the resonance effects of the substituent groups on the carboxylate ligand that there is a better correlation, if one ignores the poor correlating groups *p*-F and *m*-NMe₂, as they have σ^+ values close to 0, then the groups that have responded the most to the changes give a good correlation showing that resonance is having more an effect when it comes to the changing of the substituent on the carboxylate and the change in $\kappa^2 \Delta\nu$.

2.3.1 Crystal structure for the complexes $\text{Ru}(\kappa_2\text{-O}_2\text{CC}_6\text{H}_4\text{-R})_2(\text{PPh}_3)_2$

In some cases crystals suitable for study by X-ray Diffraction were obtained by slow diffusion of pentane into solutions of the complexes **2a** and **3a** in DCM, The crystal structure of **2a** is shown below but **3a** is yet to be fully solved. This provided further evidence that the synthesised complexes had the desired ligand configuration. The X-ray crystal structure data for complex **2a** is shown in Table 2.3.

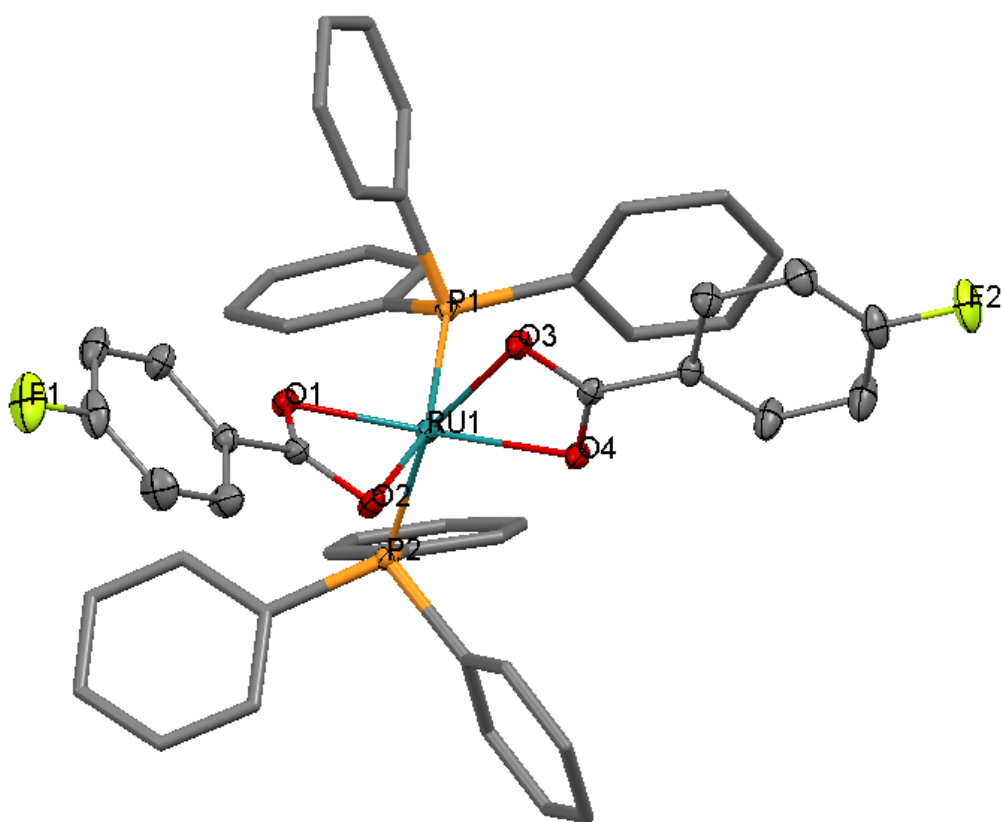


Figure 2.11: Crystal structure of **2a**, thermal ellipsoids, where shown, at the 50% probability level. Hydrogen atoms omitted for clarity.

Table 2.3 The important bond lengths (Å) and bond angles (°) for complex **2a** and those reported for $[\text{Ru}(\kappa^2\text{-O}_2\text{CPh})(\text{PPh}_3)_2]$,⁴² and $[\text{Ru}(\kappa^2\text{-OAc})(\text{PPh}_3)_2]$.¹²

Bond Length	2a / Å	$[\text{Ru}(\kappa^2\text{-O}_2\text{CPh})_2(\text{PPh}_3)_2]$ / Å	$[\text{Ru}(\kappa^2\text{-OAc})_2(\text{PPh}_3)_2]$ / Å
Ru – P(1)	2.2609(4)	2.2424(5)	2.2467(5)
Ru – P(2)	2.2424(4)	2.2664(5)	2.2463(5)
Ru – O(1)	2.1065(10)	2.1016(12)	2.1000(14)
Ru – O(2)	2.2368(10)	2.2278(13)	2.2353(15)
Ru – O(3)	2.2252(11)	2.2272(12)	2.2362(15)
Ru – O(4)	2.0986(15)	2.1017(12)	2.1072(14)
Bond Angle	2a / °	$[\text{Ru}(\kappa^2\text{O}_2\text{CPh})_2(\text{PPh}_3)_2]$ / °	$[\text{Ru}(\kappa^2\text{OAc})_2(\text{PPh}_3)_2]$ / °
P(1) – Ru – P(2)	103.828(14)	104.046(17)	100.57(2)
P(1) – Ru – O(1)	100.26(3)	97.82(4)	93.55(4)
P(1) – Ru – O(2)	156.87(3)	156.91(4)	155.75(4)
P(1) – Ru – O(3)	86.74(3)	94.92(4)	87.74(4)
P(1) – Ru – O(4)	91.00(3)	91.37(4)	98.59(4)
O(1) – Ru – O(2)	60.65(4)	-	60.48(5)
O(3) – Ru – O(4)	60.83(4)	-	60.48(5)
O(1) – Ru – O(3)	103.57(4)	-	103.56(6)
O(2) – Ru – O(3)	85.14(4)	-	85.97(6)
O(1) – Ru – O(4)	160.43(4)	-	159.15(6)
P(2) – Ru – O(1)	94.92(3)	91.35(4)	-
P(2) – Ru – O(2)	91.98(3)	86.34(4)	-
P(2) – Ru – O(3)	86.79(3)	100.06(4)	-
P(2) – Ru – O(4)	97.88(3)	156.85(4)	-

The crystal structure data for complex **2a** shows it adopts the same distorted octahedral conformation as reported for both $[\text{Ru}(\kappa^2\text{-O}_2\text{CPh})_2(\text{PPh}_3)_2]$ ⁴² and $[\text{Ru}(\kappa^2\text{OAc})_2(\text{PPh}_3)_2]$.¹²

All three crystal structures that were compared exhibited similar Ru-O bond lengths. The main differences in the complexes was that $[\text{Ru}(\kappa^2\text{-OAc})_2(\text{PPh}_3)_2]$ exhibits near equal bond lengths for Ru-P(1) and Ru-P(2) whereas **2a** and $[\text{Ru}(\kappa^2\text{-O}_2\text{CPh})_2(\text{PPh}_3)_2]$ have one of the

Ru-P bond lengths longer than the other, and if one compares the two complexes, **2a** has overall shorter Ru-P bonds.

2.3.2 Other crystal structures of interest

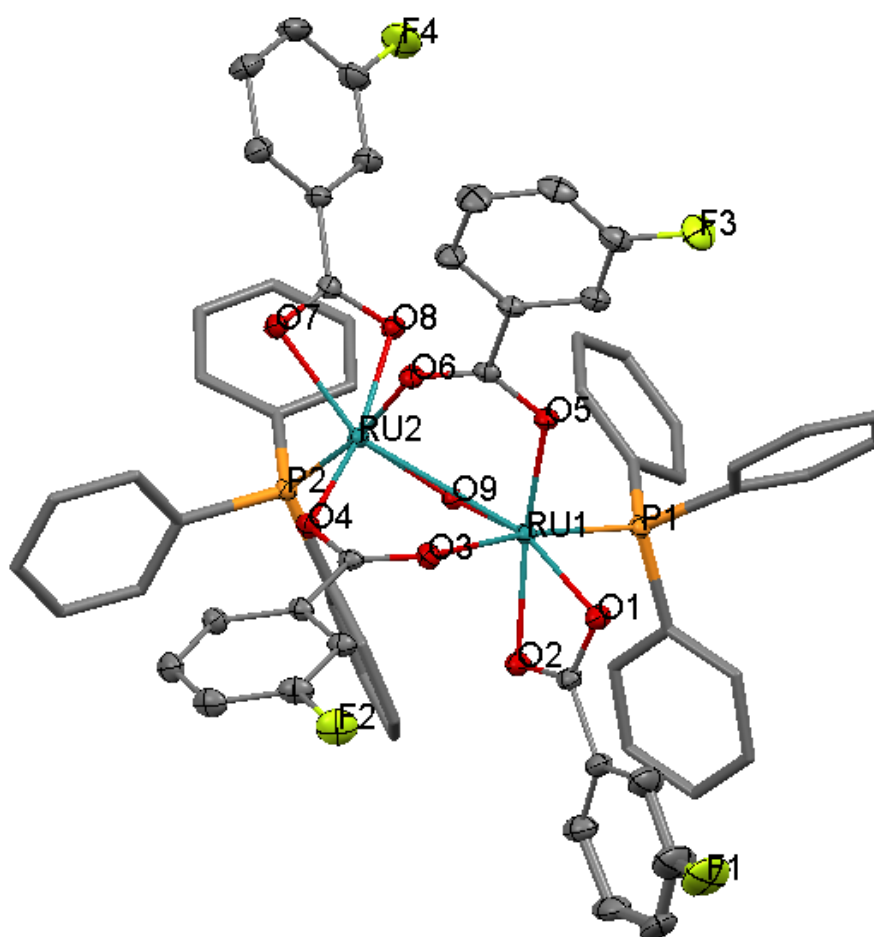


Figure 2.12: Crystal structure of $[\text{Ru}_2\text{O}(\text{O}_2\text{CC}_6\text{H}_4\text{-3-F})_4(\text{PPh}_3)_2]$ **2b**, thermal ellipsoids, where shown, at the 50 % probability level. Hydrogens and DCM molecule omitted for clarity

Other crystals were obtained from the slow diffusion of pentane and a solution of complex/DCM. But in these cases that follow the monomer species was not seen but some different degradation products. The crystal shown in Figure 2.12 was grown when trying to get a structure of complex **2b**. The solution must have come into contact with oxygen

during the crystal's growth as it formed an oxygen bridged dimer; a similar structure has been reported by Wilkinson and co-workers. Wilkinson *et al* reported that the complex $[\text{Ru}(\kappa^2\text{-OAc})_2(\text{PPh}_3)_2]$ in the presence of oxygen can form a ruthenium dimer $[\text{Ru}_2\text{O}(\text{CO}_2\text{Me})_4(\text{PPh}_3)_2]$,⁵⁴ which has two ruthenium metals bound to each other and bridged with two acetate ligands and an oxygen. A similar complex has also been reported by Werner *et al*, $[\text{Ru}_2(\text{CO}_2\text{Me})_4(\text{SbPr}^i_3)_2(\text{OH}_2)]$, which exhibited similar bridging but with a water bridging the two ruthenium centres rather than oxygen.⁵² The crystal structure of $[\text{Ru}_2\text{O}(\text{O}_2\text{CC}_6\text{H}_4\text{-3-F})_4(\text{PPh}_3)_2]$, shows this same bridging demonstrated by Wilkinson *et al*. It is possible that this was just one of the crystals in the batch but it is still of interest as at least in this instance it shows that the complexes synthesised exhibit similar chemistry to $[\text{Ru}(\kappa^2\text{-OAc})_2(\text{PPh}_3)_2]$.

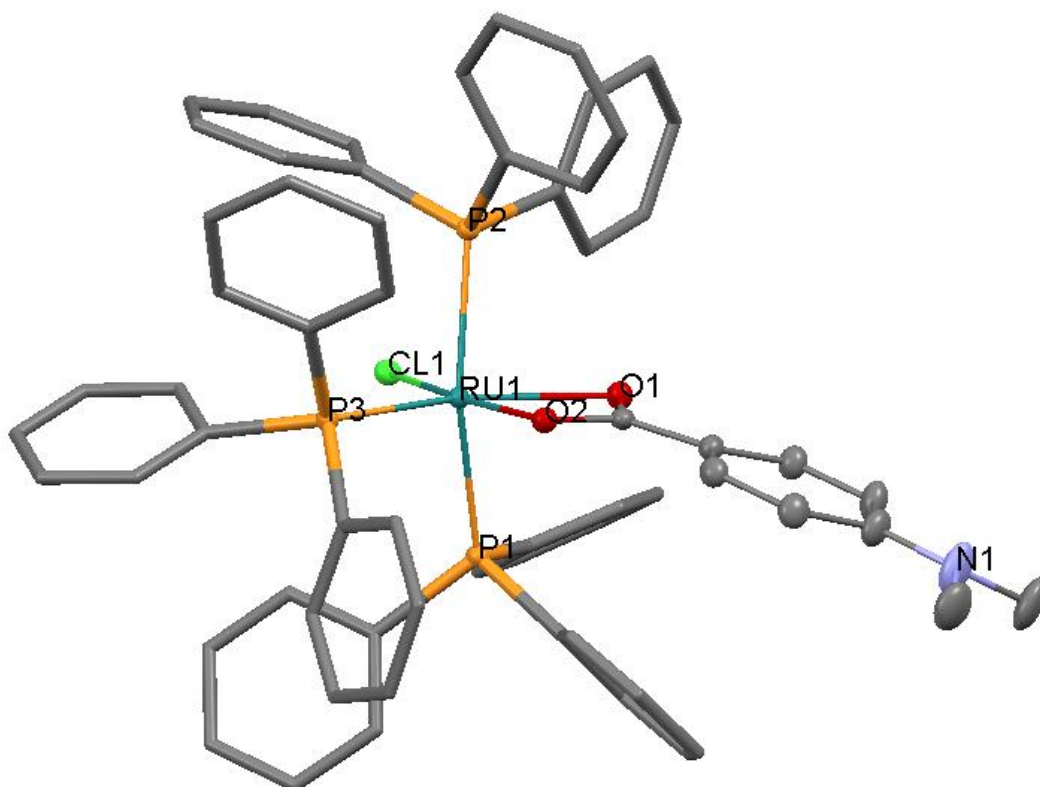


Figure 2.13: Crystal structure of $[\text{RuCl}(\text{O}_2\text{CC}_6\text{H}_4\text{-4-NMe}_2)(\text{PPh}_3)_3]$, thermal ellipsoids, where shown, at the 50 % probability level. Hydrogens and DCM molecule omitted for clarity

While trying to grow crystals of complex **5a** we managed to grow crystals of $[\text{RuCl}(\text{O}_2\text{CC}_6\text{H}_4\text{-4-NMe}_2)(\text{PPh}_3)_3]$ by slow diffusion of C_5H_{12} and a solution of complex/DCM. This product is thought to form when the crystals are left for too long in DCM and the complexes begin to degrade and is considered to be a minor product. In this case one of the acetates has dissociated and been replaced by chlorine and an extra triphenylphosphine group.

Both of these crystal structure shown are minor products that can exist while the complexes are under an inert atmosphere, as there is no evidence for these products in the data. The dimer or oxidation product shown for **2b** becomes the major product if these complexes are exposed to oxygen for a prolonged period of time while in solution.⁷⁶

3.1 Transition metal carbonyl complexes and π -back bonding

The study of the effects of different groups on the strength of the π -back bonding in transition metal carbonyl complexes is a well-studied phenomenon.^{71,77} Section 1.4.1 of the introduction discussed the chemistry that governs these types of interactions, and also that both vinylidene and carbonyl species have π -back bonding interactions that govern the strength of the metal-ligand bond. It is important to look at the carbonyl species when trying to understand the chemistry of the vinylidene π -back bonding, as they are essentially identical when it comes to this type of interaction.⁴ So by making the carbonyl derivatives of the different ruthenium carboxylate complexes that were synthesised during this project, we can use this information to predict the strength of the metal-ligand bond in the vinylidene complexes

3.2 Preparation of $[\text{Ru}(\kappa^1\text{-OAc})(\kappa^2\text{-OAc})(\text{CO})(\text{PPh}_3)_2]$

During the 1960-80's, there was a significant amount of work done by the groups of Wilkinson and Robinson, amongst others, into the synthesis, characterisation and behaviour of a range of different acetato- and trifluoroacetato- complexes of ruthenium. This work was drawn upon by Lynam and co-workers to provide new inspiration for easily prepared ruthenium precursors.

In 1974, Wilkinson reported the synthesis of the CO-containing derivative of complex $[\text{Ru}(\kappa^2\text{-OAc})(\text{PPh}_3)_2]$, $[\text{Ru}(\kappa^1\text{-OAc})(\kappa^2\text{-OAc})(\text{CO})(\text{PPh}_3)_2]$, **6**. This procedure involved bubbling CO through a solution of $[\text{Ru}(\kappa^2\text{-OAc})_2(\text{PPh}_3)_2]$ in MeOH for one hour, followed by isolation of the resulting pale yellow-green precipitate which was washed with MeOH and Et₂O.⁶⁴ Lynam *et al* have found that this complex can also be prepared by vigorously stirring a solution of $[\text{Ru}(\kappa^2\text{-OAc})(\text{PPh}_3)_2]$ in DCM under an atmosphere of CO until a colour change from red-orange to a pale yellow-green is observed. Removal of the solvent

in vacuo afforded a pale yellow-green residue which could be used without further purification. The latter method is used to conveniently generate this compound *in situ*, whilst Wilkinson's method was used to prepare the complex on a large scale.¹²

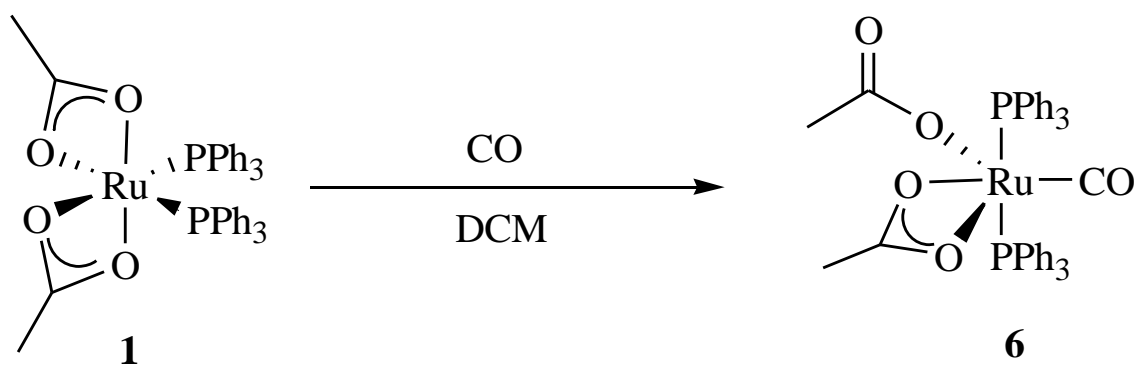


Figure 3.1: Addition of CO to [Ru(κ²-OAc)₂(PPh₃)₂].

Lynam *et al* reported that complex **6** can be readily identified by characteristic spectroscopic features, most notably in the IR spectrum where a band assigned to ν_{CO} was observed at 1946 cm^{-1} . The ^{31}P NMR spectrum of complex **6** displays a singlet at δ_{P} 39.1 ppm, indicating a *trans*-orientation of the triphenylphosphine ligands. As explained earlier the chemical shift of the singlet in the ^{31}P NMR indicative of the stereochemistry of the triphenylphosphine ligands with the *trans*-oriented occurring in the region of δ_{P} 33.0-39.9 ppm as noted for the vinylidene and carbonyl complexes. In contrast the chemical shift of *cis*-oriented triphenylphosphine occurs in the region of δ_{P} 63.0-64.0 ppm which is exhibited for the complexes of the general type [Ru(κ²O₂CR)₂(PPh₃)₂]. In the ^{13}C NMR spectrum, a triplet resonance at δ_{C} 207.4 ($^2J_{\text{PC}} = 13.2\text{ Hz}$) was observed which corresponds to the CO ligand, being split by the two equivalent PPh₃ ligands.

3.3 The preparation of complexes of the general type $[\text{Ru}(\kappa^1\text{-O}_2\text{CC}_6\text{H}_4\text{-R})(\kappa^2\text{-O}_2\text{CC}_6\text{H}_4\text{-R})(\text{CO})(\text{PPh}_3)_2]$

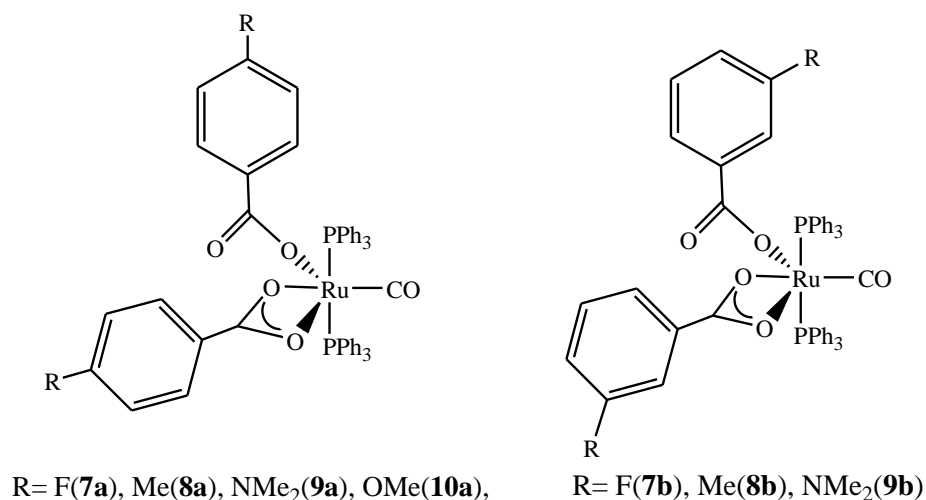


Figure 3.2: Carbonyl complexes successfully synthesised and their R group and reference number.

As discussed at the beginning of this chapter the carbonyl derivatives of the ruthenium carboxylate complexes needed to be synthesised to show the effect the different R-groups have on the π -back-bonding in the carbonyl complexes, this is because both the carbonyl and vinylidene species are essentially similar with regards to the behaviour of π -back bonding of the M-C interaction. Because judging the strength of the π -back-bonding is easier in carbonyl species then one can use the information gathered from the carbonyl complexes and compare that to what is found for vinylidene complexes and hopefully show that carbonyl species can be used to predict the π -back bonding interaction in vinylidene species, *i.e.* that using electron withdrawing groups such as fluorine will weaken the π -back bonding interaction for both species. Thus the aim of this chapter was to prepare and characterise the carbonyl derivatives $[\text{Ru}(\kappa^1\text{-O}_2\text{CC}_6\text{H}_4\text{-R})(\kappa^2\text{-O}_2\text{CC}_6\text{H}_4\text{-R})$

R)(CO)(PPh₃)₂], to show what effect changing of the R groups on the phenyl ring of the carboxylate had on the strength of the M-CO bond.

The carbonyl complexes were synthesised by reacting the desired carboxylate complex with carbon monoxide in DCM, as reported for [Ru(κ^2 -OAc)₂(PPh₃)₂].¹² Most of the compounds reacted exactly the same as the results reported for [Ru(κ^2 -O₂CPh)₂(PPh₃)₂] and [Ru(κ^2 -OAc)₂(PPh₃)₂], exhibiting a colour change in the DCM/complex solution going from orange to yellow except for **10a** which went from a dark orange to light orange. To make sure that there was no *di* substitution of carbon monoxide the reaction was monitored by IR spectroscopy. All reactions went through to completion to produce the carbonyl derivatives of the ruthenium carboxylate complexes. It was important to only have the *mono* substituted carbonyl as if there were two carbon monoxide ligands the effect that the R groups would have on the back bonding of the carbon monoxide would be altered as it would be spread between two carbon monoxide groups, and the information we want to gain from these complexes is how the groups effect the π -back bonding in one M-C environment.

All the synthesised compounds were characterised by ¹H, ³¹P and ¹³C NMR spectroscopy, IR spectra recorded in the solid state (KBr) and ESI-MS. The strongest evidence to show that the desired complex had been formed came from IR and NMR spectroscopy. The IR spectrum should have a ν_{CO} band at approximately 1900 cm⁻¹. Stretches for both coordination modes should be evident in the IR spectrum. ³¹P NMR spectra should display a singlet at approximately δ_{P} 39 ppm, indicating a *trans*-orientation of the PPh₃ ligands. In the ¹³C NMR spectrum, a triplet resonance at around δ_{C} 210 ppm (²J_{PC} = 13.2 Hz) corresponds to the carbon monoxide ligand.

To explain how the ^1H and ^{13}C NMR spectroscopic data was assigned complex, $[\text{Ru}(\kappa^1\text{-O}_2\text{CC}_6\text{H}_4\text{-4-F})(\kappa^2\text{-O}_2\text{CC}_6\text{H}_4\text{-4-F})(\text{CO})(\text{PPh}_3)_2]$ **7a**, is used as an example. The ^1H NMR spectrum was assigned as follows:

^1H δ_{H} : 6.67 (at, $^3J_{\text{HH}}$, $^3J_{\text{HF}} = 9.29\text{Hz}$, 4H, *m*- $\text{C}_6\text{H}_4\text{F}$), 7.17 (m, 4H, *o*- $\text{C}_6\text{H}_4\text{F}$), 7.24 (m, 18H, ***Ph***), 7.51 (m, 12H, ***Ph***). The assignment reasons are identical to that as described for the carboxylate complexes the only difference being that because the carboxylate ligands are fluctuating rapidly between κ^1 and κ^2 binding modes the *ortho*-protons on the carboxylate exhibited more complicated signals and further splitting turned this from an apparent triplet into a multiplet. The ppm shifts of the protons appear similar region to those of the carboxylate complex. The reason the peaks do not occur at the exact same ppm shift as those of the carboxylate complex is due to this fluctuation of the carboxylate ligand between κ^1 and κ^2 binding modes.

The ^{13}C NMR spectrum for complex **7a** was assigned in the following way for the following reasons:

$^{13}\text{C}\{^1\text{H}\}$: δ_{C} 113.5 (d, $^2J_{\text{CF}} = 21.6\text{ Hz}$, *m*- $\text{C}_6\text{H}_4\text{F}$), 128.2 (at, $^3J_{\text{PC}} = 4.6\text{ Hz}$, *m*-***PPh***₃), 129.7 (vt, $^1J_{\text{PC}} + ^3J_{\text{PC}} = 21.9\text{ Hz}$, *i*-***PPh***), 130.2 (s, *p*-***PPh***), 130.5 (d, $^3J_{\text{CF}} = 8.8\text{ Hz}$, *o*- $\text{C}_6\text{H}_4\text{F}$), 134.2 (at, $^2J_{\text{PC}} = 4.9\text{ Hz}$, *o*-***PPh***), 164.3 (d, $^1J_{\text{CF}} = 248.6\text{ Hz}$, *p*- $\text{C}_6\text{H}_4\text{F}$), 175.2 (s, $\text{CO}_2\text{C}_6\text{H}_4\text{F}$), 206.8 (t, $^2J_{\text{PC}} = 12.6\text{ Hz}$, ***CO***) ppm. The peaks were assigned for the same reasons given for the carboxylate ligand, but as with the proton spectrum the fluctuating binding mode has shifted the ppm of the peaks for the carboxylate ligand, most notably the quaternary carbon $\text{CO}_2\text{C}_6\text{H}_4\text{F}$, which has shifted from 181.7 to 175.2 ppm. The ***CO*** carbon appears as a triplet at 206.8 ppm and is coupled to the two phosphorus atoms.

Table 3.1: Common characteristic NMR spectroscopic features of complexes **7a-10a** and **7b-9b** (CD₂Cl₂).

	³¹ P NMR δ _P /ppm PPh ₃	¹³ C NMR δ _C /ppm CO	¹³ C ² J _{CP} /Hz
7a	39.1	206.8	12.6
8a	38.5	207.4	13.5
9a	37.8	208.2	14.3
10a	38.6	207.9	14.5
7b	39.2	206.9	13.9
8b	38.7	207.8	14.7
9b	38.8	207.4	14.4

Table 3.2: Selected IR spectroscopic features of complexes **7a-10a** and **7b-9b** (CD₂Cl₂).

	Vibration cm ⁻¹						
	7a	8a	9a	10a	7b	8b	9b
P-Ph	1482	1482	1482	1482	1482	1482	1482
κ¹-OCO_{sym}	1347	1350	1343	1349	1348	1343	1351
κ¹-OCO_{asym}	1625	1587	1570	1589	1584	1575	1559
κ¹-Δν	278	237	227	240	226	232	208
κ²-OCO_{sym}	1434	1429	1428	1424	1436	1436	1436
κ²-OCO_{asym}	1502	1504	1519	1506	1507	1506	1507
κ²-Δν	68	75	91	82	71	70	71
CO	1948	1946	1942	1945	1950	1947	1945

The IR spectroscopic data shows that changing the R-group has an effect on the CO stretching frequency, although the effects are minor (1942-1950 cm^{-1}). Even in the ^{13}C NMR spectra the CO triplet only moves by fractions of ppm (206.8-208.2 ppm).

To show the trend that the R groups have on the stretching frequency of the CO in the IR spectra, a Hammett plot of the σ constants against the IR stretching frequency was plotted.

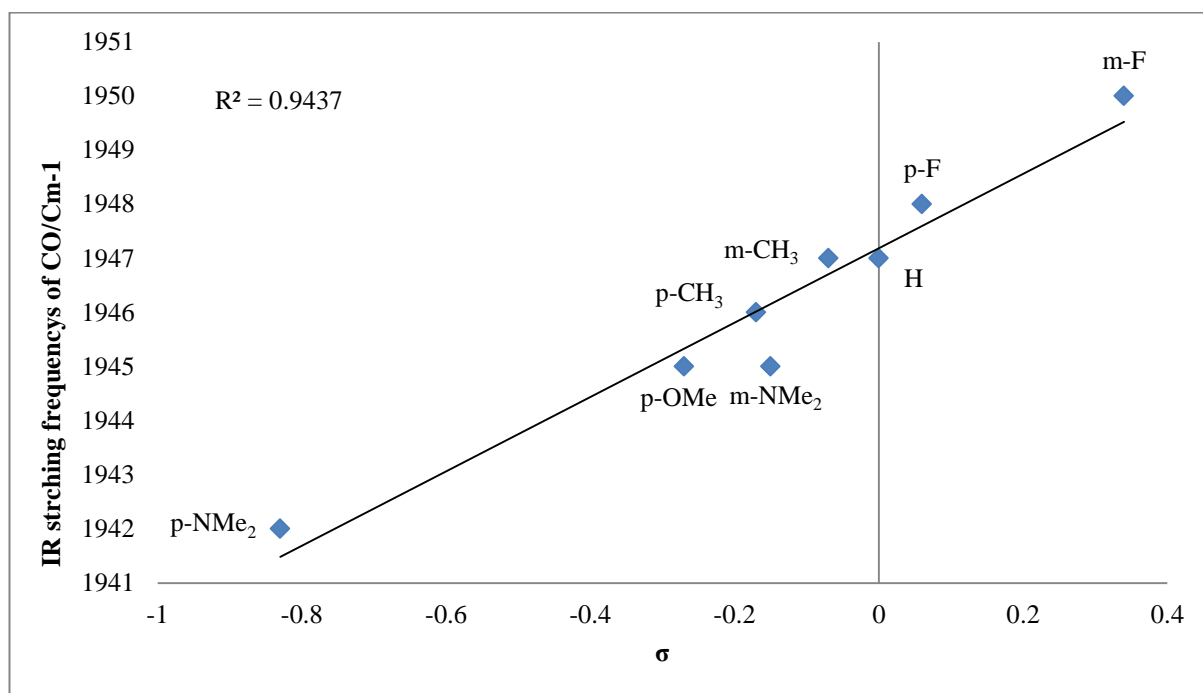


Figure 3.3: A plot of Hammett σ constants against IR stretching frequencies for CO

The data gathered for the ν CO stretching frequency for this series of ruthenium carbonyl complexes shows that these complexes behave as predicted in the literature. The literature predicts that as you change from electron withdrawing group to an electron donating groups that there should be a decrease in the stretching frequency. The lower the value for ν CO the greater the back-bonding to the carbonyl group thus the stronger the M-C bond. The electron donating groups here have a lower ν CO value than $[\text{Ru}(\kappa^2\text{-O}_2\text{CPh})(\kappa^1\text{-O}_2\text{CPh})(\text{CO})(\text{PPh}_3)_2]$ **7**, which had a ν CO of 1947 cm^{-1} ,⁴² for example compared to that of $[\text{Ru}(\kappa^2\text{-O}_2\text{CC}_6\text{H}_4\text{-4-NMe}_2)(\kappa^1\text{-O}_2\text{CC}_6\text{H}_4\text{-4-NMe}_2)(\text{CO})(\text{PPh}_3)_2]$ **9a**, which had a ν CO of

1942 cm^{-1} , thus meaning that the back-bonding for the complexes with electron donating groups have strengthened the M-C bond whereas in the complexes with the electron withdrawing groups they exhibit a larger $\nu \text{ CO}$, for example $[\text{Ru}(\kappa^2\text{-O}_2\text{CC}_6\text{H}_4\text{-4-F})(\kappa^1\text{-O}_2\text{CC}_6\text{H}_4\text{-4-F})(\text{CO})(\text{PPh}_3)_2]$ which had a $\nu \text{ CO}$ of 1950 cm^{-1} , which shows that these are weakening the back-bonding interactions. As stated before these effects are very small as the $\nu \text{ CO}$ is only being changed by a few wavelengths.

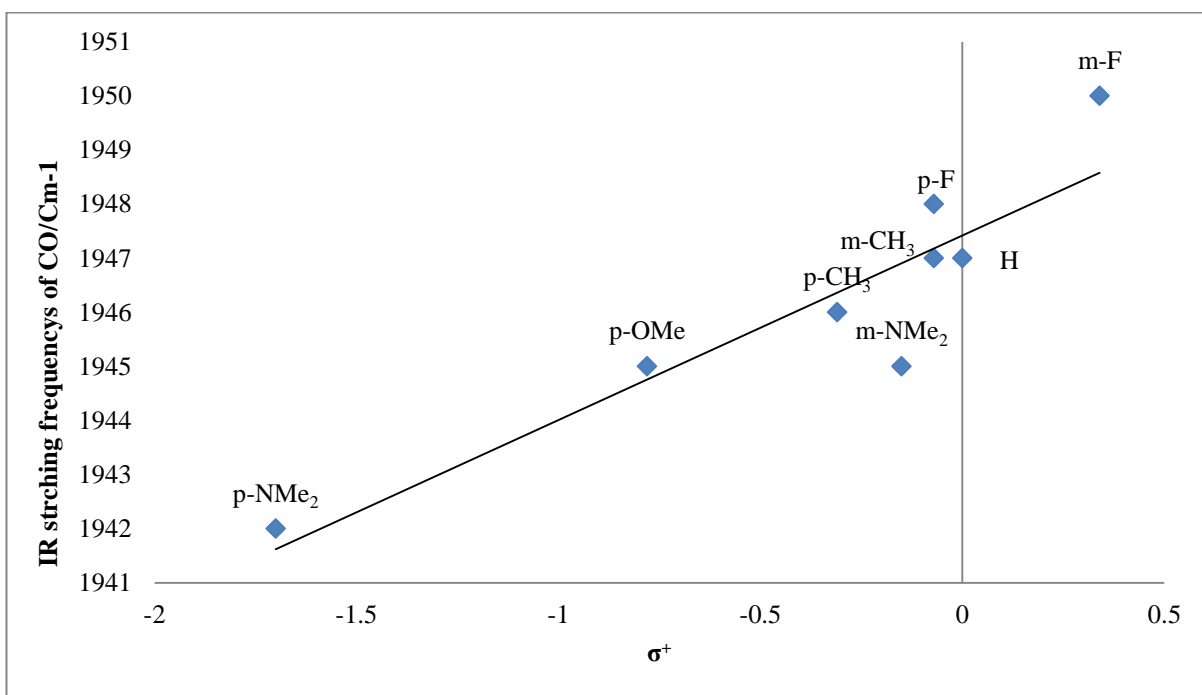


Figure 3.3: A plot of Hammett σ^+ constants against IR stretching frequencies for CO.

When the resonance effect is taken into account the correlation is poorer, this is not to say that resonance does not play a role in these compounds just that the Hammett σ^+ constants are derived for a system that is very different to this which is shown by the poor correlation.

4.1 Synthesis of complexes of the general type $[\text{Ru}(\kappa^1\text{-O}_2\text{CC}_6\text{H}_4\text{-R})(\kappa^2\text{-O}_2\text{CC}_6\text{H}_4\text{-R})(=\text{C}=\text{HPh})(\text{PPh}_3)_2]$

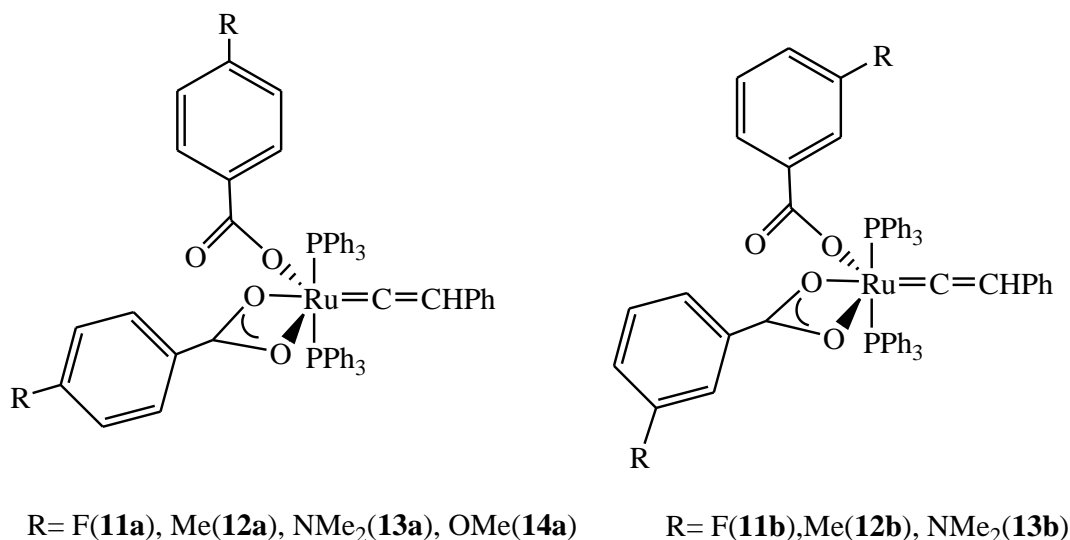


Figure 4.1: Complexes that were successfully synthesised and their R group and compound numbers.

Having successfully synthesised the carbonyl derivatives of the carboxylate complexes and thus gained evidence that would help predict the behaviour each R group would have on the π -back bonding in these ruthenium complexes, the next objective for this project was to test whether the $[\text{Ru}(\kappa^2\text{-R-C}_6\text{H}_4\text{CO}_2)_2(\text{PPh}_3)_2]$ complexes exhibit similar reactivity to $[\text{Ru}(\kappa^2\text{-OAc})_2(\text{PPh}_3)_2]$, and produce the vinylidene derivatives $[\text{Ru}(\kappa^1\text{-O}_2\text{CC}_6\text{H}_4\text{-R})(\kappa^2\text{-O}_2\text{CC}_6\text{H}_4\text{-R})(=\text{C}=\text{HPh})(\text{PPh}_3)_2]$. This was done by reaction of the desired carboxylate complex with phenyl acetylene in a solution of DCM that was stirred at room temperature for 1 hour.

All the compounds reacted exactly the same as the results reported for $[\text{Ru}(\kappa^2\text{-OAc})_2(\text{PPh}_3)_2]$ and went through to completion to produce the vinylidene derivatives of the ruthenium acetate complexes. Only the complex $[\text{Ru}(\kappa^1\text{-O}_2\text{CC}_6\text{H}_4\text{-3-OMe})(\kappa^2\text{-O}_2\text{CC}_6\text{H}_4\text{-3-OMe})(=\text{C}=\text{HPh})(\text{PPh}_3)_2]$ was not synthesised, as complex **5b** had proved

difficult to obtain as a pure product the complex would appear in all the different washing stages, the most awkward of these being the water wash to remove the NaCl as exposure to water can lead to the complex oxidising and producing a dimer like that shown in Figure 2.12.

All the synthesised compounds were characterised by ^1H , ^{31}P and ^{13}C NMR spectroscopy, IR spectra recorded in the solid state (KBr), ESI-MS and elemental analysis. The NMR spectra should show a characteristic triplet for the proton on the β carbon, which is observed in the ^1H NMR spectra at around δ_{H} 5.2 ppm the triplet is due to the proton on the β carbon being coupled to the protons on the *ortho* position of the phenyl ring. The corresponding triplet of the β carbon in the ^{13}C NMR occurs around δ_{C} 112 ppm, this is a triplet due to the coupling to the phosphorus ($^3J_{\text{CP}}$). Also the ^{31}P NMR spectra show a singlet at δ_{P} 33-34 ppm which shows that the triphenylphosphine ligands have changed from the *cis*-position found in the carboxylate complexes, to the *trans*-position as previously reported for these vinylidene ruthenium complexes.^{12, 42}

To see the peaks in the ^{13}C NMR spectra that correspond to those of the vinylidene requires a completely saturated NMR sample and approximately 20K scans on a 500 MHz NMR machine; early attempts to detect these peaks failed as the vinylidene complexes were not very soluble in CD_2Cl_2 . A different route was attempted by preparing the ruthenium complexes *in situ* but the complexes would crash out of solution once formed. The final solution was to use ^{13}C labelled phenyl acetylene, [$^{13}\text{C}=\text{CHPh}$] to make the complexes *in situ*. This method allowed the α C of the vinylidene to be detected in very few scans.

The NMR spectra of most of the ^{13}C labelled complexes showed multiple triplets in the region that is associated with the shift of the α C of the vinylidene, other than those

attributed to the α and β carbons of the vinylidene ligand, with some giving rise to broad peaks which is normally indicative of some sort of exchange process. As there was evidence in the NMR spectra for free phenyl acetylene, it was probable that *in situ* the phenyl acetylene was freely exchanging with the vinylidene ligand as this has been observed in work by Lynam and co-workers (some ruthenium half-sandwich complexes also gave broad peaks).⁷⁸ To test this hypothesis the solvent and any excess phenyl acetylene were removed *in vacuo* for one of the samples where a broad peak was observed, and the NMR sample re-made with fresh solvent.

The ^{13}C NMR spectra still showed a broad peak in the region where the α C of the vinylidene is usually observed and no peaks due to free phenyl acetylene. Exactly what is causing this phenomenon is unknown at this present moment but future studies by variable temperature NMR might be able to show some insight into what precisely is going on. The data for complex **13b** was unable to be collected, as the sample had decomposed by the time the labelling studies were carried out.

Table 4.1: Common characteristic NMR features of complexes **11a-14a** and **11b-13b**
(CD_2Cl_2)

	^{31}P NMR $\delta_{\text{P}}/\text{PPh}_3$ ppm	^{13}C NMR $\delta_{\text{C}}/\text{C}_\alpha$ ppm	^{13}C $^2J_{\text{CP}}$ / Hz
11a	34.2	359.0	16.1
12a	34.2	353.5	-
13a	33.3	344.3	-
14a	33.7	355.0	16.5
11b	34.2	357.2	16.6
12b	33.9	356.5	16.6
13b	33.2	-	-

IR spectroscopy showed stretching frequencies for both the κ^1 and κ^2 binding mode. As discussed in the introduction, to create a vacant site at which the alkyne can coordinate to the metal centre to form a vinylidene, one of the labile acetate ligands switches from the bidentate (κ^2) to the unidentate (κ^1) binding mode; it can be established by NMR spectroscopic analysis if the carboxylate ligands of the ruthenium-vinylidene complexes are binding in the desired fashion. The NMR spectroscopic data showed that the vinylidene has been formed on the metal centre and that the phosphorus ligands are in the desired *trans*-position.

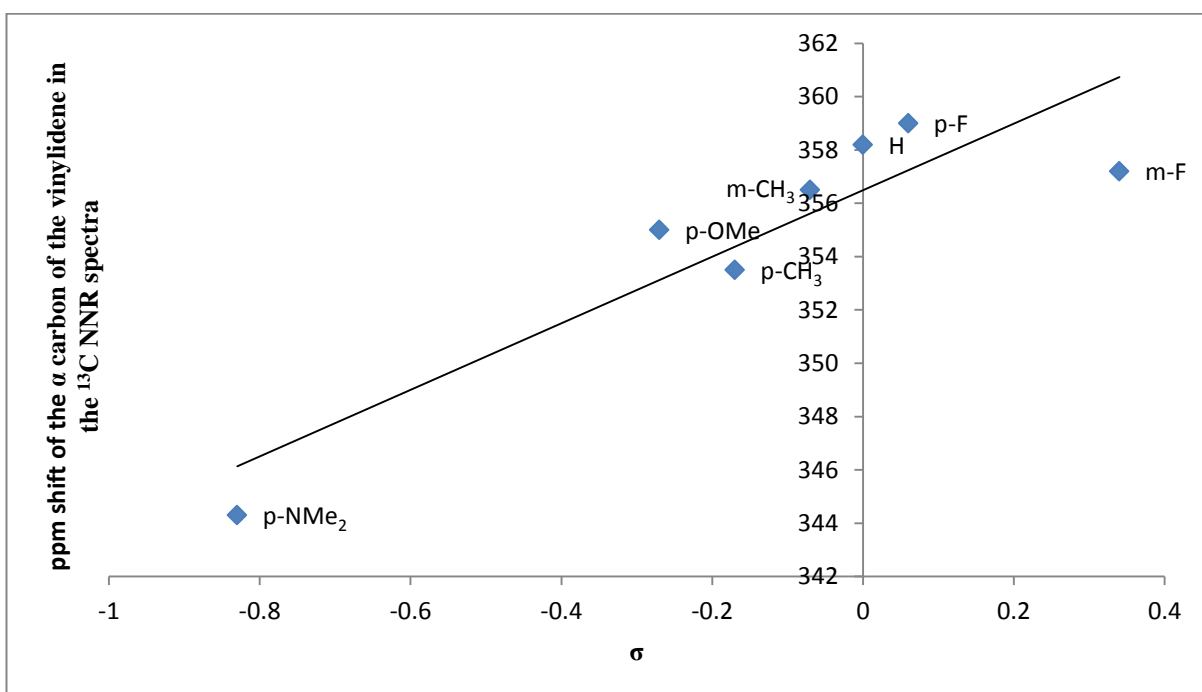


Figure 4.2: A Hammett plot of the σ constants against the ppm shift for the α carbon of the vinylidene in the ^{13}C NMR spectra.

The Hammett plot shows that the trend predicted for the carbonyl complexes regarding the M-C bond strength is also present in the vinylidene complexes. The more electron donating groups have strengthened the π -back bonding on the metal vinylidene bond and the

electron withdrawing groups have weakened this interaction. This is shown by the change in the chemical shift of the α carbon in the ^{13}C NMR spectra.

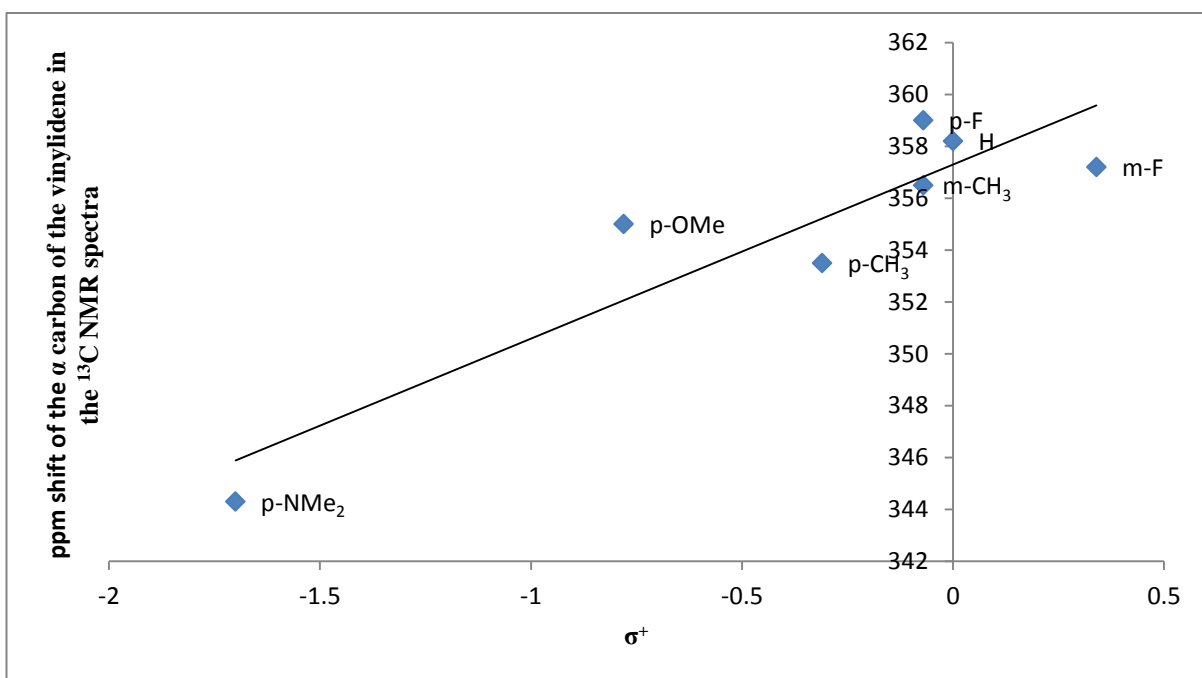


Figure 4.3: Hammett plot of σ^+ constants against the ppm shift of the α carbon of the vinylidene in the ^{13}C NMR spectra.

When taking into account the resonance effect of the substituted carboxylates has on the ppm shift of the α carbon of the vinylidene in the ^{13}C NMR spectra, there is a poorer correlation but it still showing the same effect as discussed before for the Hammett plot in Figure 4.2.

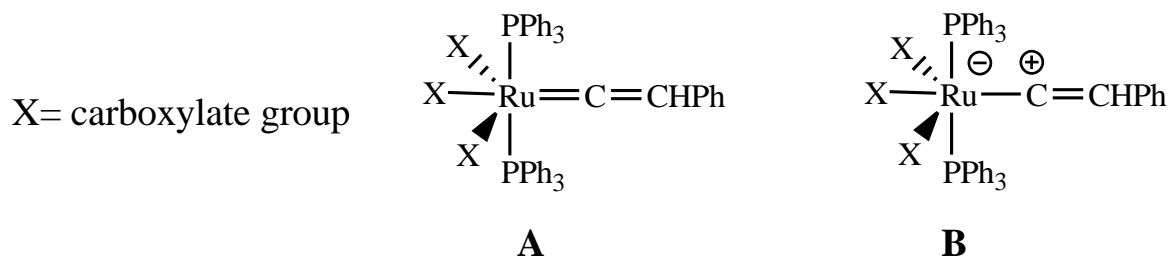


Figure 4.4: Resonance structures of vinylidenes

The vinylidene complexes with electron donating carboxylate groups are exhibiting a resonance structure **A**, the triplet of the α carbon in the ^{13}C NMR spectrum occurs at a lower ppm, as these groups are giving electron density to the metal centre which is in turn strengthening the M-C bond due to the strengthening of the metal d orbital to vinylidene p orbital via back donation, thus stabilising the vinylidene. As such there is more electron density on the α carbon of the vinylidene which means it will occur at a lower chemical shift. The electron withdrawing groups are pulling away electron density from the metal centre so the complexes are exhibiting a resonance structure **B** meaning that the M-C bonding is weaker as the ruthenium is not donating electron density into the M-C bond, due to the weakening of the metal d orbital to vinylidene p-orbital via back donation, thus stabilising the vinylidene. So triplet of the α carbon in the ^{13}C NMR spectrum occurs at a higher chemical shift due to the lack of electron density on the α carbon.

Crystals suitable for X-ray diffraction were obtained for **12a** and **11b** by slow diffusion of a complex/DCM solution added to pentane. The crystal structures for **12a** and **11b** and Table 4.3 comparing the bond lengths and angles of complexes **12a**, **11b**, **15** ($[\text{Ru}(\kappa^1\text{-O}_2\text{CPh})(\kappa^2\text{-O}_2\text{CPh})(=\text{C}=\text{CHPh})(\text{PPh}_3)_2]$)⁴² and **16** ($[\text{Ru}(\kappa^1\text{-OAc})(\kappa^2\text{-O}_2\text{Ac})(=\text{C}=\text{CHPh})(\text{PPh}_3)_2]$),¹² are shown in Figures 4.4, 4.5 and Table 4.3 respectively.

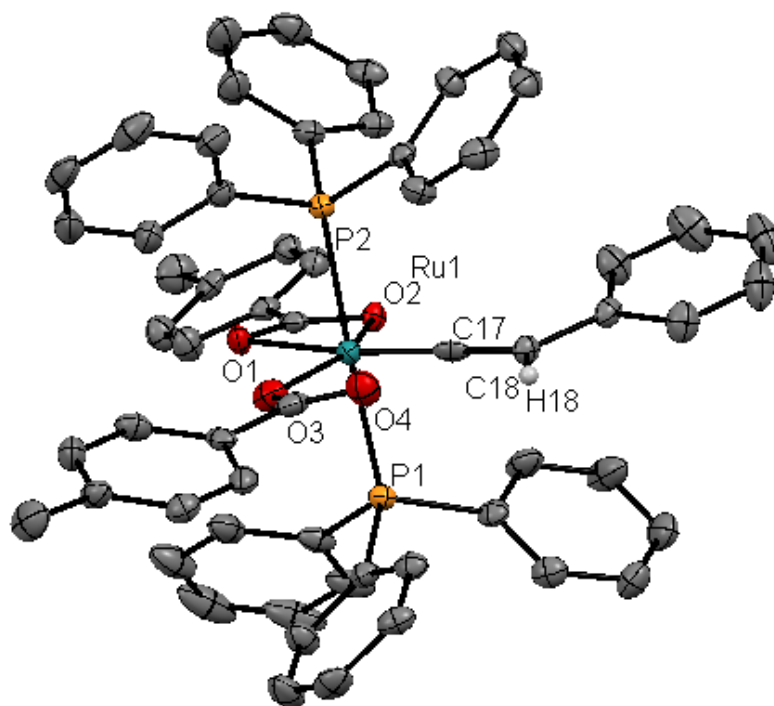


Figure 4.5: Crystal structure diagram of **12a**, thermal ellipsoids, where shown, are at the 50% probability level. Hydrogen atoms, except for H(18), are omitted for clarity.

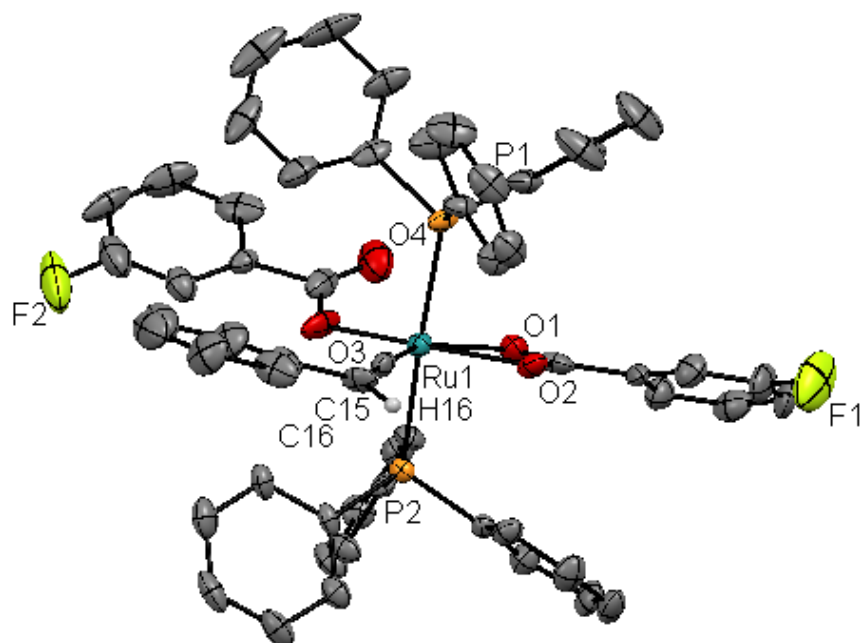


Figure 4.6: Crystal structure diagram of **11b**, thermal ellipsoids, where shown, are at the 50% probability level. Hydrogen atoms, except for H(16), are omitted for clarity.

Table 4.3: Important bond lengths (Å) and angles (°) for complexes **15**, **16**, **12a** and **11b**

Bond Length	16	15	12a	11b
Ru – P(1)	2.3853(7)	2.4031(6)	2.3882(14)	2.3733(7)
Ru – P(2)	2.3910(7)	2.3925(6)	2.3830(14)	2.3883(7)
Ru – O(1)	2.1139(17)	2.110(3)	2.258(5)	2.251(2)
Ru – O(2)	2.2863(18)	2.313(4)	2.190(5)	2.148(2)
Ru – O(3)	2.0699(17)	2.0464(18)	2.057(7)	2.013(3)
Ru – C _α	1.786(3)	1.794(9)	1.801(9)	1.797(4)
C _α – C _β	1.318(4)	1.312(10)	1.471(17)	1.302(5)

Bond Angle	16	15	12a	11b
P(1) – Ru – P(2)	178.89(3)	178.08(2)	177.25(3)	177.28(8)
P(1) – Ru – O(1)	89.08(5)	82.30(7)	95.02(6)	94.27(14)
P(1) – Ru – O(2)	98.59(5)	92.66(13)	88.7(6)	85.03(13)
P(1) – Ru – O(3)	93.06(5)	95.12(5)	89.18(7)	96.5(2)
O(1) – Ru – O(2)	59.08(6)	-	59.76(8)	58.30(19)
O(1) – Ru – O(3)	168.17(7)	-	91.84(9)	112.4(2)
O(2) – Ru – O(3)	109.09(7)	-	151.20(10)	170.7(3)
P(2) – Ru – O(1)	-	97.36(8)	87.73(6)	84.01(13)
P(2) – Ru – O(2)	-	85.56(13)	92.63(6)	92.27(12)
P(2) – Ru – O(3)	-	84.75(5)	90.83(7)	86.15(19)
P(1) – Ru – C _α	87.77(8)	-	85.95(12)	90.6(3)
P(2) – Ru – C _α	91.58(8)	-	91.34(12)	89.8(3)
P(1) – Ru – O(1)	97.81(9)	82.3(7)	95.02(6)	94.27(14)
P(1) – Ru – O(2)	98.59(5)	92.66(13)	88.70(6)	85.03(13)
P(1) – Ru – O(3)	93.90(9)	95.12(5)	96.5(2)	89.18(7)
Ru – C _α – C _β	176.5(2)	176.9(8)	179.3(5)	177.3(9)

The structures obtained show that both **12a** and **11b** adopt a distorted octahedral structure like that reported for both **16** and **15**. The majority of the angles about the ruthenium are close to that of an ideal octahedron; however significant distortions arise due to the constraints of a κ^2 -OAc ligand. The P(1)–Ru–P(2) angle is close to linear in both **12a** and **11b**, 177.25(3)° and 177.28(8)° respectively, which is similar to the angle to P(1)–Ru–

P(2) reported for **16** (178.89(3)°) and **15** (178.08(2)°). The Ru–C_α–C_β angle of **12a** and **11b** are almost linear being 179.3(3)° and 177.3(9)° respectively, which is similar to that shown for **16** (176.5(2)°), this provides further evidence for the distorted octahedral structure.

Bruce has reported that the M=C=C bond are “essentially linear, the angle at C_α being in the range 167-180°”.⁴ He also suggests the M=C moiety has a bond order of two whilst the bond order of C=C is typically between two and three, in a range of 1.25-1.41 Å. The Ru–C_α–C_β angle of **12a** and **11b** are 179.3(5)° and 177.3 (9)° respectively; both are more linear than **16** with its Ru–C_α–C_β bond angle being 176.5(2)°. The bond length of the vinylidene moiety is typical in **12a**; both Ru–C_α and C_α–C_β are short at 1.797(4) Å and 1.302(5) Å respectively. This is similar to those reported for **16**; both Ru–C_α and C_α–C_β are 1.786(3) Å and 1.318(4) Å respectively. In complex **15** these bonds are reported to be 1.794(9) Å for the Ru–C_α. In complex **11b** the Ru–C_α is similar to **15** (1.797(4) Å), whereas **12a** is only slightly longer at 1.801(9) Å, and its C_α–C_β bond 1.471(17) Å, does not adhere to the parameters set out by Bruce of 1.25-1.41 Å,⁴ **12a** is which is 0.06 Å longer than the limits proposed by Bruce; this is much larger than those reported for both **16** and **15** by 1.318(4) Å and 1.312(10) Å respectively.

5. Conclusions

5.1 Synthesis of precursors 2a-5a and 2b-5b.

The first objective of the project was to synthesise a series of novel ruthenium carboxylate complexes of the general type $[\text{Ru}(\kappa^2\text{-O}_2\text{C-R})_2(\text{PPh}_3)_2]$ and this has been achieved.

By using different substituted benzoic carboxylates a series of complexes of the general type $[\text{Ru}(\kappa^2\text{-O}_2\text{CC}_6\text{H}_4\text{-R})_2(\text{PPh}_3)_2]$ have been prepared. The incorporation of the phenyl group on the carboxylate ligand, meant that not only could the effect of having different substituents be studied, but the effects of incorporating the groups to different positions on the phenyl ring could be examined.

Through making these ruthenium complexes a synthetic method has been developed, by which to date any carboxylic acid group may be employed to synthesise a range of complexes of the general type $[\text{Ru}(\kappa^2\text{-O}_2\text{C-R})_2(\text{PPh}_3)_2]$. The method by which to achieve this was as follows;

- Reacting a sodium carboxylate with $[\text{RuCl}_2(\text{PPh}_3)]$ in ${}^t\text{BuOH}$ for 1 hour at $90\text{ }^\circ\text{C}$, to get the desired product;
- Creating a sodium carboxylate could be achieved reacting sodium with ${}^t\text{BuOH}$ at $90\text{ }^\circ\text{C}$ for 2 hours to make ${}^t\text{BuONa}$, then reacting this with a carboxylic acid for 10-30 minutes to create a sodium carboxylate.

From the numerous methods tried to develop this synthetic method we found that the sodium counter-ion was important as reactions using a different ion such as potassium rarely worked.

5.2 Synthesis of carbonyl complexes **7a-10a** and **7b-9b**

The next objective of the project was to investigate the chemistry of these novel ruthenium complexes, in order to determine if they exhibited the same chemistry as $[\text{Ru}(\kappa^2\text{-OAc})_2(\text{PPh}_3)_2]$ and $[\text{Ru}(\kappa^2\text{-O}_2\text{Ph})(\text{PPh}_3)_2]$ with regards to being able to form the complexes of the general type $[\text{Ru}(\kappa^1\text{-O}_2\text{CC}_6\text{H}_4\text{-R})(\kappa^2\text{-O}_2\text{CC}_6\text{H}_4\text{-R})(\text{CO})(\text{PPh}_3)_2]$. This was successfully achieved for all the complexes. This was an important observation, as not only did it show that these complexes exhibited the same chemistry as $[\text{Ru}(\kappa^2\text{-OAc})_2(\text{PPh}_3)_2]$ and $[\text{Ru}(\kappa^2\text{-O}_2\text{Ph})_2(\text{PPh}_3)_2]$, but by examining the stretching frequency of the carbonyl group in the IR spectra, the strength of the M-C bond could be determined and the effect of the R groups on the M-C back bonding interaction determined. The electron withdrawing groups such as in complex **7a** weaken the M-C bond and the electron donating groups strengthen the M-C bond. The Hammett plot of the $\Delta\nu \text{C}\equiv\text{O}$ against the Hammett constants (σ , σ^+) displayed a strong correlation indicating that these substituent groups had a strong effect on the stretching frequency of the carbonyl group.

As the substituents on the carboxylate ligands had the same effect in both the carbonyl and the vinylidene ruthenium complexes, the carbonyl complexes become of great interest due to the fact that judging the strength of π back bonding is far easier to observe than in the case of the vinylidene species. This is because the M-C stretching frequency in the IR spectrum for vinylidene ligands is weaker and thus difficult to obtain. The only way to accurately infer the strength of the back bonding is through measuring the M-C bond length from crystal structures whereas there in the carbonyl complexes this can be inferred from the $\Delta\nu \text{CO}$ stretching frequencies.

5.3 Synthesis of the vinylidene complexes 11a-14a and 11b-13b

It has also been shown that these complexes exhibit similar behaviour to $[\text{Ru}(\kappa^2\text{-OAc})_2(\text{PPh}_3)_2]$ and $[\text{Ru}(\kappa^2\text{-O}_2\text{Ph})_2(\text{PPh}_3)_2]$ in that one can form the vinylidene intermediate by reaction with phenyl acetylene. The Hammett plots of the sigma constants (σ , σ^+) against the chemical shift of the α carbon demonstrates that the various substituents had the same effect as observed with the $\text{C}\equiv\text{O}$ stretching frequencies. This was expected as the π back-bonding in both vinylidene and carbonyl complexes are similar.

If you compare the Hammett studies of the $\text{C}\equiv\text{O}$ stretching frequencies in the IR spectra for the carbonyl species and the chemical shift of the α carbon in the ^{13}C NMR spectra for the vinylidene species both show a strong correlation but the gradient of the Hammett plot for $\text{C}\equiv\text{O}$ stretching frequencies of the carbonyl species is steeper indicating that this is more sensitive to the change in the groups on the carboxylate than the chemical shift of the α carbon in the ^{13}C NMR spectra of the vinylidene species.

5.4 Further work

Although the R-substituted phenyl groups did not have a huge effect on the strength of the carbonyl/vinylidene back bonding, the substituted acetate ligands could be used to modulate the electronic effects on series of different types of compounds. By looking into changing the phosphine groups on compounds of the general type $[\text{Ru}(\kappa^2\text{-O}_2\text{CR})_2(\text{PR}_n)_2]$ that are being studied further by Lynam *et al*, in conjunction with changing the carboxylate group the electronic effects of these compounds can hopefully be further understood thus leading to compounds of this general type being able to be tuned to give a desired effect in a specific reactions whether that be to strengthen or weaken a M-C π back bonding interaction.

Also as the complexes of the general type $[\text{Ru}(\kappa^2\text{-O}_2\text{CC}_6\text{H}_4\text{-R})_2(\text{PPh}_3)_2]$ can be used to make vinylidenes then they should be capable of undergoing the reaction with propargyl alcohols, as shown by Christine Welby (from the Lynam group) for $[\text{Ru}(\kappa^2\text{-OAc})_2(\text{PPh}_3)_2]$,¹² and it would be of interest if they exhibit the same chemistry.

6 .Experimental

All experiments were carried out under an atmosphere of dinitrogen using standard Schlenk line and glove box techniques. CH₂Cl₂, pentane, hexane were purified with the aid of an Innovative Technologies anhydrous solvent engineering system. The ^tBuOH was degassed by purging with dinitrogen before use. The Et₂O and MeOH was AR grade and used without any further purification unless stated. The CD₂Cl₂ used for NMR was dried over CaH₂ and degassed with three freeze-pump-thaw cycles. The solvent was vacuum transferred into NMR tubes fitted with PTFE Young's taps. NMR spectra were acquired on a JEOL 400 ¹H 399.78 MHz, ¹³C 100.52 MHz, ¹⁹F 376.17 MHz and ³¹P 161.83 MHz spectrometer. Mass spectrometry measurements were performed on a Bruker micrOTOF (ESI) instrument or Waters GCT Premier MS (LIFDI). IR spectra were acquired on a Thermo-Nicolet Avatar 370 FTIR spectrometer either using CsCl solution cells or as KBr discs. RuCl₂(PPh₃)₃ was prepared by the literature method.⁷⁴ All chemicals used were obtained from Sigma Aldrich Chemicals and used as supplied except for *p*-RC₆H₄COOH (R = OMe, F, NMe₂) and HC≡CPh which were obtained from Acros Organics and used without any further purification.

6.1 Synthesis of $\text{RuCl}_2(\text{PPh}_3)_3$

This was prepared with slight alterations to the published literature method. One equivalent of $\text{RuCl}_3 \cdot (\text{H}_2\text{O})_3$ (5.00 g / 0.0215 mol) was added to a Schlenk vessel containing 200ml of degassed MeOH. This was then transferred to a round bottom flask (containing a further 800ml of degassed MeOH) via cannula transfer. To this was added 6 equivalents of PPh_3 (31.5 g / 0.12 mol). The mixture was refluxed with stirring for 3 hours; over the course of this time the mixture changed colour from a very dark brown to pitch black. After the 3 hours, the mixture was left to cool overnight (the product precipitated out as black crystals slowly on cooling). The next stage was to filter off all the MeOH, once this was done the black solid was washed with 3 x 200 ml portions of degassed Et_2O . The product was dried *in vacuo*. 17 g of product was obtained giving a yield of 82.4 %.

6.2 Synthesis and characterisation of 2a-5a and 2b-5b

6.2.1 General procedure for the synthesis of $\text{Ru}(\kappa_2\text{-O}_2\text{C}_6\text{H}_4\text{-R})_2(\text{PPh}_3)_2$ 2a-5a and 2b-5b

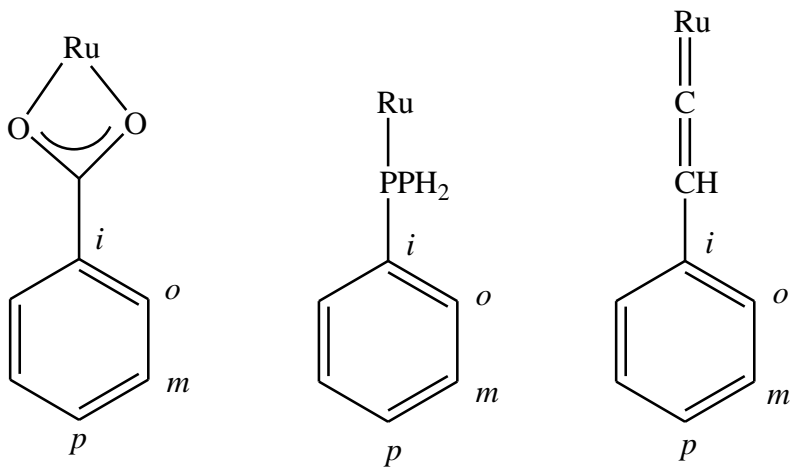
10 equivalents of Na (0.24g, 0.0104 mol) was added to a Schlenk vessel containing 75 ml of degassed $t\text{BuOH}$ (degassed with N_2 for 2 hours); the solution was heated at 90 °C for approximately 2 hours until all the Na had dissolved. To this, 10 equivalents of $\text{R-C}_6\text{H}_4\text{COOH}$ (0.0104 mol) were added and the mixture was stirred for 15 minutes. One equivalent of $\text{RuCl}_2(\text{PPh}_3)_3$ (1 g, 0.0010 mol) was added and the mixture was allowed to react for at least 1 hour with constant stirring and heating (90 °C), until the solution changed colour from grey to an orange/yellow. Whilst still warm, the resulting solution was filtered through a sintered funnel and washed with 80 ml of H_2O , 50 ml of MeOH,

50ml of Et₂O/pentane (unless stated in the individual procedures), and the resulting solid was dried *in vacuo*

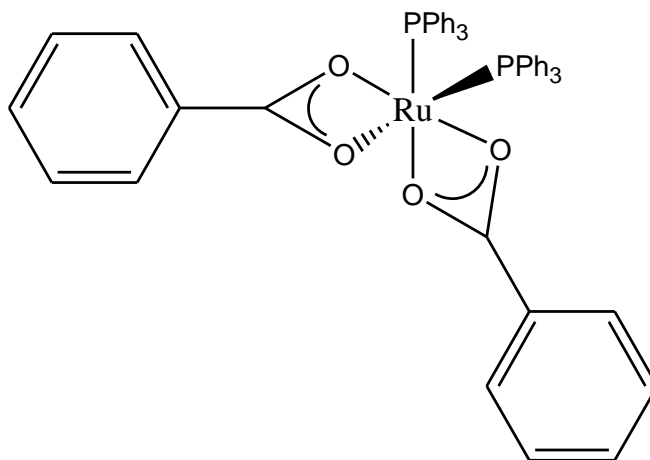
Key to NMR abbreviations:

s (singlet); br (broad singlet); d (doublet); dd (doublet of doublets); ad (apparent doublet);

t (triplet); dt (doublet of triplets); vt (virtual triplets); at (apparent triplet); m (multiplet)

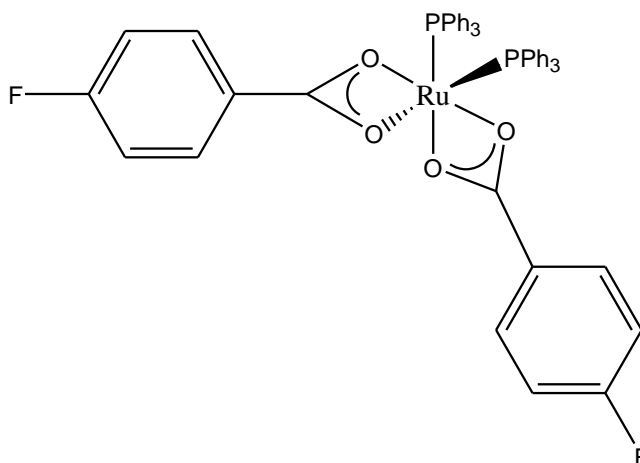


6.2.2 Synthesis of $[\text{Ru}(\kappa^2\text{-O}_2\text{CPh})_2(\text{PPh}_3)_2]$. 2



The synthesis of this was carried out according to the literature preparation reported for this compound.⁴² NaO_2CPh (0.45g, 0.0031 mol) was added to a Schlenk vessel containing 14 ml of degassed $^t\text{BuOH}$ (degassed with N_2 for 30 minutes); the solution was heated at 50 °C for approximately 30 minutes. To this, 10 equivalents of $\text{R-C}_6\text{H}_4\text{COOH}$ (0.0104 mol) were added and the mixture was stirred for 15 minutes. One equivalent of $\text{RuCl}_2(\text{PPh}_3)_3$ (0.3 g, 0.00031 mol) was added and the mixture was allowed to react for at least 1 hour with constant stirring and heating (90 °C), until the solution changed colour from grey to an orange/yellow. Whilst still warm, the resulting solution was filtered through a sintered funnel and washed with 10 ml of H_2O , 8 ml of MeOH , 4 ml of Et_2O /pentane (unless stated in the individual procedures), and the resulting solid was dried *in vacuo*.

6.2.3 Synthesis of $[\text{Ru}(\kappa^2\text{-O}_2\text{C}_6\text{H}_4\text{-4-F})_2(\text{PPh}_3)_2]$. 2a



The complex was synthesised according to the general procedure. As the reaction mixture was very viscous occasional stirring with a spatula was required in addition to the mixing provided by the stirrer bar. The reaction mixture changed colour from grey to orange/yellow on completion. The complex was washed with 80ml of water, 50ml of MeOH and 50ml of Et₂O. An orange solid was obtained. Crystals suitable for X-ray diffraction were obtained from a CH₂Cl₂/ n-pentane solution.

Yield = 0.80g (85%)

NMR Spectra (CD₂Cl₂):

¹H: 6.84 (at, ³J_{HH}, ³J_{HF} = 8.8 Hz, 4H, *m*-C₆H₄F), 7.01 (at, ³J_{HH}, ⁴J_{HP} = 7.5 Hz, 12H, *Ph*), 7.18-7.11(m, 18H, *Ph*), 7.60(dd, ³J_{HH} = 8.8Hz, ⁴J_{HF} = 5.66Hz, 4H, *o*-C₆H₄F) ppm.

³¹P {¹H}: 63.5 (s, *PPh*₃) ppm.

¹³C {¹H}: 114.4 (d, ²J_{CF} = 22.7 Hz, *m*-C₆H₄F), 127.5 (at, ³J_{PC} = 4.8 Hz, *m-PPh*₃), 128.5 (d, ⁴J_{CF} = 3.0 Hz, *i*-C₆H₄F), 129.2 (s, *p-PPh*), 130.5 (d, ³J_{CF} = 9.07 Hz, *o*-C₆H₄F), 134.2 (at, ²J_{PC} = 5.0 Hz, *o-PPh*), 134.8 (vt, ¹J_{PC} + ³J_{PC} = 45.3 Hz, *i-PPh*), 165.0 (d, ¹J_{CF} = 251 Hz *p*-C₆H₄F), 181.7 (s, CO₂C₆H₄F) ppm.

^{19}F $\{^1\text{H}\}$: -108.6 (s, *p*- $\text{FC}_6\text{H}_4\text{CO}_2$).

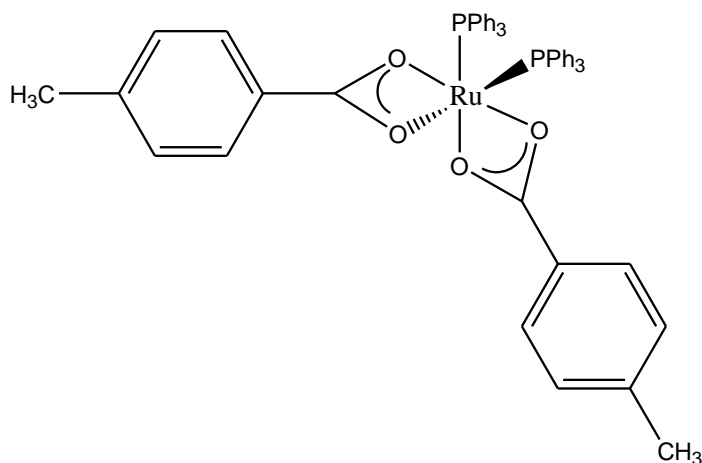
IR (KBr): 1427 cm^{-1} (κ^2 -OCOsym), 1482 cm^{-1} (P-Ph₃), 1495 cm^{-1} (κ^2 -OCOasym), $\Delta\nu$ (chelate) 68 cm^{-1} .

MS (ESI): 927.1140 m/z ($[\text{M}]^+\text{Na}$ expected for $\text{C}_{50}\text{H}_{38}\text{F}_2\text{NaO}_4\text{P}_2\text{Ru}$ 927.1155), 904.1247 m/z ($[\text{M}]^+$ expected for $\text{C}_{50}\text{H}_{38}\text{F}_2\text{NaO}_4\text{P}_2\text{Ru}$ 904.1257), 806.1302 m/z ($[\text{Ru}(\text{O}_2\text{CC}_6\text{H}_4\text{-4-F})(\text{PPh}_3)_2(\text{CNCH}_3)]^+$ expected for $\text{C}_{52}\text{H}_{41}\text{F}_2\text{NO}_4\text{P}_2\text{Ru}$ 806.1327), 765.1038 m/z ($[\text{Ru}(\text{O}_2\text{CC}_6\text{H}_4\text{-4-F})(\text{PPh}_3)_2]^+$ expected for $\text{C}_{43}\text{H}_{34}\text{FO}_2\text{P}_2\text{Ru}$ 765.1062).

Elemental Analysis for $\text{C}_{50}\text{H}_{38}\text{F}_2\text{NaO}_4\text{P}_2\text{Ru}$: (Calculated %) C 66.44, H 4.24; (Found %) C 66.12, H 4.252

Table 1: Crystal data and structure refinement for jml1126	
Identification code	jml1126
Empirical formula	C ₅₀ H ₃₈ F ₂ O ₄ P ₂ Ru
Formula weight	903.81
Temperature / K	110.0
Crystal system	triclinic
Space group	P-1
a / Å, b / Å, c / Å	10.9788(7), 12.8555(11), 16.3875(10)
α /°, β /°, γ /°	81.267(6), 72.065(5), 67.840(7)
Volume / Å ³	2036.3(2)
Z	2
ρ_{calc} / mg mm ⁻³	1.474
μ / mm ⁻¹	0.520 F(000) 924
Crystal size / mm ³	0.3619 × 0.1883 × 0.0682
2 Θ range for data collection	5.72 to 64.38°
Index ranges	-16 ≤ h ≤ 16, -19 ≤ k ≤ 19, -24 ≤ l ≤ 23
Reflections collected	48274
Independent reflections	13186[R(int) = 0.0324]
Data/restraints/parameters	13186/0/532
Goodness-of-fit on F ²	1.039
Final R indexes [I > 2 σ (I)]	R ₁ = 0.0287, wR ₂ = 0.0656
Final R indexes [all data]	R ₁ = 0.0340, wR ₂ = 0.0688
Largest diff. peak/hole / e Å ⁻³	0.560/-0.579

6.2.4 Synthesis of $[\text{Ru}(\kappa^2\text{-O}_2\text{C}_6\text{H}_4\text{-4-CH}_3)_2(\text{PPh}_3)_2]$. **3a**



The complex was synthesised according to the general procedure. The reaction mixture goes from a grey through to an orange/yellow colour on completion. The complex was washed with 80ml of water, 50ml of MeOH and 50ml of Et₂O. An orange solid was obtained.

Yield = 0.561g (60%)

NMR Spectra (CD₂Cl₂):

¹H: 2.23 (s, 6H, CO₂C₆H₄CH₃), 7.48 (ad, ³J_{HH} = 8.1Hz, 4H, *m*-C₆H₄CH₃), 7.04-6.95 (m, 16H, *PPh*+ *o*-C₆H₄CH₃), 7.18-7.11 (m, 18H, *PPh*) ppm.

³¹P{¹H}: 63.5 (s, *PPh*₃) ppm.

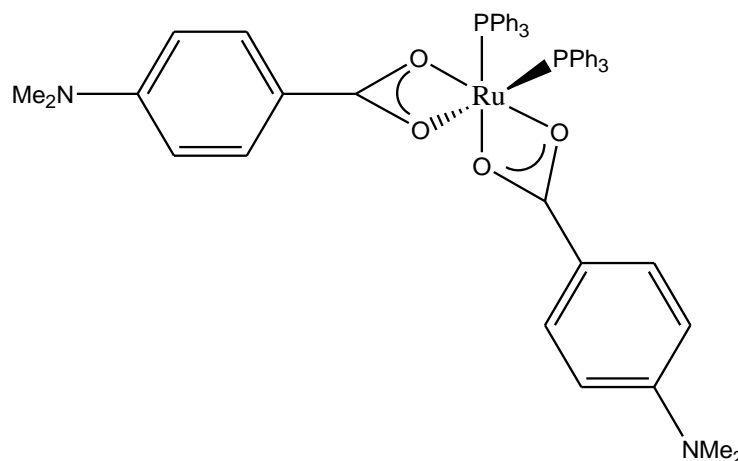
¹³C{¹H}: 21.3 (s, CO₂C₆H₄CH₃), 127.5 (at, ³J_{PC} + ⁵J_{PC} = 4.8 Hz, *m*-*PPh*₃), 128.1 (s, *i*-C₆H₄CH₃), 128.2 (s, *m*-C₆H₄CH₃), 129.1 (s, *p*-*PPh*), 129.7 (s, *o*-C₆H₄CH₃), 134.2 (at, ²J_{PC} + ⁴J_{PC} = 4.9 Hz, *o*-*PPh*), 134.9 (vt, ¹J_{PC} + ³J_{PC} = 44.8 Hz, *i*-*PPh*), 142 (s, *C*₄-C₆H₄CH₃), 183 (s, CO₂C₆H₄CH₃) ppm.

IR (KBr): 1423 cm^{-1} (κ^2 -OCOsym), 1480 cm^{-1} (P-Ph₃), 1505 cm^{-1} (κ^2 -OCOasym), $\Delta\nu$ (chelate) 82 cm^{-1} ; (CH₂Cl₂) 1424 cm^{-1} (κ^2 -OCOsym), 1481 cm^{-1} (P-Ph₃), 1505 cm^{-1} (κ^2 -OCOasym), $\Delta\nu$ (chelate) 83 cm^{-1} .

MS (ESI): 919.1665 m/z ([M]⁺Na expected for C₅₂H₄₄NaO₄P₂Ru 919.1656), 897.1840 m/z ([M]⁺H expected for C₅₂H₄₅O₄P₂Ru 897.1837), 802.1580 m/z ([Ru(O₂CC₆H₄-4-CH₃)(PPh₃)₂(CNCH₃)]⁺ expected for 802.1578), 761.1322 m/z ([Ru(O₂CC₆H₄-4-CH₃)(PPh₃)₂]⁺ expected for 761.1312).

Elemental Analysis for C₅₂H₄₄O₄P₂Ru: (Calculated %) C 69.71, H 4.95; (Found %) C 67.69, H 4.8.

6.2.5 Synthesis of [Ru(κ^2 -O₂CC₆H₄-4-NMe₂)₂(PPh₃)₂]. 4a



The complex was synthesised according to the general procedure. As the reaction mixture was very viscous so occasional stirring with a spatula was required in addition to the mixing provided by the stirrer bar. The reaction mixture goes from a grey solution through to an orange/yellow color on completion. The complex was washed with 70ml of water, 50ml of MeOH, 50ml of C₅H₁₂ and 25ml of Et₂O. A yellow/brown solid was obtained

Yield = 0.82g (83%)

NMR Spectra (CD₂Cl₂):

¹H: 2.88 (s, 12H, C₆H₄N(CH₃)₂), 6.42 (d, ³J_{HH} = 8.89Hz, 4H, *m*-C₆H₄N(CH₃)₂), 7.0 (at, ³J_{HH}, ³J_{HP} = 7.52 Hz 12H, *PPh*), 7.17-7.1(m, 18H, *PPh*), 7.48 (d, ³J_{HH} = 8.89Hz, 4H, *o*-C₆H₄N(CH₃)₂) ppm.

³¹P{¹H}: 63.63 (s, *PPh*₃) ppm.

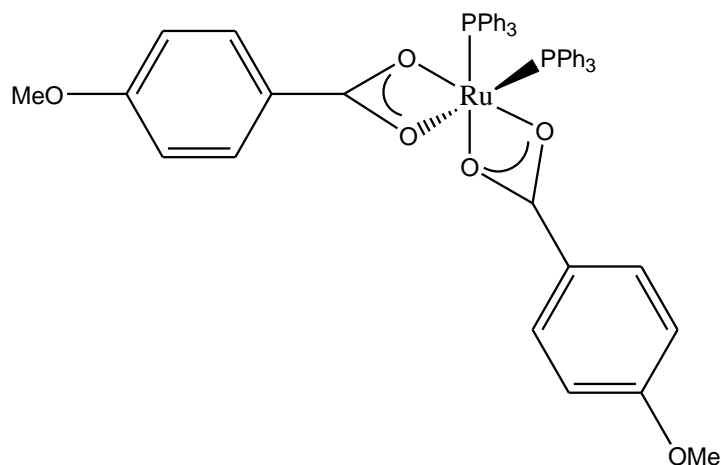
¹²C{¹H}: 39.9 (s, CO₂C₆H₄N(CH₃)₂), 110.1 (s, *m*-C₆H₄NMe₂), 120.2 (s, *p*-C₆H₄NMe₂), 127.3 (at, ³J_{PC} + ⁵J_{PC} = 4.79 Hz, *m*-*PPh*₃), 128.89 (s, *o*-C₆H₄NMe₂), 129.5 (s, *p*-*PPh*), 134.2 (at, ²J_{PC} + ⁴J_{PC} = 4.94 Hz, *o*-*PPh*), 135.48 (vt, ¹J_{PC} + ³J_{PC} = 43.66 Hz, *i*-*PPh*), 152.67 (s, *p*-C₆H₄NMe₂), 183.58 (s, CO₂C₆H₄NMe₂) ppm.

IR (KBr): 1414 cm⁻¹ (κ²-OCOsym), 1480 cm⁻¹ (P-Ph₃), 1539 cm⁻¹ (κ²-OCOasym), Δν (chelate) 189 cm⁻¹; (CH₂Cl₂) 1419 cm⁻¹ (κ²-OCOsym), 1481 cm⁻¹ (P-Ph₃), 1539 cm⁻¹ (κ²-OCOasym), Δν (chelate) 185 cm⁻¹.

MS (ESI): 955.23 *m/z* ([M]⁺), 831.18 *m/z* ([Ru(*p*-NMe₂C₆H₄CO₂)(PPh₃)₂(CNCH₃)]⁺), 790.15 *m/z* ([Ru(*p*-NMe₂C₆H₄CO₂)(PPh₃)₂]⁺).

Elemental Analysis: (Calculated %) C 67.91, H 5.28, N 2.94; (Found %) C 66.73, H 5.24, N 2.69

6.2.6 Synthesis of $[\text{Ru}(\kappa^2\text{-O}_2\text{C}_6\text{H}_4\text{-4-OMe})_2(\text{PPh}_3)_2]$. 5a



The complex was synthesised according to the general procedure. The reaction mixture goes from a grey solution through to an orange/brown colour on completion. The complex was washed with 100ml of water 100ml of MeOH and 75ml of pentane, 70ml Et₂O. An orange/brown solid was obtained.

Yield = 0.65g (67%)

NMR Spectra (CD₂Cl₂):

¹H: 3.79 (s, 6H, CO₂C₆H₄OCH₃), 6.75 (ad, ³J_{HH} = 8.7 Hz, 4H, *m*-C₆H₄OCH₃), 6.88-7.33 (m, 30H, *PPh*), 7.65 (ad, ³J_{HH} = 8.7 Hz, 4H, *o*-C₆H₄OCH₃) ppm.

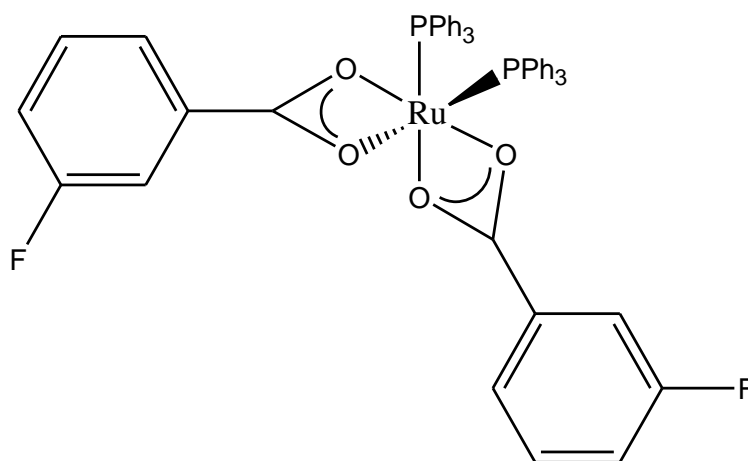
³¹P{¹H}: 63.6 (s, *PPh*₃) ppm.

¹³C{¹H}: 55.3 (s, O₂CC₆H₄OCH₃), 112.7 (s, *m*-C₆H₄OCH₃), 127.5 (at, ³J_{PC} + ⁵J_{PC} = 4.82 Hz *m*-*PPh*₃), 128.5 (s, *i*-C₆H₄OCH₃), 129.1 (s, *p*-*PPh*₃), 130 (s, *o*-C₆H₄OCH₃), 134.3 (at, ²J_{PC} + ⁴J_{PC} = 4.9 Hz, *o*-*PPh*₃), 135 (vt, ¹J_{PC} + ³J_{PC} = 44.6 Hz, *i*-*PPh*₃), 162.5 (s, *p*-C₆H₄OCH₃), 182.7 (s, CO₂C₆H₄OCH₃) ppm.

IR (KBr): 1422 cm^{-1} (κ^2 -OCOsym), 1480 cm^{-1} (P-Ph₃), 1506 cm^{-1} (κ^2 -OCOasym), $\Delta\nu$ (chelate) 84 cm^{-1} ; (CH₂Cl₂) 1424 cm^{-1} (κ^2 -OCOsym), 1481 cm^{-1} (P-Ph₃), 1506 cm^{-1} (κ^2 -OCOasym), $\Delta\nu$ (chelate) 82 cm^{-1} .

MS (ESI): 929.1763 m/z ([M]⁺H expected for C₅₂H₄₅O₆P₂Ru 929.1725), 818.1529 m/z ([Ru(O₂CC₆H₄-4-OMe)(PPh₃)₂(CNCH₃)]⁺ expected for C₄₆H₄₀NO₃P₂Ru 818.1527), 777.1265 m/z ([Ru(O₂CC₆H₄-4-OMe)(PPh₃)₂]⁺ expected for C₄₄H₃₇O₃P₂Ru 777.1261).

6.2.7 Synthesis of [Ru(κ^2 -O₂CC₆H₄-3-F)₂(PPh₃)₂]. 2b



The complex was synthesised according to the general procedure. The reaction mixture goes from a grey solution to a yellow solution, through to an orange colour on completion. The complex was washed with 100ml of water 50ml of MeOH and 75ml of Et₂O. An orange solid was obtained.

Yield = 0.44g (47%)

NMR Spectra (CD₂Cl₂):

¹H: 6.9-7.28 (m, 36H, PPh), 7.4 (d, ³J_{HF} = 7.14Hz, 2H, *o*(H₂)-C₆H₄F) ppm.

³¹P{¹H}: 63.4 (s, PPh₃) ppm.

$^{13}\text{C}\{^1\text{H}\}$: 114.7 (d, $^2J_{\text{CF}} = 22.34$ Hz, $p,o(\text{C}_2)\text{-C}_6\text{H}_4\text{F}$), 118.53 (d, $^3J_{\text{CF}} = 21.65$ Hz, $i,m(\text{C}_5)\text{-C}_6\text{H}_4\text{F}$), 123.8 (d, $^4J_{\text{CF}} = 2.4$ Hz, $o(\text{C}_6)\text{-C}_6\text{H}_4\text{F}$), 127.55 (at, $^3J_{\text{PC}} + ^5J_{\text{PC}} = 4.64$ Hz, $m\text{-PPh}$), 129.2 (s, $p\text{-PPh}$), 134.2 (at, $^2J_{\text{PC}} + ^4J_{\text{PC}} = 4.87$ Hz, $o\text{-PPh}$), 134.4 (vt, $^1J_{\text{PC}} + ^3J_{\text{PC}} = 45.37$ Hz, $i\text{-PPh}$), 162.14 (d, $^1J_{\text{CF}} = 245\text{Hz}$, $m(\text{C}_3)\text{-C}_6\text{H}_4\text{F}$), 181.38 (s, $\text{CO}_2\text{C}_6\text{H}_4\text{F}$) ppm.

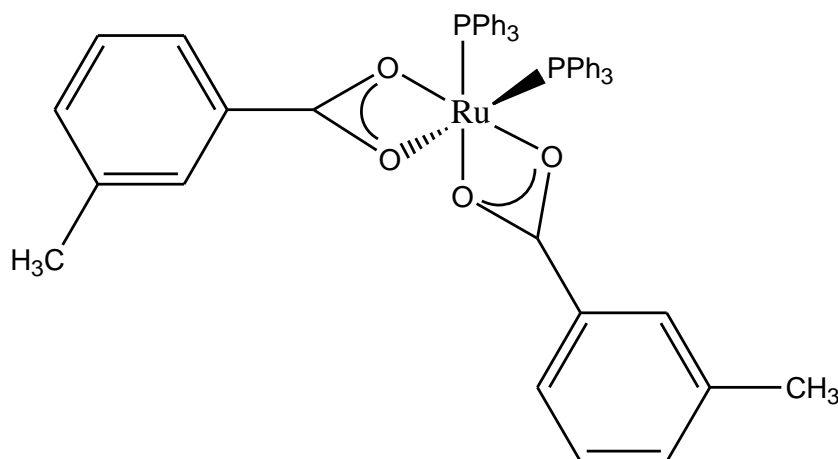
$^{19}\text{F}\{^1\text{H}\}$: -114.2 (s, $m\text{-FC}_6\text{H}_4\text{CO}_2$) ppm.

IR (KBr): 1414 cm^{-1} ($\kappa^2\text{-OCOsym}$), 1482 cm^{-1} (P-Ph₃), 1503 cm^{-1} ($\kappa^2\text{-OCOasym}$), $\Delta\nu$ (chelate) 189 cm^{-1} ; (CH₂Cl₂) 1419 cm^{-1} ($\kappa^2\text{-OCOsym}$), 1481 cm^{-1} (P-Ph₃), 1539 cm^{-1} ($\kappa^2\text{-OCOasym}$), $\Delta\nu$ (chelate) 185 cm^{-1} .

MS (ESI): 927.11 m/z ([M]Na⁺), 904.12 m/z ([M]⁺), 806.13 m/z ([Ru($m\text{-FC}_6\text{H}_4\text{CO}_2$)(PPh₃)₂(CNCH₃)]⁺), 765.1 m/z ([Ru($m\text{-FC}_6\text{H}_4\text{CO}_2$)(PPh₃)₂]⁺).

Elemental Analysis: (Calculated %) C 66.44, H 4.24; (Found %) C 66.07, H 4.24.

6.2.8 Synthesis of [Ru($\kappa^2\text{-O}_2\text{CC}_6\text{H}_4\text{-3-CH}_3$)₂(PPh₃)₂]. **3b**



The complex was synthesised according to the general procedure. The reaction mixture goes from a grey solution through to an orange/yellow on completion. The complex was washed with 80 ml of water 50 ml of MeOH and 50 ml of Et₂O. An orange solid was obtained.

Yield = 0.57 g (61%)

NMR Spectra (CD₂Cl₂):

¹H: 2.2 (s, 6H, CO₂C₆H₄CH₃), 7.38 (ad, ³J_{HH} = 9.41Hz, 4H, *m,o*(H₂)-C₆H₄CH₃), 7.07-6.98 (m, 14H, *PPh* + *p*-C₆H₄CH₃), 7.18-7.11(m, 20H, *PPh* + *o*(H₅)-C₆H₄CH₃) ppm.

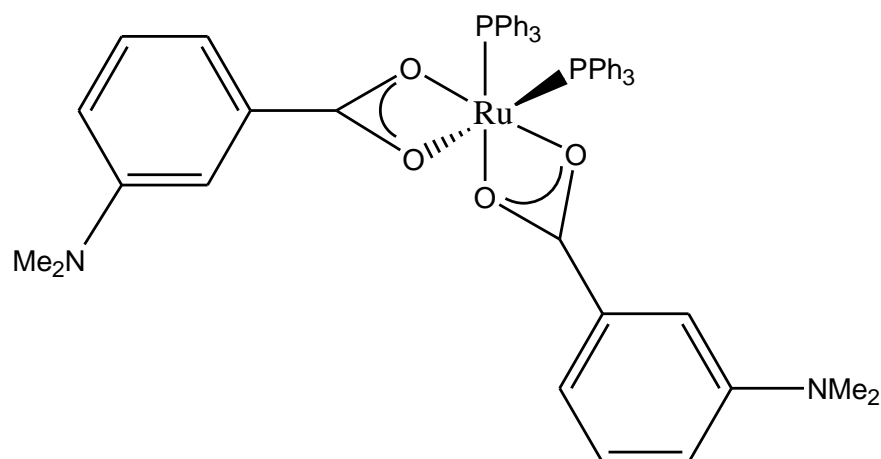
³¹P{¹H}: δ_p63.5 (s, *PPh*₃) ppm.

¹³C{¹H}: 20.9 (s, C₆H₄CH₃), 125.2 (s, *o*(C₆)-C₆H₄CH₃), 127.4 (s, *o*(C₂)-C₆H₄CH₃), 127.5 (at, ³J_{PC} + ⁵J_{PC} = 4.8 Hz *m-PPh*₃), 128.6 (s, *i*-C₆H₄CH₃), 129.1 (s, *p-PPh*), 132.2 (s, *m*(C₅)-C₆H₄CH₃), 132.3 (s, *p*-C₆H₄CH₃), 134.2 (at, ²J_{PC} + ⁴J_{PC} = 4.91 Hz, *o-PPh*), 134.9 (vt, ¹J_{PC} + ³J_{PC} = 44.74 Hz, *i-PPh*), 137.4 (s, *m*(C₃)-C₆H₄CH₃), 183.2 (s, CO₂C₆H₄CH₃) ppm.

IR (KBr): MS (ESI): 919 *m/z* ([M]Na⁺), 897.18 *m/z* ([M]⁺), 802.15 *m/z* ([Ru(*m*-CH₃C₆H₄CO₂)(PPh₃)₂(CNCH₃)]⁺), 761.13 *m/z* ([Ru(*m*-CH₃C₆H₄CO₂)(PPh₃)₂]⁺).

Elemental Analysis: (Calculated %) C 69.71, H 4.95; (Found %) C 69.43, H 5.017.

6.2.9 Synthesis of $[\text{Ru}(\kappa^2\text{-O}_2\text{CC}_6\text{H}_4\text{-3-NMe}_2)_2(\text{PPh}_3)_2]$. **4b**



The complex was synthesised according to the general procedure. The reaction was heated for 20 hours at 90°C instead of the usual 1 hour. The reaction mixture goes from a grey colour through to a yellow solution on completion. It was washed with 100ml of water, 100ml of MeOH, 75ml of C₅H₁₂ and 75ml of Et₂O. A yellow solid was obtained. 0.40 g was purified further *via* recrystallization of the complex in a DCM/C₅H₁₂ solution. The DCM/C₅H₁₂ filtrate was extracted by canular transfer to another Schlenk flask leaving a white precipitate behind. The filtrate was then removed in *vacuo* down to leave an orange solid, which was left under vacuum to dryness.

Yield = 0.26g (65%).

NMR Spectra (CD₂Cl₂):

¹H: 2.84 (s, 12H, C₆H₄N(CH₃)₂), 6.66 (d, ³J_{HH} = 8.88 Hz, 2H, *p*-C₆H₄NMe₂), 6.97-6.93 (m, 4H, *o*-C₆H₄CH₃), 7.02 (at, ³J_{HH}, ⁴J_{HP} = 7.52 Hz, 12H, PPh), 7.2-7.1 (m, 20H, PPh + *m*-C₆H₄NMe₂) ppm.

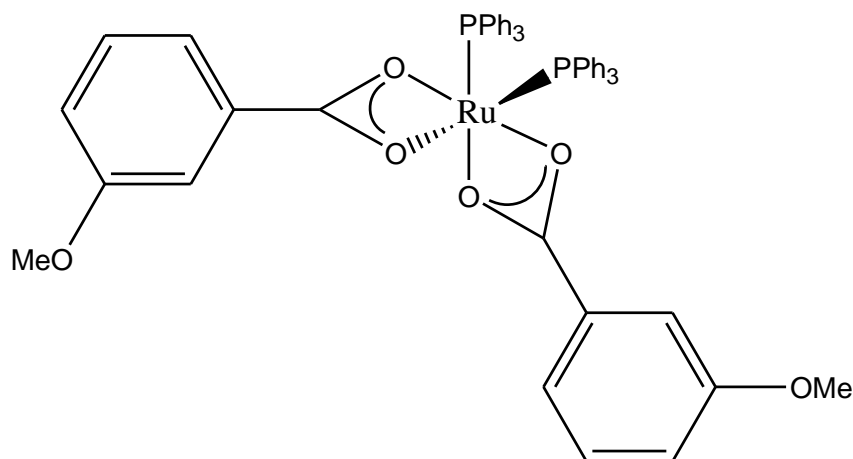
³¹P{¹H}: 63.3 (s, PPh₃) ppm.

$^{13}\text{C}\{^1\text{H}\}$: 39.6 (s, $\text{CO}_2\text{C}_6\text{H}_4\text{N}(\text{CH}_3)_2$), 111.2 (s, $o(\text{C}_2)\text{-C}_6\text{H}_4\text{NMe}_2$), 114.8 (s, $p\text{-C}_6\text{H}_4\text{NMe}_2$), 115.6 (s, $o(\text{C}_6)\text{-C}_6\text{H}_4\text{NMe}_2$), 126.6 (at, $^3J_{\text{PC}} + ^5J_{\text{PC}} = 4.76$ Hz $m\text{-PPh}_3$), 127.3 (s, $i\text{-C}_6\text{H}_4\text{NMe}_2$), 128.3 (s, $p\text{-PPh}$), 130.0 (s, $m(\text{C}_5)\text{-C}_6\text{H}_4\text{NMe}_2$), 133.5 (at, $^2J_{\text{PC}} + ^4J_{\text{PC}} = 4.90$ Hz, $o\text{-PPh}$), 134.16 (vt, $^1J_{\text{PC}} + ^3J_{\text{PC}} = 44.7$ Hz, $i\text{-PPh}$), 149.33 (s, $m(\text{C}_3)\text{-C}_6\text{H}_4\text{NMe}_2$), 182.84 (s, $\text{CO}_2\text{C}_6\text{H}_4\text{NMe}_2$) ppm.

IR (CH_2Cl_2): 1419 cm^{-1} ($\kappa^2\text{-OCOsym}$), 1482 cm^{-1} (P- Ph_3), 1508 cm^{-1} ($\kappa^2\text{-OCOasym}$), $\Delta\nu$ (chelate) 89 cm^{-1}

MS (ESI): 977.21 m/z ($[\text{M}]\text{Na}^+$), 955.23 m/z ($[\text{M}]^+$), 831.18 m/z ($[\text{Ru}(p\text{-NMe}_2\text{C}_6\text{H}_4\text{CO}_2)(\text{PPh}_3)_2(\text{CNCH}_3)]^+$), 790.15 m/z ($[\text{Ru}(p\text{-NMe}_2\text{C}_6\text{H}_4\text{CO}_2)(\text{PPh}_3)_2]^+$).

6.2.10 Synthesis of $[\text{Ru}(\kappa^2\text{-O}_2\text{CC}_6\text{H}_4\text{-3-OMe})_2(\text{PPh}_3)_2]$. **5b**



The complex was synthesised according to the general procedure. The reaction mixture goes from a grey solution through an orange/yellow colour on completion. The complex was washed with 80ml of water 80ml of MeOH and 50ml of C_6H_{12} . A yellow/brown solid was obtained.

Yield = 0.51g (53%)

NMR Spectra (CD₂Cl₂):

¹H: 7.40 (s, 6H, O₂CC₆H₄OCH₃), 7.00-7.23 (m, 38H, *PPh*) ppm.

³¹P{¹H}: 63.3 (s, *PPh*₃) ppm.

¹³C{¹H}: 55.3 (s, O₂CC₆H₄OCH₃), 112.4 (s, *o*(C₂)-C₆H₄OCH₃), 118.2 (s, *p*-C₆H₄OCH₃), 120.6 (s, *o*(C₆)-C₆H₄OCH₃), 127.5 (at, ³J_{PC} + ⁵J_{PC} = 4.8 Hz *m-PPh*₃), 128.6 (s, *i*-C₆H₄OCH₃), 129.2 (s, *p-PPh*), 133.5 (s, *m*(C₅)-C₆H₄OCH₃), 134.3 (at, ²J_{PC} + ⁴J_{PC} = 4.7 Hz, *o-PPh*), 134.7 (vt, ¹J_{PC} + ³J_{PC} = 44.8 Hz, *i-PPh*), 159.0 (s, *m*(C₃)-C₆H₄OCH₃), 182.6 (s, CO₂C₆H₄OCH₃).

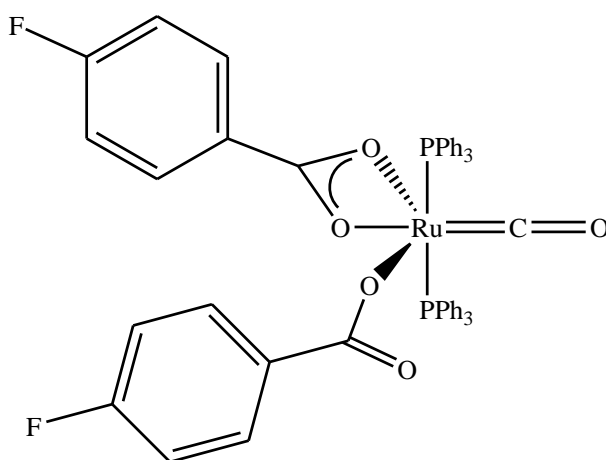
MS (ESI): 951.15 *m/z* ([M]Na⁺), 929.17 *m/z* ([M]), 818.15 *m/z* ([Ru(*m*-OMeC₆H₄CO₂)(PPh₃)₂(CNCH₃)]⁺), 777.12 *m/z* ([Ru(*m*-OMeC₆H₄CO₂)(PPh₃)₂]⁺).

6.3 Synthesis and characterisation of 7a-10a and 7b-9b

6.3.1 General procedure for the synthesis of $[\text{Ru}(\kappa^2\text{-O}_2\text{CC}_6\text{H}_4\text{-R})(\kappa^1\text{-O}_2\text{CC}_6\text{H}_4\text{-R})(\text{CO})(\text{PPh}_3)_2]$ 7a-10a and 7b-9b.

0.1g of $\text{Ru}(\kappa_2 \text{ R-C}_6\text{H}_4\text{CO}_2)_2(\text{PPh}_3)_2$ was added to a Schlenk vessel containing approximately 14ml of dichloromethane. This was then reacted with gaseous carbon monoxide (length of time stated for each complex in singular procedures). After the elapsed time the carbon monoxide was removed *in vacuo* out of the Schlenk vessel and replaced with N_2 and the DCM was removed *in vacuo* to leave the product; they were purified with a C_5H_{12} wash. If further purification was needed then the product was washed with 10 ml MeOH and 10 ml Et_2O . After filtration, the solid powder was dried *in vacuo*.

6.3.2 Synthesis of $[\text{Ru}(\kappa^2\text{-O}_2\text{CC}_6\text{H}_4\text{-4-F})(\kappa^1\text{-O}_2\text{CC}_6\text{H}_4\text{-4-F})(\text{CO})(\text{PPh}_3)_2]$. 7a



The complex was synthesised according to the general procedure. 100 mg of **2a** was reacted with carbon monoxide for approximately 5 minutes until the solution went from an orange colour through to a yellow solution.

NMR Spectra (CD₂Cl₂):

¹H: 6.67 (at, ³J_{HH}, ³J_{HF} = 9.3 Hz, 4H, *m*-C₆H₄F), 7.17 (m, 4H, *o*-C₆H₄F), 7.24 (m, 18H, *PPh*), 7.51 (m, 12H, *PPh*) ppm.

³¹P{¹H}: 39.1 (s, *PPh*) ppm.

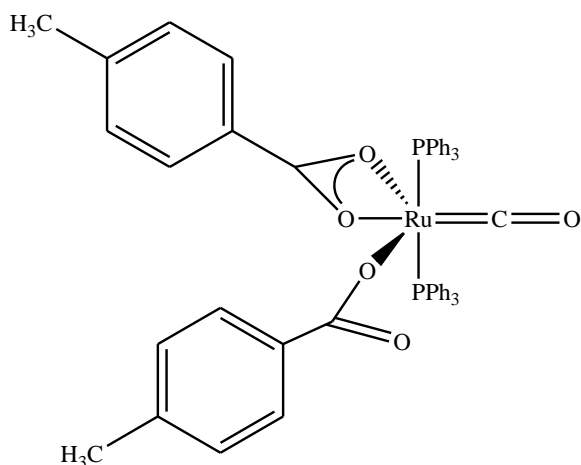
¹³C{¹H}: 113.5 (d, ²J_{CF} = 21.6 Hz, *m*-C₆H₄F), 128.2 (at, ³J_{PC} = 4.6 Hz, *m-PPh*), 129.7 (vt, ¹J_{PC} + ³J_{PC} = 21.9 Hz, *i-PPh*), 130.2 (s, *p-PPh*), 130.5 (d, ³J_{CF} = 8.8 Hz, *o*-C₆H₄F), 134.2 (at, ²J_{PC} = 4.9 Hz, *o-PPh*), 164.3 (d, ¹J_{CF} = 248.6 Hz, *p*-C₆H₄F), 175.2 (s, CO₂C₆H₄F), 206.8 (²J_{PC} = 12.6 Hz, CO) ppm.

¹⁹F {¹H}: -110.6 (s, *p*-FC₆H₄CO₂).

IR (KBr): 1434 cm⁻¹ (κ²-OCOsym), 1482 cm⁻¹ (P-Ph₃), 1502 cm⁻¹ (κ²-OCOasym), Δν (chelate) 68 cm⁻¹, 1347 cm⁻¹ (κ¹-OCOsym), 1625 cm⁻¹ (κ¹-OCOasym), Δν (unidentate) 278 cm⁻¹, 1948 cm⁻¹ (CO)

MS (ESI): 834.12 *m/z* ([Ru(*p*-FC₆H₄CO₂)(PPh₃)₂(CO)(CNCH₃)]⁺), 793.10 *m/z* ([Ru(*p*-FC₆H₄CO₂)(CO)(PPh₃)₂]⁺).

6.3.3 Synthesis of $[\text{Ru}(\kappa^2\text{-O}_2\text{CC}_6\text{H}_4\text{-4-CH}_3)(\kappa^1\text{-O}_2\text{CC}_6\text{H}_4\text{-4-CH}_3)(\text{CO})(\text{PPh}_3)_2]$. **8a**



The complex was synthesised according to the general procedure. 50 mg of **3a** was reacted with the carbon monoxide for approximately 5 minutes until the solution went from an orange colour through to a yellow solution.

NMR Spectra (CD_2Cl_2):

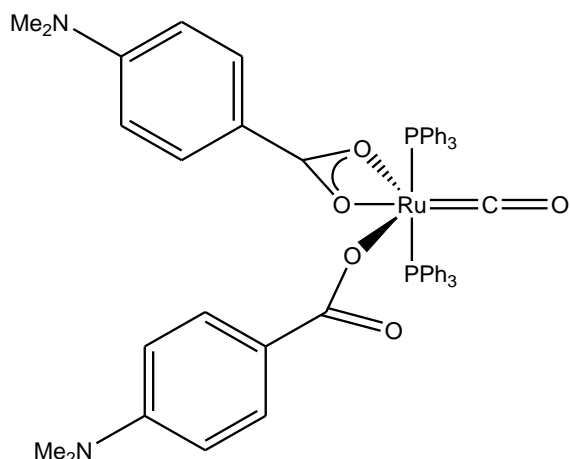
^1H : 2.23 (s, 6H, $\text{C}_6\text{H}_4\text{CH}_3$), 6.81 (d, 8.06 Hz, $^3J_{\text{HH}}$, 4H, $m\text{-C}_6\text{H}_4$), 7.06 (d, 8.06 Hz, $^3J_{\text{HH}}$, 4H, $o\text{-C}_6\text{H}_4$), 7.25 (m, 18H, PPh), 7.53 (m, 12H, PPh) ppm.

$^{31}\text{P}\{^1\text{H}\}$: 38.5 (s, PPh) ppm.

$^{13}\text{C}\{^1\text{H}\}$: 21.25 (s, $\text{CO}_2\text{C}_6\text{H}_4\text{CH}_3$), 127.4 (s, $p\text{-PPh}$), 128.15 (at, $^3J_{\text{PC}} + ^5J_{\text{PC}} = 4.79$ Hz $m\text{-PPh}_3$), 128.2 (s, $m\text{-C}_6\text{H}_4\text{CH}_3$), 129.7 (s, $o\text{-C}_6\text{H}_4\text{CH}_3$), 130.0 (vt, $^1J_{\text{PC}} + ^3J_{\text{PC}} = 43.9$ Hz, $i\text{-PPh}$), 132.6 (s, $i\text{-C}_6\text{H}_4\text{CH}_3$), 134.7 (at, $^2J_{\text{PC}} + ^4J_{\text{PC}} = 5.90$ Hz, $o\text{-PPh}$), 140.6 (s, $p\text{-C}_6\text{H}_4\text{CH}_3$), 174.5 (s, $\text{CO}_2\text{C}_6\text{H}_4\text{CH}_3$), 207.4 (t, $^2J_{\text{CP}} = 13.5$ Hz, CO) ppm.

IR (KBr): 1429 cm^{-1} ($\kappa^2\text{-OCOsym}$), 1482 cm^{-1} (P-Ph_3), 1504 cm^{-1} ($\kappa^2\text{-OCOasym}$), $\Delta\nu$ (chelate) 75 cm^{-1} , 1350 cm^{-1} ($\kappa^1\text{-OCOsym}$), 1587 cm^{-1} ($\kappa^1\text{-OCOasym}$), $\Delta\nu$ (unidentate) 237 cm^{-1} , 1946 cm^{-1} (CO).

6.3.4 Synthesis of $[\text{Ru}(\kappa^2\text{-O}_2\text{CC}_6\text{H}_4\text{-4-NMe}_2)(\kappa^1\text{-O}_2\text{CC}_6\text{H}_4\text{-4-NMe}_2)(\text{CO})(\text{PPh}_3)_2]$. **9a**



The complex was synthesised according to the general procedure. 35 mg of **4a** was reacted with carbon monoxide for approximately 2 minutes until the solution went from a dark orange colour through to a yellow solution.

NMR Spectra (CD_2Cl_2):

^1H : 2.8 (s, 12H, $\text{C}_6\text{H}_4\text{N}(\text{CH}_3)_2$), 6.19 (d, 8.83 Hz, $^3J_{\text{HH}}$, 4H, *m*- C_6H_4), 6.90 (d, 8.94 Hz, $^3J_{\text{HH}}$, 4H, *o*- C_6H_4), 7.17 (m, 18H, *PPh*), 7.46 (m, 12H, *PPh*) ppm.

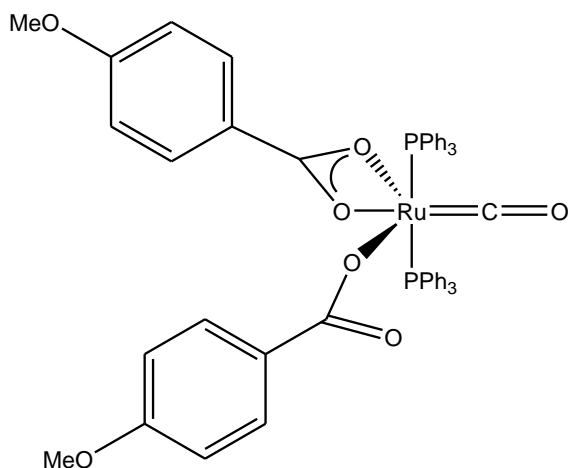
$^{31}\text{P}\{^1\text{H}\}$: 37.8 (s, *PPh*) ppm.

$^{13}\text{C}\{^1\text{H}\}$: 40.5 (s, $\text{CO}_2\text{C}_6\text{H}_4\text{N}(\text{CH}_3)_2$), 110.11 (s, *m*- $\text{C}_6\text{H}_4\text{NMe}_2$), 122.1 (s, *i*- $\text{C}_6\text{H}_4\text{NMe}_2$), 128.4 (at, $^3J_{\text{PC}} + ^5J_{\text{PC}} = 4.97$ Hz *m*-*PPh*), 130.1 (s, *o*- $\text{C}_6\text{H}_4\text{NMe}_2$), 130.4 (s, *p*-*PPh*), 130.9 (vt, $^1J_{\text{PC}} + ^3J_{\text{PC}} = 43.41$ Hz, *i*-*PPh*), 135.18 (at, $^2J_{\text{PC}} + ^4J_{\text{PC}} = 6.0$ Hz, *o*-*PPh*), 152.3 (s, *p*- $\text{C}_6\text{H}_4\text{NMe}_2$), 177.2 (s, $\text{CO}_2\text{C}_6\text{H}_4\text{NMe}_2$), 208.2 (t, $^2J_{\text{CP}} = 14.3$ Hz, CO) ppm.

IR (CD_2Cl_2): 1428 cm^{-1} (κ^2 -OCOsym), 1482 cm^{-1} (P-Ph₃), 1519 cm^{-1} (κ^2 -OCOasym), $\Delta\nu$ (chelate) 91 cm^{-1} , 1343 cm^{-1} (κ^1 -OCOsym), 1570 cm^{-1} (κ^1 -OCOasym), $\Delta\nu$ (unidentate) 227 cm^{-1} , 1942 cm^{-1} (CO)

MS (ESI): 983.23([M]H⁺), 859.17 *m/z* ([Ru(*p*-NMe₂C₆H₄CO₂)(PPh₃)₂(CO)(CNCH₃)]⁺), 818.15 *m/z* ([Ru(*p*-NMe₂C₆H₄CO₂)(CO)(PPh₃)₂]⁺).

6.3.5 Synthesis of [Ru(κ²-O₂CC₆H₄-4-OMe)(κ¹-O₂CC₆H₄-4-OMe)(CO)(PPh₃)₂]. 10a



The complex was synthesised according to the general procedure. 100mg of **5a** was reacted with carbon monoxide for approximately 3-4 minutes until the solution went from a dark orange colour through to a light orange solution

NMR Spectra (CD₂Cl₂):

¹H: 3.79 (s, 6H, CO₂C₆H₄OCH₃), 6.75 (ad, ³J_{HH} = 8.7 Hz, 4H, *m*-C₆H₄OCH₃), 6.88-7.33 (m, 30H, *PPh*), 7.65 (ad, ³J_{HH} = 8.7 Hz, 4H, *o*-C₆H₄OCH₃) ppm.

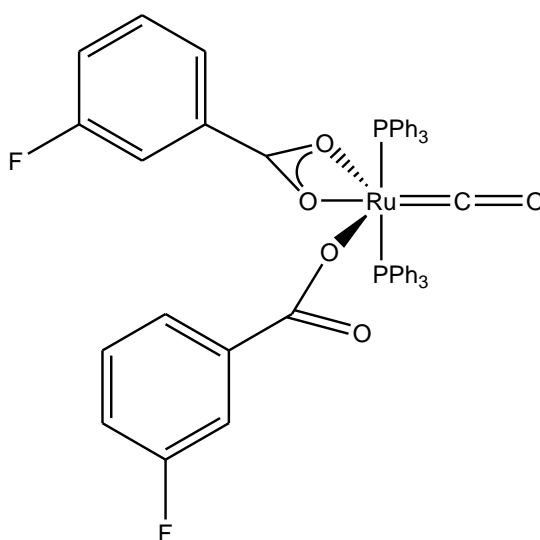
³¹P{¹H } : 38.6 (s, *PPh*) ppm.

¹³C{¹H } : 55.51 (s, O₂CC₆H₄OCH₃), 112.1 (s, *m*-C₆H₄OCH₃), 126.2 (s, *i*-C₆H₄OCH₃), 127.8 (at, ³J_{PC} + ⁵J_{PC} = 4.6 Hz *m*-*PPh*), 129.1 (s, *p*-*PPh*), 131.1 (s, *o*-C₆H₄OCH₃), 134.3 (at, ²J_{PC} + ⁴J_{PC} = 4.9 Hz, *o*-*PPh*), 135.4 (vt, ¹J_{PC} + ³J_{PC} = 45.0 Hz, *i*-*PPh*), 161.7 (s, *p*-C₆H₄OCH₃), 176.4 (s, CO₂C₆H₄OCH₃), 207.9 (t, ²J_{PC} = 14.5 Hz, CO) ppm.

IR (KBr): 1424 cm^{-1} (κ^2 -OCOSym), 1482 cm^{-1} (P-Ph₃), 1506 cm^{-1} (κ^2 -OCOasym), $\Delta\nu$ (chelate) 82 cm^{-1} , 1349 cm^{-1} (κ^1 -OCOSym), 1589 cm^{-1} (κ^1 -OCOasym), $\Delta\nu$ (unidentate) 240 cm^{-1} , 1945 cm^{-1} (CO)

MS (ESI): 846.1473 m/z ([Ru(O₂CC₆H₄-4-OMe)(PPh₃)₂(CO)(CNCH₃)]⁺), 805.1204 m/z ([Ru(O₂CC₆H₄-4-OMe)(PPh₃)₂(CO)]⁺).

6.3.6 Synthesis of [Ru(κ^2 -O₂CC₆H₄-3-F)(κ^1 -O₂CC₆H₄-3-F)(CO)(PPh₃)₂]. **7b**



The complex was synthesised according to the general procedure. 100 mg of **2b** was reacted with carbon monoxide for approximately 3 minutes until the solution went from an orange colour through to a yellow solution.

NMR Spectra (CD₂Cl₂):

¹H: 6.90-7.28(m, 36H, *PPh*), 7.40 (d, ³J_{HF} = 7.14 Hz, 2H, *o*(H₂)-C₆H₄F) ppm.

³¹P{¹H}: 39.15 (s, *PPh*₃) ppm.

¹³C{¹H}: 114.7 (d, ²J_{CF} = 22.17 Hz, *p,o*(C₂)-C₆H₄F), 118.5 (d, ³J_{CF} = 21.6 Hz, *i,m*(C₅)-C₆H₄F), 123.8 (d, ⁴J_{CF} = 2.4 Hz, *o*(C₆)-C₆H₄F), 127.6 (at, ³J_{PC} + ⁵J_{PC} = 4.64 Hz, *m-PPh*), 129.2 (s, *p-PPh*), 134.2 (at, ²J_{PC} + ⁴J_{PC} = 4.87 Hz, *o-PPh*), 134.4 (vt, ¹J_{PC} + ³J_{PC} = 45.37

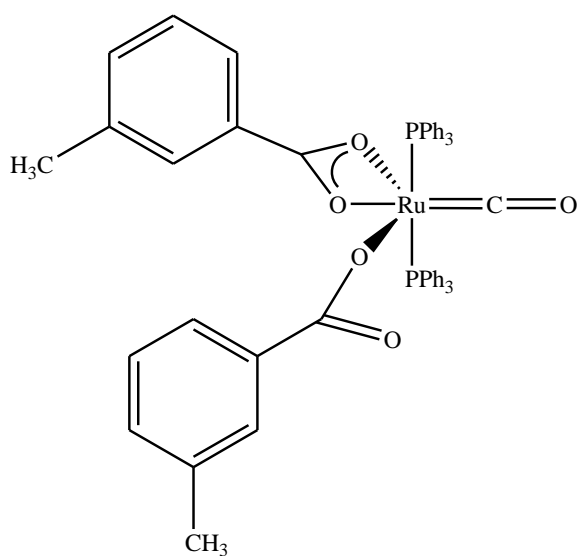
Hz, *i*-PPh), 162.14 (d, $^1J_{CF} = 245$ Hz, $m(C_3)$ -C₆H₄F), 181.38 (s, CO₂C₆H₄F), 206.9 (t, $^2J_{CP} = 13.9$ Hz, CO) ppm.

^{19}F { ^1H }: -114.2 (s, *m*-FC₆H₄CO₂) ppm.

IR (CD₂Cl₂): 1436 cm⁻¹ (κ^2 -OCOsym), 1482 cm⁻¹ (P-Ph₃), 1507cm⁻¹ (κ^2 -OCOasym), $\Delta\nu$ (chelate) 71 cm⁻¹, 1348 cm⁻¹ (κ^1 -OCOsym), 1584 cm⁻¹ (κ^1 -OCOasym), $\Delta\nu$ (unidentate) 236 cm⁻¹, 1950 cm⁻¹ (CO).

MS (ESI): 834.13 *m/z* ([Ru(*p*-NMe₂C₆H₄CO₂)(PPh₃)₂(CO)(CNCH₃)]⁺), 793.10 *m/z* ([Ru(*p*-NMe₂C₆H₄CO₂)(CO)(PPh₃)₂]⁺).

6.3.7 Synthesis of [Ru(κ^2 -O₂CC₆H₄-3-CH₃)(κ^1 -O₂CC₆H₄-3-CH₃)(CO)(PPh₃)₂]. **8b**



The complex was synthesised according to the general procedure. 100 mg of **3b** was reacted with carbon monoxide for approximately 3 minutes until the solution went from an orange colour through to a yellow solution.

NMR Spectra (CD₂Cl₂):

¹H: 2.16 (s, 6H, CO₂C₆H₄CH₃), 6.84-6.97 (m, 8H, C₆H₄CH₃), 7.10-7.30 (m, 18H, PPh), 7.51 (m, 12H, PPh) ppm.

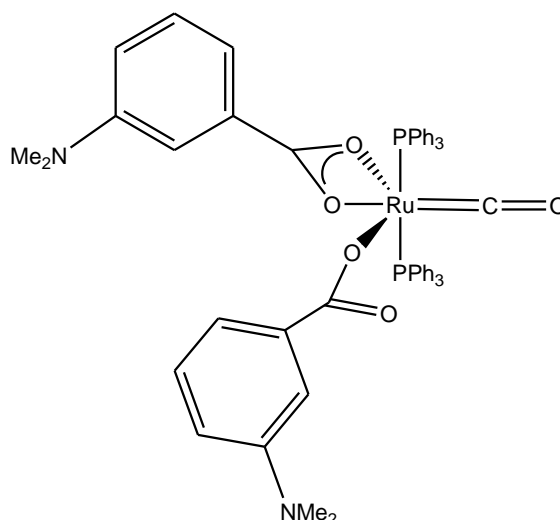
³¹P{¹H}: 38.7 (s, PPh) ppm.

¹³C{¹H}: 21.4 (s, C₆H₄CH₃), 125.7 (s, *o*(C₆)-C₆H₄CH₃), 127.0 (s, *o*(C₂)-C₆H₄CH₃), 128.5 (at, ³J_{PC} + ⁵J_{PC} = 4.9 Hz *m*-PPh₃), 129.2 (s, *i*-C₆H₄CH₃), 130.4 (vt, ¹J_{PC} + ³J_{PC} = 44.7 Hz, *i*-PPh), 130.5 (s, *m*-PPh), 131.4 (s, *m*(C₅)-C₆H₄CH₃), 133.9 (s, *p*-C₆H₄CH₃), 135.2 (at, ²J_{PC} + ⁴J_{PC} = 5.9 Hz, *o*-PPh), 136.7 (s, *m*(C₃)-C₆H₄CH₃), 177.1 (s, CO₂C₆H₄CH₃), 207.8 (t, ²J_{PC} = 14.7 Hz, (CO) ppm.

IR (CH₂Cl₂): 1436 cm⁻¹ (κ²-OCOsym), 1482 cm⁻¹ (P-Ph₃), 1506 cm⁻¹ (κ²-OCOasym), Δν (chelate) 70 cm⁻¹, 1343 cm⁻¹ (κ¹-OCOsym), 1575 cm⁻¹ (κ¹-OCOasym), Δν (unidentate) 232 cm⁻¹, 1947 cm⁻¹ (CO).

MS (ESI): 925.18 *m/z* ([M]H⁺), 830.15 *m/z* ([Ru(*m*-CH₃C₆H₄CO₂)(PPh₃)₂(CNCH₃)]⁺), 789.12 *m/z* ([Ru(*m*-CH₃C₆H₄CO₂)(CO)(PPh₃)₂]⁺).

6.3.8 Synthesis of $[\text{Ru}(\kappa^2\text{-O}_2\text{CC}_6\text{H}_4\text{-3-NMe}_2)(\kappa^1\text{-O}_2\text{CC}_6\text{H}_4\text{-3-NMe}_2)(\text{CO})(\text{PPh}_3)_2]$. **9b**



The complex was synthesised according to the general procedure. 35 mg of **4b** was reacted with carbon monoxide for approximately 2 minutes until the solution went from a dark orange colour through to a yellow solution.

NMR Spectra (CD_2Cl_2):

^1H : 2.82 (s, 12H, $\text{C}_6\text{H}_4\text{N}\{\text{CH}_3\}_2$), 5.88-6.49 (m, 6H, $\text{C}_6\text{H}_4\text{CH}_3$), 6.85 (at, $^3J_{\text{HH}} = 7.82$ Hz, 2H, *m*(H_5)- $\text{C}_6\text{H}_4\text{NMe}_2$), 7.31-7.24 (m, 18H, *PPh*), 7.52-7.58 (m, 12H, *PPh*) ppm.

$^{31}\text{P}\{^1\text{H}\}$: 38.8 (s, *PPh*) ppm.

$^{13}\text{C}\{^1\text{H}\}$: 40.6 (s, $\text{CO}_2\text{C}_6\text{H}_4\text{N}\{\text{CH}_3\}_2$), 112.6 (s, *o*(C_2)- $\text{C}_6\text{H}_4\text{NMe}_2$), 114.7 (s, *p*- $\text{C}_6\text{H}_4\text{NMe}_2$), 116.9 (s, *o*(C_6)- $\text{C}_6\text{H}_4\text{NMe}_2$), 127.6 (s, *i*- $\text{C}_6\text{H}_4\text{NMe}_2$), 128.2 (at, $^3J_{\text{PC}} + ^5J_{\text{PC}} = 5.02$ Hz *m*-*PPh*), 129.2 (s, *p*-*PPh*), 130.2 (s, *m*(C_5)- $\text{C}_6\text{H}_4\text{NMe}_2$), 130.3 (vt, $^1J_{\text{PC}} + ^3J_{\text{PC}} = 43.7$ Hz, *i*-*PPh*), 134.7 (at, $^2J_{\text{PC}} + ^4J_{\text{PC}} = 4.90$ Hz, *o*-*PPh*), 149.7 (s, *m*(C_3)- $\text{C}_6\text{H}_4\text{NMe}_2$), 177.2 (s, $\text{CO}_2\text{C}_6\text{H}_4\text{NMe}_2$), 207.4 (t, $^3J_{\text{CP}} = 14.4$ Hz, *CO*) ppm.

IR (CH₂Cl₂): 1436 cm⁻¹ (κ^2 -OCOSym), 1482 cm⁻¹ (P-Ph₃), 1507 cm⁻¹ (κ^2 -OCOasym), $\Delta\nu$ (chelate) 71 cm⁻¹, 1351 cm⁻¹ (κ^1 -OCOSym), 1559 cm⁻¹ (κ^1 -OCOasym), $\Delta\nu$ (unidentate) 208 cm⁻¹, 1945 cm⁻¹ (CO).

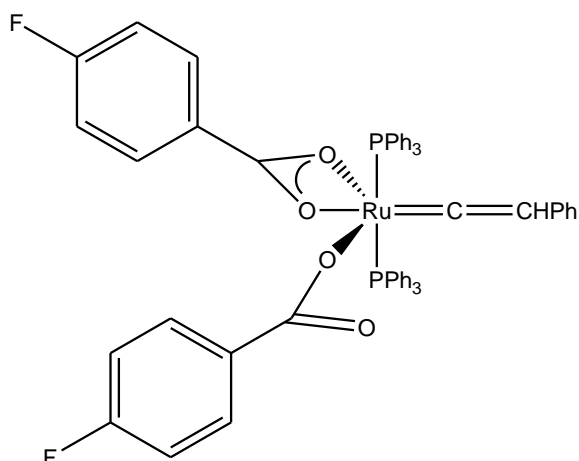
MS (ESI): 859.1787 *m/z* ([Ru(O₂CC₆H₄-3-NMe₂)(PPh₃)₂(CO)(CNCH₃)]⁺), 818.1518 *m/z* ([Ru(O₂CC₆H₄-3-NMe₂)(PPh₃)₂(CO)]⁺).

6.4 Synthesis and characterisation of 11a-14a and 11b-13b

6.4.1 General procedure for the synthesis of $[\text{Ru}(\kappa^2\text{-O}_2\text{CC}_6\text{H}_4\text{-R})(\kappa^1\text{-O}_2\text{CC}_6\text{H}_4\text{-R})(=\text{C}=\text{HPh})(\text{PPh}_3)_2]$ 11a-14a and 11b-13b

0.2 g of $[\text{Ru}(\kappa^2\text{-R-C}_6\text{H}_4\text{CO}_2)_2(\text{PPh}_3)_2]$ was added to a Schlenk vessel containing approximately 40 ml of CH_2Cl_2 . Approximately 1 equivalent of phenylacetylene was added to the solution. After stirring for 1 hour most of the DCM was removed by *vacuo* and the product was precipitated out by the addition of pentane. After filtration, the solid powder was washed two times with pentane and dried *in vacuo*

6.4.2 Synthesis of $[\text{Ru}(\kappa^2\text{-O}_2\text{CC}_6\text{H}_4\text{-4-F})(\kappa^1\text{-O}_2\text{CC}_6\text{H}_4\text{-4-F})(=\text{C}=\text{HPh})(\text{PPh}_3)_2]$. 11a



The complex was synthesised according to the general procedure. 50 ml of pentane was used to precipitate out the product and it was washed further with 2 x 30 ml of water and pentane.

0.16g (73%) of pink/orange solid was obtained.

NMR Spectra (CD_2Cl_2):

^1H : 5.2 (t, 3.76 Hz, $^4J_{\text{HH}}$, 1H, $=\text{C}=\text{CHPh}$), 6.65 (at, $^3J_{\text{HH}}$, $^3J_{\text{HF}} = 8.79$ Hz, 4H, *m*- $\text{C}_6\text{H}_4\text{F}$), 6.77-6.85 (m, 3H, $=\text{C}=\text{CHPh}$), 7.00-7.20 (m, 24H, *Ph*), 7.43-7.37(m, 12H, *o*-*Ph*) ppm.

$^{31}\text{P}\{^1\text{H}\}$: 34.17 (s, **PPh**₃) ppm.

$^{13}\text{C}\{^1\text{H}\}$: 112.7 (t, $^3J_{\text{CP}} = 4.89$ Hz, =C=CHPh), 114.1 (d, $^2J_{\text{CF}} = 21.6$ Hz, *m*-C₆H₄F), 122.5 (s, **CHPh**-*p*), 124.3 (s, **CHPh**-*o,m*), 128.3 (t, $^3J_{\text{PC}} = 4.74$ Hz, *m*-**PPh**), 129.4 (s, *p*-**PPh**), 129.63 (vt, $^1J_{\text{PC}} + ^3J_{\text{PC}} = 43.42$ Hz, *i*-**PPh**), 130.12 (ad, $^4J_{\text{CF}} = 2.95$ Hz, *i*-C₆H₄F) 131.17 (d, $^3J_{\text{CF}} = 8.96$ Hz, *o*-C₆H₄F), 133.61 (at, $^4J_{\text{PC}} = 2.47$ Hz, **CHPh**-*i*), 135.24 (t, $^2J_{\text{PC}} = 5.97$ Hz, *o*-**PPh**), 164.78 (d, $^1J_{\text{CF}} = 249$ Hz, *p*-C₆H₄F), 173.87 (s, CO₂C₆H₄F) ppm.

$^{19}\text{F}\{^1\text{H}\}$: -111 (s, *p*-FC₆H₄CO₂) ppm.

^{13}C labelling data

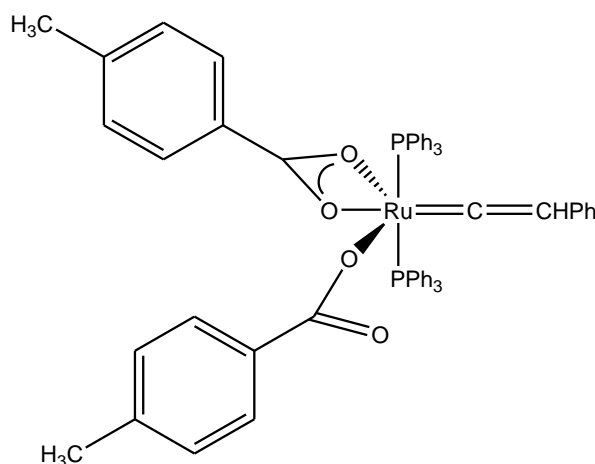
$^{13}\text{C}\{^1\text{H}\}$: 359.0 (t, $^2J_{\text{PC}} = 16.1$ Hz, =C=CHPh), $^{31}\text{P}\{^1\text{H}\}$: 34.17 (d, $^2J_{\text{PC}} = 16.1$ Hz, **PPh**₃).

IR (KBr): 1434 cm⁻¹ (κ²-OCOsym), 1482 cm⁻¹ (P-Ph₃), 1503 cm⁻¹ (κ²-OCOasym), Δν (chelate) 69 cm⁻¹, 1335 cm⁻¹ (κ¹-OCOsym), 1602 cm⁻¹, (κ¹-OCOasym), Δν (unidentate) 267 cm⁻¹.

MS (ESI): 1029.16 *m/z* ([M]Na⁺), 1007.17 *m/z* ([M]⁺), 908.17 *m/z* ([Ru(*p*-FC₆H₄CO₂)(PPh₃)₂(=C=CHPh)(CNCH₃)]⁺), 867.15 *m/z* ([Ru(*p*-FC₆H₄CO₂)(=C=CHPh)(PPh₃)₂]⁺).

Elemental Analysis: (Calculated %) C 69.18, H 4.50; (Found %) C 66.63, H 4.33.

6.4.3 Synthesis of $[\text{Ru}(\kappa^2\text{-O}_2\text{CC}_6\text{H}_4\text{-4-CH}_3)(\kappa^1\text{-O}_2\text{CC}_6\text{H}_4\text{-4-CH}_3)(=\text{C}=\text{HPh})(\text{PPh}_3)_2]$. 12a



The complex was synthesised according to the general procedure. 50 ml of pentane was used to precipitate out the product and it was washed further with 2 x 30 ml of water and pentane.

0.158g (72%) of an orange solid was obtained.

NMR Spectra (CD_2Cl_2):

^1H : 2.17 (s, 6H, $\text{C}_6\text{H}_4\text{CH}_3$), 5.18 (t, 3.72Hz, $^4J_{\text{HH}}$, 1H, $=\text{C}=\text{CHPh}$), 6.7-6.8 (m, 6H, **Ph**), 6.9-7.15(m, 25H, **Ph**), 7.38-7.45 (m, 12H, *o*-**PPh**) ppm.

$^{31}\text{P}\{^1\text{H}\}$: 34.17 (s, **PPh**) ppm.

$^{13}\text{C}\{^1\text{H}\}$: 21.13 (s, $\text{CO}_2\text{C}_6\text{H}_4\text{CH}_3$), 124.7 (s, **CHPh-*o,m***), 127.5 (s, **CHPh-*p***), 127.7 (at, $^3J_{\text{PC}} + ^5J_{\text{PC}} = 4.98$ Hz, *m*-**PPh**), 127.8 (s, *i*- $\text{C}_6\text{H}_4\text{CH}_3$), 128.4 (s, *m*- $\text{C}_6\text{H}_4\text{CH}_3$), 129.5 (vt, $^1J_{\text{PC}} + ^3J_{\text{PC}} = 43.34$ Hz, *i*-**PPh**), 129.7 (s, *o*- $\text{C}_6\text{H}_4\text{CH}_3$), 130.8 (s, *p*-**PPh**), 134.75 (at, $^2J_{\text{PC}} + ^4J_{\text{PC}} = 5.91$ Hz, *o*-**PPh**), 140.59 (s, *p*- $\text{C}_6\text{H}_4\text{CH}_3$), 174.6 (s, $\text{CO}_2\text{C}_6\text{H}_4\text{CH}_3$) ppm.

^{13}C labelling data

$^{13}\text{C}\{^1\text{H}\}$: 353.5 (br, $=\text{C}=\text{CHPh}$), $^{31}\text{P}\{^1\text{H}\}$: 31.78 (br, **PPh**) ppm.

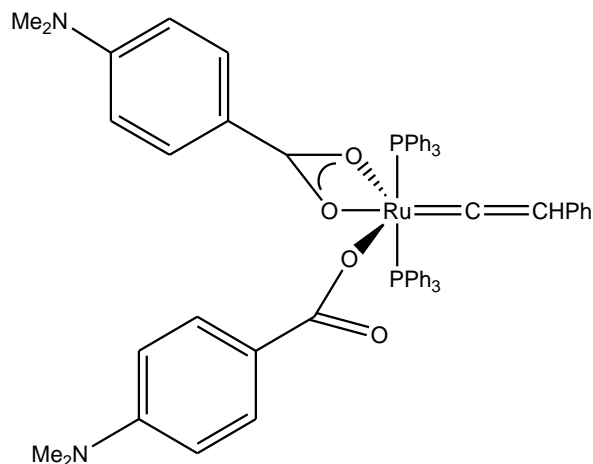
IR (KBr): 1431 cm^{-1} (κ^2 -OCOSym), 1481 cm^{-1} (P-Ph₃), 1521 cm^{-1} (κ^2 -OCOasym), $\Delta\nu$ (chelate) 90 cm^{-1} , 1334 cm^{-1} (κ^1 -OCOSym), 1594 cm^{-1} , (κ^1 -OCOasym), $\Delta\nu$ (unidentate) 260 cm^{-1} .

MS (ESI): 999.23 m/z ([M]⁺), 908.17 m/z ([Ru(*p*-CH₃C₆H₄CO₂)(PPh₃)₂(=C=CHPh)(CNCH₃)]⁺), 867.15 m/z ([Ru(*p*-CH₃C₆H₄CO₂)(=C=CHPh)(PPh₃)₂]⁺).

Elemental Analysis: (Calculated %) C 72.20, H 5.05; (Found %) C 70.89, H 5.06.

Crystal data and structure refinement for jml1120	
Identification code	jml1120
Empirical formula	C ₆₀ H ₅₀ O ₄ P ₂ Ru
Formula weight	998.01
Temperature/K	110.0
Crystal system	monoclinic
Space group	P2 ₁ /n
a/Å	20.2280(3)
b/Å	23.5455(3)
c/Å	21.7027(3)
α /°	90.00
β /°	113.3119(18)
γ /°	90.00
Volume/Å ³	9492.7(2)
Z	8
ρ _{Calculated} mg/mm ³	1.397
μ /mm ⁻¹	0.448
F(000)	4128
Crystal size/mm ³	0.3107 × 0.1512 × 0.0886
2 θ range for data collection	5.7 to 57.62°
Index ranges	-26 ≤ h ≤ 24, -31 ≤ k ≤ 25, -26 ≤ l ≤ 27
Reflections collected	46057
Independent reflections	20974[R(int) = 0.0332]
Data/restraints/parameters	20974/5/1307
Goodness-of-fit on F ²	1.042
Final R indexes [$I \geq 2\sigma(I)$]	R ₁ = 0.0431, wR ₂ = 0.0893
Final R indexes [all data]	R ₁ = 0.0757, wR ₂ = 0.1075
Largest diff. peak/hole / e Å ⁻³	0.658/-0.996

6.4.4. Synthesis of [Ru(κ^2 -O₂CC₆H₄-4-NMe₂)(κ^1 -O₂CC₆H₄-4-NMe₂)(=C=HPh)(PPh₃)₂]. 13a



The complex was synthesised according to the general procedure. 50 ml of pentane was used to precipitate out the product and it was washed further with 2 x 30 ml of water and pentane.

NMR Spectra (CD₂Cl₂):

¹H: 2.99 (s, 12H, O₂CC₆H₄N{CH₃})₂, 5.34 (t, 3.7Hz, ⁴J_{HH}, 1H, =C=CHPh), 6.42 (ad, 9.15 Hz, ³J_{HH}, 4H, *m*-C₆H₄NMe₂), 7.20-7.35(m, 27H, **Ph**), 7.57-7.65(m, 12H, *o*-PPh) ppm.

³¹P{¹H}: 33.3 (s, PPh₃) ppm.

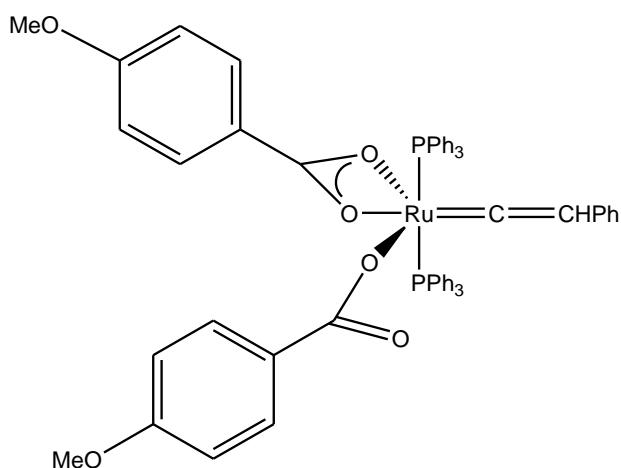
¹³C{¹H}: 39.2 (s, O₂CC₆H₄N{CH₃})₂, 108.9 (s, *m*-C₆H₄N{CH₃})₂, 123.8 (s, *i*-C₆H₄N{CH₃})₂, 128.8 (s, =C=CHPh-*p*)/*p*-PPh), 126.8 (at, ³J_{PC} + ⁵J_{PC} = 4.5 Hz, *m*-PPh), 127.0 (s, CHPh-*o,m*), 128.7 (s, =C=CHPh-*i*), 129.1(s, *o*-C₆H₄N{CH₃})₂, 129.4 (vt, ¹J_{PC} + ³J_{PC} = 42.2 Hz, *i*-PPh), 134.0 (at, ²J_{PC} + ⁴J_{PC} = 5.91 Hz, *o*-PPh), 151.1 (s, *p*-C₆H₄N{CH₃})₂, 174.3 (s, O₂CC₆H₄N{CH₃})₂ ppm.

¹³C labelling data:

¹³C{¹H}: 344.3(br, =C=CHPh), ³¹P{¹H}: 33.3 (d, ²J_{PC} = 16.6 Hz, PPh₃) ppm.

MS (ESI): 1057.2854 *m/z* ([M]H⁺), 933.2333 *m/z* ([Ru(O₂C C₆H₄-4-NMe₂ (=C=CHPh)(PPh₃)₂ (CNCH₃)]⁺).

6.4.5 Synthesis of [Ru(κ²-O₂CC₆H₄-4-OMe)(κ¹-O₂CC₆H₄-4-OMe)(=C=HPh)(PPh₃)₂]. 14a



The complex was synthesised according to the general procedure. 50 ml of pentane was used to precipitate out the product and it was washed further with 2 x 30 ml of water and pentane.

NMR Spectra (CD₂Cl₂):

¹H: 3.66 (s, 6H, C₆H₄OCH₃), 5.18 (t, 3.82Hz, ⁴J_{HH}, 1H, =C=CHPh), 6.49 (ad, 8.73 Hz, ³J_{HH} 4H, *m*-C₆H₄OMe), 6.79 (m, 2H, =C=CHPh-*o*), 6.98-7.17 (m, 25H, Ph), 7.38-7.45 (m, 12H, *o*-PPh) ppm.

³¹P{¹H}: 33.7 (s, PPh₃) ppm.

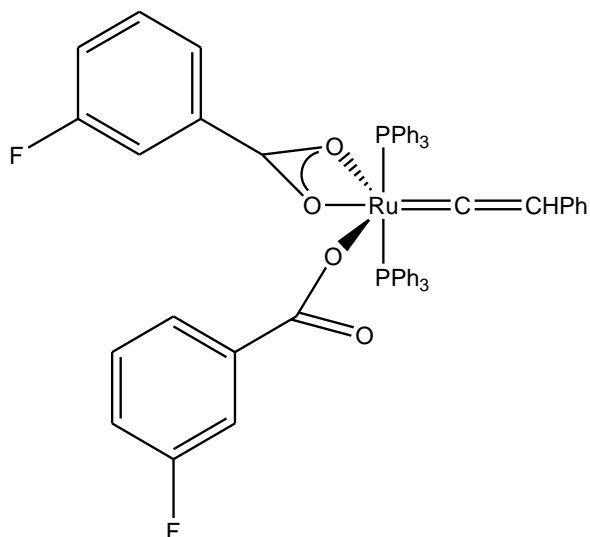
$^{13}\text{C}\{^1\text{H}\}$: 54.38 (s, $\text{C}_6\text{H}_4\text{OCH}_3$), 111.69 (s, *m*- $\text{C}_6\text{H}_4\text{OCH}_3$), 122.8 (s, $=\text{C}=\text{CHPh-}p$), 123.8, (s, $\text{CHPh-}m,o$), 128.9 (s, *p*-**PPh**), 126.9 (at, $^3J_{\text{PC}} + ^5J_{\text{PC}} = 4.87$ Hz *m*-**PPh**), 127.0 (s, *i*- $\text{C}_6\text{H}_4\text{OCH}_3$), 128.7 (vt, $^1J_{\text{PC}} + ^3J_{\text{PC}} = 43.4$ Hz, *i*-**PPh**), 128.9 (s, $=\text{C}=\text{CHPh-}i$), 129.38 (s, *o*- $\text{C}_6\text{H}_4\text{OCH}_3$), 133.9 (at, $^2J_{\text{PC}} + ^4J_{\text{PC}} = 5.83$ Hz, *o*-**PPh**), 160.6 (s, *p*- $\text{C}_6\text{H}_4\text{OCH}_3$), 173.4 (s, $\text{CO}_2\text{C}_6\text{H}_4\text{OCH}_3$) ppm.

^{13}C labelling data:

$^{13}\text{C}\{^1\text{H}\}$: 355.0 (t, $^2J_{\text{PC}} = 16.5$ Hz, $=\text{C}=\text{CHPh}$), $^{31}\text{P}\{^1\text{H}\}$: 33.8 (d, $^2J_{\text{PC}} = 16.5$ Hz, **PPh**₃)

MS (ESI): 1031.22 *m/z* ($[\text{M}]\text{H}^+$), 920.19 *m/z* ($[\text{Ru}(p\text{-MeOC}_6\text{H}_4\text{CO}_2)(\text{PPh}_3)_2(=\text{C}=\text{CHPh})(\text{CNCH}_3)]^+$), 769.13 *m/z* ($[\text{Ru}(p\text{-MeOC}_6\text{H}_4\text{CO}_2)(=\text{C}=\text{CHPh})_2(\text{PPh}_3)]^+$).

6.4.6 Synthesis of $[\text{Ru}(\kappa^2\text{-O}_2\text{CC}_6\text{H}_4\text{-3-F})(\kappa^1\text{-O}_2\text{CC}_6\text{H}_4\text{-3-F})(=\text{C}=\text{HPh})(\text{PPh}_3)_2]$. 11b



The complex was synthesised according to the general procedure. 50ml of pentane was used to precipitate out the product and it was washed further with 2 x 30 ml of water and pentane.

0.125g (56%) of pink solid was obtained

NMR Spectra (CD₂Cl₂):

¹H: 5.0 (1H, =C=CHPh), 6.75-6.85 (m, 6H, **Ph**), 6.90-7.00 (m, 4H, **Ph**), 7.01-7.20 (m, 21 H, **Ph**), 7.40-7.30 (m, 12H, *o*-PPh) ppm.

³¹P{¹H}: 34.19 (s, PPh₃) ppm.

¹³C{¹H}: 114.9 (d, ²J_{CF} = 21.9 Hz, *o*(C₂), *p*(C₄)-C₆H₄F), 117.1 (d, ³J_{CF} = 21.9 Hz, *i*(C₁), *m*(C₅)-C₆H₄F), 123.8 (s, *m*-CHPh), 124.0 (d, ⁴J_{CF} = 2.8 Hz, *o*(C₆)-C₆H₄F), 124.7 (s, *o,m*-CHPh), 127.7 (at, ³J_{PC} + ⁵J_{PC} = 4.68 Hz, *o*-PPh₃), 127.8 (s, *p*-CHPh), 128.9 (vt, ¹J_{PC} + ³J_{PC} = 43.3 Hz, *i*-PPh), 128.24 (d, 8.11Hz, *i*-CHPh), 129.8 (s, *p*-PPh), 134.6 (at, ²J_{PC} = 5.65 Hz, *o*-PPh), 166.8 (d, ¹J_{CF} = 246.5 Hz, *m*-C₆H₄F), 174.2 (s, CO₂C₆H₄F) ppm.

¹⁹F{¹H}: -115.4 (s, *m*-FC₆H₄CO₂).

¹³C labelling data

¹³C{¹H}: 357.2 (t, ²J_{PC} = 16.6 Hz, =C=CHPh), ³¹P{¹H}: 34.1 (d, ²J_{PC} = 16.6 Hz, PPh₃) ppm.

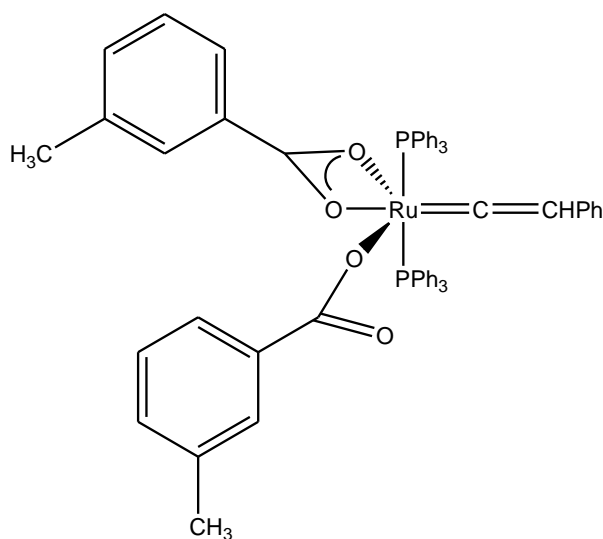
IR (KBr): 1434 cm⁻¹ (κ²-OCOsym), 1482 cm⁻¹ (P-Ph₃), 1491 cm⁻¹ (κ²-OCOasym), Δν (chelate) 57 cm⁻¹, 1340 cm⁻¹ (κ¹-OCOsym), 1593 cm⁻¹, (κ¹-OCOasym), Δν (unidentate) 253 cm⁻¹

MS (ESI): 1029.16 *m/z* ([M]Na⁺), 1007.17 *m/z* ([M]H⁺), 908.18 *m/z* ([Ru(*m*-FC₆H₄CO₂)(PPh₃)₂(=C=CHPh)(CNCH₃)]⁺), 745.09 *m/z* ([Ru(*m*-FOC₆H₄CO₂)(=C=CHPh)₂(PPh₃)]⁺).

Elemental Analysis: (Calculated %) C 69.25, H 4.41; (Found %) C 68.02, H 4.51

Crystal data and structure refinement for jml1143	
Identification code	jml1143
Empirical formula	C ₅₈ H ₄₄ F ₂ O ₄ P ₂ Ru
Formula weight	1005.94
Temperature/K	109.9(4)
Crystal system	orthorhombic
Space group	Pca2 ₁
a/Å	18.4523(6)
b/Å	16.6112(7)
c/Å	15.3290(6)
α/°	90.00
β/°	90.00
γ/°	90.00
Volume/Å ³	4698.6(3)
Z	4
ρ _{Calculated} mg/mm ³	1.422
m/mm ⁻¹	0.459
F(000)	2064
Crystal size/mm ³	0.2435 × 0.1378 × 0.1072
2θ range for data collection	5.7 to 58.12°
Index ranges	-23 ≤ h ≤ 13, -20 ≤ k ≤ 15, -20 ≤ l ≤ 14
Reflections collected	12573
Independent reflections	7223[R(int) = 0.0499]
Data/restraints/parameters	7223/111/657
Goodness-of-fit on F ²	1.063
Final R indexes [I >= 2σ (I)]	R ₁ = 0.0534, wR ₂ = 0.1106
Final R indexes [all data]	R ₁ = 0.0695, wR ₂ = 0.1250
Largest diff. peak/hole / e Å ⁻³	0.711/-0.881
Flack Parameter	-0.04(4)

6.4.7 Synthesis of $[\text{Ru}(\kappa^2\text{-O}_2\text{C}_6\text{H}_4\text{-3-CH}_3)(\kappa^1\text{-O}_2\text{C}_6\text{H}_4\text{-3-CH}_3)(=\text{C=HPh})(\text{PPh}_3)_2]$. 12b



The complex was synthesised according to the general procedure. 50ml of pentane was used to precipitate out the product and it was washed further with 2 x 30 ml of water and pentane.

0.16g (72%) of an orange solid was obtained

NMR Spectra (CD₂Cl₂):

¹H: 2.13 (s, 6H, C₆H₄CH₃), 5.17 (t, 3.47Hz, ⁴J_{HH}, 1H, =C=CHPh), 6.80 (m, 6H, **Ph**), 6.90 (m, 4H, **Ph**), 7-7.15 (m, 21H, **Ph**), 7.4-7.45 (m, 12H, *o*-P**Ph**) ppm.

³¹P{¹H}: 33.9 (s, PPh₃).

¹³C{¹H}: 20.9 (s, CO₂C₆H₄CH₃), 123.7 (s, *p*-CH**Ph**), 124.7 (s, *o*-CH**Ph**), 125.4 (s, *m*-CH**Ph**), 127.7 (at, ³J_{PC} + ⁵J_{PC} = 4.68 Hz, *m*-P**Ph**), 127.9 (s, *i*-C₆H₄CH₃), 129.2 (vt, ¹J_{PC} + ³J_{PC} = 42.07 Hz, *i*-P**Ph**), 129.7 (s, *o*(C₂)-C₆H₄CH₃), 131.0 (s, *p*-P**Ph**), 133.3 (s, *o*(C₅)-C₆H₄CH₃), 133.4 (s, *p*-C₆H₄CH₃), 134.7 (at, ²J_{PC} + ⁴J_{PC} = 5.92 Hz, *o*-P**Ph**), 136.6 (s, *m*(C₃)-C₆H₄CH₃), 174.8 (s, CO₂C₆H₄CH₃) ppm.

¹³C labelling data

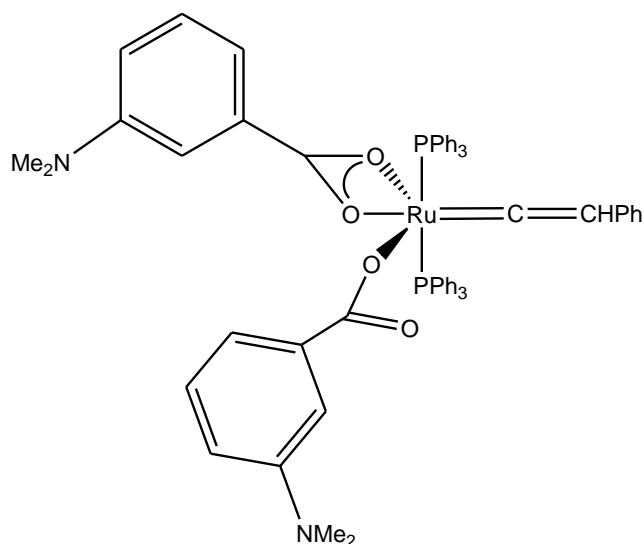
¹³C {¹H}: 356.5 (t, ²J_{PC} = 16.6 Hz, =C=CHPh), ³¹P {¹H}: 33.9 (d, ²J_{PC} = 16.6 Hz, PPh₃) ppm.

IR (KBr): 1433 cm⁻¹ (κ²-OCO_{sym}), 1481cm⁻¹ (P-Ph₃), 1521 cm⁻¹ (κ²-OCO_{asym}), Δν (chelate) 88 cm⁻¹, 1323 cm⁻¹ (κ¹-OCO_{sym}), 1592 cm⁻¹, (κ¹-OCO_{asym}), Δν (unidentate) 269 cm⁻¹.

MS (ESI): 999.23 *m/z* ([M]H⁺), 904.2 *m/z* ([Ru(*m*-CH_{12a6}H₄CO₂)(PPh₃)₂(=C=CHPh)(CNCH₃)]⁺), 863.17 *m/z* ([Ru(*m*-CH_{12a6}H₄CO₂)(=C=CHPh)(PPh₃)₂]⁺).

Elemental Analysis: (Calculated %) C 72.20, H 5.05; (Found %) C 71.01 H 5.01.

6.4.8 Synthesis of [Ru(κ²-O₂CC₆H₄-3-NMe₂)(κ¹-O₂CC₆H₄-3-NMe₂)(=C=HPh)(PPh₃)₂]. 13b



The complex was synthesised according to the general procedure. 50ml of pentane was used to precipitate out the product and it was washed further with 3 x 30 ml of water and pentane.

0.155g (70%) of a pink solid was obtained

NMR Spectra (CD₂Cl₂):

¹H: δ_H 2.7 (s, 12H, C₆H₄N(CH₃)₂), 5.13 (t, ⁴J_{HH} = 3.75 Hz, =C=CHPh), 6.5- 6.6 (m, 6H, H_{4,5,6}-C₆H₄NMe₂), 6.73-6.86 (m, 5H, CHPh), 6.98 (at, ⁴J_{HH} = 7.75 Hz, 2H, o(H₂)-C₆H₄NMe₂), 7.05-7.17 (m, 18H, m,p-PPh), 7.14-7.48 (m, 12H, o-PPh) ppm.

³¹P{¹H}: 33.18 (s, PPh₃) ppm.

¹³C{¹H}: 40.5 (s, CO₂C₆H₄N(CH₃)₂), 112.6 (s, o(C₂)-C₆H₄NMe₂), 114.6 (s, p-C₆H₄NMe₂), 116.9 (s, o(C₆)-C₆H₄NMe₂), 123.5 (s, p-CHPh), 124.6 (s, o-CHPh), 127.31 (s, m-CHPh), 127.6 (at, ³J_{PC} + ⁵J_{PC} = 4.9 Hz, m-PPh₃), 129.14 (s, p-PPh), 129.7 (vt, ¹J_{PC} + ³J_{PC} = 43.9 Hz, i-PPh), 134.15 (s, o(C₅)-C₆H₄NMe₂), 134.7 (at, ²J_{PC} + ⁴J_{PC} = 5.87 Hz, o-PPh), 136.32 (s, i-C₆H₄NMe₂), 149.5 (s, m(C₃)-C₆H₄NMe₂), 176.72 (s, CO₂C₆H₄NMe₂) ppm.

MS (ESI): 1057.17 m/z ([M]H⁺), 933.23 m/z ([Ru(m-NMe₂C₆H₄CO₂)(PPh₃)₂(=C=CHPh)(CNCH₃)]⁺), 892.2 m/z ([Ru(m-NMe₂C₆H₄CO₂)(PPh₃)₂(=C=CHPh)]H⁺), 795.19 m/z ([Ru(m-NMe₂C₆H₄CO₂)(=C=CHPh)₂(PPh₃)]⁺).

7. Abbreviations

Å - Angstrom

AMLA-Ambiphilic Metal Ligand Activation

Bu-Butyl

°C-Degrees Celsius

cm⁻¹-Wavenumber

CMD-Concerted Metalation Deprotonation

Cp-Cyclopentadienyl

DCM-Dichloromethane

δ-Chemical shift in ppm

DFT-Density Functional Theory

EI-Electron Ionisation

ESI-Electrospray Ionisation

Et-Ethyl

Et₂O-Diethyl ether

EtOH-Ethanol

g-gram

(g)-Gas

HOMO-Highest Occupied Molecular Orbital

LUMO-Lowest Unoccupied Molecular Orbital

IR-Infrared

J-Joules

J-Coupling constant (in Hertz)

kJ-kilojoules

(l)-Liquid

LAPS-Ligand-Assisted Proton Shuttle

LIFDI-Liquid Injection Field Desorption Ionisation

LUMO-Lowest Unoccupied Molecular Orbital

Me-Methyl

MeOH-Methanol

mg-milligram

mL-millilitre

mmol-millimol

μ L-microliter

μ mol-micromole

MS-Mass Spectrometry

m/z-mass/charge ratio

NMR-Nuclear Magnetic Resonance

OAc-Acetate

PES-Potential Energy Surface

Ph-Phenyl

(s)-Solid

^tBuOH-*tert*-Butyl alcohol (*t*-butanol)

THF-Tetrahydrofuran

TMS-trimethylsilyl

VT-Variable Temperature

8. References

1. Johnson, D. G.; Lynam, J. M.; Slattery, J. M.; Welby, C. E., *Dalton Trans.*, **39**, 10432-10441.
2. Christian Bruneau, P. H. D., *Angew. Chem., Int. Ed.* **2006**, *45*, 2176-2203.
3. Lynam, J. M., *Chem. Eur. J.*, **16**, 8238-8247.
4. Bruce, M. I., *Chem. Rev.* **1991**, *91*, 197-257.
5. Sasaki, Y.; Dixneuf, P. H., *J. Chem. Soc., Chem. Commun.* **1986**, 790-791.
6. Mahe, R.; Dixneuf, P. H.; Lecolier, S., *Tetrahedron Lett.* **1986**, *27*, 6333-6336.
7. King, R. B.; Saran, M. S., *J. Chem. Soc., Chem. Commun.* **1972**, 1053-1054.
8. De Angelis, F.; Sgamellotti, A.; Re, N., *Organometallics* **2002**, *21*, 2715-2723.
9. Albertin, G.; Autoniutti, S.; Bordignon, E.; Cazzaro, F.; Ianelli, S.; Pelizzi, G., *Organometallics* **1995**, *14*, 4114-4125; Field, L. D.; Magill, A. M.; Jensen, P., *Organometallics* **2008**, *27*, 6539-6546.
10. Bianchini, C.; Innocenti, P.; Peruzzini, M.; Romerosa, A.; Zanobini, F., *Organometallics* **1996**, *15*, 272-285.
11. De Angelis, F.; Sgamellotti, A.; Re, N., *Organometallics* **2002**, *21*, 5944-5950.
12. Lynam, J. M.; Welby, C. E.; Whitwood, A. C., *Organometallics* **2009**, *28*, 1320-1328.
13. Cowley, M. J.; Lynam, J. M.; Slattery, J. M., *Dalton Trans.* **2008**, 4552-4554.
14. Wakatsuki, Y.; Koga, N.; Werner, H.; Morokuma, K., *J. Am. Chem. Soc.* **1997**, *119*, 360-366.
15. Werner, H., *J. Organomet. Chem.* **1994**, *475*, 45-55.
16. Katayama, H.; Nakayama, M.; Nakano, T.; Wada, C.; Akamatsu, K.; Ozawa, F., *Macromolecules* **2004**, *37*, 13-17.
17. Bianchini, C.; Innocenti, P.; Meli, A.; Peruzzini, M.; Zanobini, F.; Zanello, P., *Organometallics* **1990**, *9*, 2514-2522.
18. Bianchini, C.; Mantovani, N.; Marchi, A.; Marvelli, L.; Masi, D.; Peruzzini, M.; Rossi, R.; Romerosa, A., *Organometallics* **1999**, *18*, 4501-4508.
19. Puerta, M. C.; Valerga, P., *Coord. Chem. Rev.* **1999**, *193-5*, 977-1025.
20. Oliván, M.; Clot, E.; Eisenstein, O.; Caulton, K. G., *Organometallics* **1998**, *17*, 3091-3100.
21. Gauss, C.; Veghini, D.; Orama, O.; Berke, H., *J. Organomet. Chem.* **1997**, *541*, 19-38; Cadierno, V.; Gamasa, M. P.; Gimeno, J., *Coord. Chem. Rev.* **2004**, *248*, 1627-1657.
22. Werner, H.; Schulz, M.; Windmueller, B., *Organometallics* **1995**, *14*, 3659-3668.
23. Adams, J. S.; Bitcon, C.; Brown, J. R.; Collison, D.; Cunningham, M.; Whiteley, M. W., *J. Chem. Soc., Dalton Trans.* **1987**, 3049-3053; Meng, X. J.; Kim, S., *Org. Biomol. Chem.* **2011**, *9*, 4429-4431.
24. Grime, R. W.; Helliwell, M.; Hussain, Z. I.; Lancashire, H. N.; Mason, C. R.; McDouall, J. J. W.; Mydlowski, C. M.; Whiteley, M. W., *Organometallics* **2008**, *27*, 857-871; Adams, J. S.; Cunningham, M.; Whiteley, M. W., *J. Organomet. Chem.* **1985**, *293*, C13-C14.
25. Ipaktschi, J.; Rooshenas, P.; Dulmer, A., *Organometallics* **2005**, *24*, 6239-6243.
26. Connelly, N. G.; Geiger, W. E.; Lagunas, C.; Metz, B.; Rieger, A. L.; Rieger, P. H.; Shaw, M. J., *J. Am. Chem. Soc.* **1995**, *117*, 12202-12208.
27. Antonova, A. B.; Chudin, O. S.; Pavlenko, N. I.; Sokolenko, W. A.; Rubaylo, A. I.; Vasiliev, A. D.; Verpekin, V. V.; Semeikin, O. V., *Russ. Chem. B+*. **2009**, *58*, 955-963.

28. Shor, E. A. I.; Nasluzov, V. A.; Shor, A. M.; Antonova, A. B.; Rosch, N., *J. Organomet. Chem.* **696**, 3445-3453.
29. Werner, H.; Stark, A.; Schulz, M.; Wolf, J., *Organometallics* **1992**, *11*, 1126-1130; Miki, K.; Uemura, S.; Ohe, K., *Chem. Letters* **2005**, *34*, 1068-1073.
30. Wakatsuki, Y., *J. Organomet. Chem.* **2004**, *689*, 4092-4109.
31. Bruneau, C.; Dixneuf, P. H., *Angew. Chem., Int. Ed.* **2006**, *45*, 2176-2203.
32. Bustelo, E.; Carbo, J. J.; Lledos, A.; Mereiter, K.; Puerta, M. C.; Valerga, P., *J. Am. Chem. Soc.* **2003**, *125*, 3311-3321.
33. Katayama, H.; Ozawa, F., *Coord. Chem. Rev.*
- Vinylidene, Allenylidene, and Metallacumulene Complexes* **2004**, *248*, 1703-1715.
34. Trost, B. M.; McClory, A., *Chem. Asia. J.* **2008**, *3*, 164-194.
35. Bullock, R. M., *J. Chem. Soc., Chem. Commun.* **1989**, 165-167.
36. Grotjahn, D. B.; Zeng, X.; Cooksy, A. L., *J. Am. Chem. Soc.* **2006**, *128*, 2798-2799.
37. Davison, A.; Selegue, J. P., *J. Am. Chem. Soc.* **1978**, *100*, 7763-7765.
38. Davison, A.; Selegue, J. P., *J. Am. Chem. Soc.* **1980**, *109*, 2455-2456.
39. Yasuo, W., *J. Organomet. Chem.* **2004**, *689*, 4092-4109.
40. Slugovc, C.; Sapunov, V. N.; Wiede, P.; Mereiter, K.; Schmid, R.; Kirchner, K., *J. Chem. Soc., Dalton Trans.* **1997**, 4209-4216.
41. Edgar Haak, *Eu. J. Org. Chem.* **2007**, *2007*, 2815-2824; Borguet, Y.; Sauvage, X.; Zaragoza, G.; Demonceau, A.; Delaude, L., *Organometallics* **2011**, *30*, 2730-2738; Varela, J. A.; Gonzalez-Rodriguez, C.; Rubin, S. G.; Castedo, L.; Saa, C., *Pure and Applied Chem.* **2008**, *80*, 1167-1177.
42. Hiett, N. P.; Lynam, J. M.; Welby, C. E.; Whitwood, A. C., *J. Organomet. Chem.* **696**, 378-387.
43. Kostic, N. M.; Fenske, R. F., *Organometallics* **1982**, *1*, 974-982.
44. De Angelis, F.; Sgamellotti, A.; Re, N., *Organometallics*, **2007**, *26*, 5285-5288.
45. Grotjahn, D. B.; Zeng, X.; Cooksy, A. L.; Kassel, W. S.; DiPasquale, A. G.; Zakharov, L. N.; Rheingold, A. L., *Organometallics* **2007**, *26*, 3385-3402.
46. Tokunaga, M.; Suzuki, T.; Koga, N.; Fukushima, T.; Horiuchi, A.; Wakatsuki, Y., *J. Am. Chem. Soc.* **2001**, *123*, 11917-11924.
47. Bruce, M.; Wallis, R., *Aus. J. Chem.* **1979**, *32*, 1471-1485; Bruce, M. I.; Wong, F. S.; Skelton, B. W.; White, A. H., *J. Chem. Soc., Dalton Trans.* **1982**, 2203-2207; Bruce, M.; Koutsantonis, G., *Aus. J. Chem.* **1991**, *44*, 207-217; Lompfrey, J. R.; Selegue, J. P., *J. Am. Chem. Soc.* **1992**, *114*, 5518-5523; Gamasa, M. P.; Gimeno, J.; Martin-Vaca, B. M.; Borge, J.; Garcia-Granda, S.; Perez-Carreno, E., *Organometallics* **1994**, *13*, 4045-4057.
48. Le Lagadec, R.; Roman, E.; Toupet, L.; Mueller, U.; Dixneuf, P. H., *Organometallics* **1994**, *13*, 5030-5039.
49. Bruce, M. I.; Hall, B. C.; Zaitseva, N. N.; Skelton, B. W.; White, A. H., *J. Organomet. Chem.* **1996**, *522*, 307-310.
50. Wakatsuki, Y.; Koga, N.; Yamazaki, H.; Morokuma, K., *J. Am. Chem. Soc.* **1994**, *116*, 8105-8111.
51. Arikawa, Y.; Yamasaki, H.; Yamaguchi, M.; Umakoshi, K.; Onishi, M., *Organometallics* **2009**, *28*, 5587-5589.
52. Grunwald, C.; Laubender, M.; Wolf, J.; Werner, H., *J. Chem. Soc., Dalton Trans.* **1998**, 833-839.
53. Nguyen, S. T.; Johnson, L. K.; Grubbs, R. H.; Ziller, J. W., *J. Am. Chem. Soc.* **1992**, *114*, 3974-3975; Czelusniak, I.; Handzlik, J., *J. Organomet. Chem.* **2009**, *694*, 1427-1434; Dias, E. L.; Nguyen, S. T.; Grubbs, R. H., *J. Am. Chem. Soc.* **1997**, *119*, 3887-3897; Jens O. Krause, O. N., Klaus Wurst, Michael R. Buchmeiser., *Chem. Eur. J.* **2004**, *10*, 777-

- 784; Love, J. A.; Sanford, M. S.; Day, M. W.; Grubbs, R. H., *J. Am. Chem. Soc.* **2003**, *125*, 10103-10109; Lynn, D. M.; Mohr, B.; Grubbs, R. H., *J. Am. Chem. Soc.* **1998**, *120*, 1627-1628; Sanford, M. S.; Love, J. A.; Grubbs, R. H., *Organometallics* **2001**, *20*, 5314-5318; Scholl, M.; Trnka, T. M.; Morgan, J. P.; Grubbs, R. H., *Tetrahedron Lett.* **1999**, *40*, 2247-2250; Scholl, M.; Ding, S.; Lee, C. W.; Grubbs, R. H., *Org. Lett.* **1999**, *1*, 953-956; Schwab, P.; Grubbs, R. H.; Ziller, J. W., *J. Am. Chem. Soc.* **1996**, *118*, 100-110; Trnka, T. M.; Grubbs, R. H., *Acc. Chem. Res.* **2001**, *34*, 18-29; Wu, Z.; Nguyen, S. T.; Grubbs, R. H.; Ziller, J. W., *J. Am. Chem. Soc.* **1995**, *117*, 5503-5511.
54. Mitchell, R. W.; Spencer, A.; Wilkinson, G., *J. Chem. Soc., Dalton Trans.* **1973**, 846-854.
55. Wakatsuki, Y.; Koga, N.; Yamazaki, H.; Morokuma, K., *J. Am. Chem. Soc.* **1994**, *116*, 8105-8111.
56. Zhang, L.; Chen, X.; Xue, P.; Sun, H. H. Y.; Williams, I. D.; Sharpless, K. B.; Fokin, V. V.; Jia, G., *J. Am. Chem. Soc.* **2005**, *127*, 15998-15999.
57. Lynam, J. M.; Nixon, T. D.; Whitwood, A. C., *J. Organomet. Chem.* **2008**, *693*, 3103-3110; Bassetti, M.; Cadierno, V.; Gimeno, J.; Pasquini, C., *Organometallics* **2008**, *27*, 5009-5016.
58. Laungani, A. C.; Keller, M.; Slattery, J. M.; Krossing, I.; Breit, B., *Chem. Eur. J.* **2009**, *15*, 10405-10422; Laungani, A. C.; Slattery, J. M.; Krossing, I.; Breit, B., *Chem. Eur. J.* **2008**, *14*, 4488-4502.
59. Davies, D. L.; Donald, S. M. A.; Macgregor, S. A., *J. Am. Chem. Soc.* **2005**, *127*, 13754-13755.
60. Boutadla, Y.; Davies, D. L.; Macgregor, S. A.; Poblador-Bahamonde, A. I., *Dalton Trans.* **2009**, 5820-5831.
61. Boutadla, Y.; Davies, D. L.; Macgregor, S. A.; Poblador-Bahamonde, A. I., *Dalton Trans.* **2009**, 5887-5893.
62. Fairlamb, I., *Plat. Met. Rev.* **2011**, *55*, 91-97.
63. Bruce, M. I., *Chem. Rev.* **1998**, *98*, 2797-2858; Selegue, J. P., *Organometallics* **1982**, *1*, 217-218; Rigaut, S.; Touchard, D.; Dixneuf, P. H., *Coord. Chem. Rev.* **2004**, *248*, 1585-1601.
64. Spencer, A.; Wilkinson, G., *J. Chem. Soc., Dalton Trans.* **1974**, 786-792.
65. Salah, O. M. A.; Bruce, M. I., *J. Chem. Soc., Dalton Trans.* **1974**, 2302-2304; Sullivan, B. P.; Smythe, R. S.; Kober, E. M.; Meyer, T. J., *J. Am. Chem. Soc.* **1982**, *104*, 4701-4703; Knaup, W.; Werner, H., *J. Organomet. Chem.* **1991**, *411*, 471-489; Mountassir, C.; Hadda, T. B.; Le Bozec, H., *J. Organomet. Chem.* **1990**, *388*, c13-c16; Bianchini, C.; Casares, J. A.; Peruzzini, M.; Romerosa, A.; Zanobini, F., *J. Am. Chem. Soc.* **1996**, *118*, 4585-4594.
66. Yang, S.-M.; Chan, M. C.-W.; Cheung, K.-K.; Che, C.-M.; Peng, S.-M., *Organometallics* **1997**, *16*, 2819-2826; Bruce, M. I.; Swincer, A. G.; Wallis, R. C., *J. Organomet. Chem.* **1979**, *171*, C5-C8; Oro, L. A.; Ciriano, M. A.; Campo, M.; Foces-Foces, C.; Cano, F. H., *J. Organomet. Chem.* **1985**, *289*, 117-131; Mezzetti, A.; Consiglio, G.; Morandini, F., *J. Organomet. Chem.* **1992**, *430*, C15-C18.
67. Datta, S.; Chang, C.-L.; Yeh, K.-L.; Liu, R.-S., *J. Am. Chem. Soc.* **2003**, *125*, 9294-9295.
68. Hocking, R. K.; Hambley, T. W., *Organometallics* **2007**, *26*, 2815-2823.
69. Crabb, E.; Moore, E.; Smart, L., *Concepts in Transition Metal Chemistry*. RSC
70. Hocking, R. K.; Hambley, T. W., *Organometallics* **2007**, *26*, 2815-2823.
71. Cotton, F. A.; Wilkinson, G., *Advanced inorganic chemistry 5th ed.* Wiley: 1988.
72. L, Shilling., Insights into the regioselectivity of the ruthenium-mediated addition of carboxylic acid to terminal alkynes. University of York, **2011**.

73. Robinson, S. D.; Uttley, M. F., *J. Chem. Soc., Dalton Trans.* **1973**, 1912-1920.
74. Stephenson, T. A.; Wilkinson, G., *J. Inorg. Nucl. Chem.* **1966**, 28, 945-956.
75. Hammett, L. P., *J. Am. Chem. Soc.* **1937**, 59, 96-103.
76. Gilbert, J. D.; Wilkinson, G., *J. Chem. Soc. A* **1969**, 1749-1753.
77. Hocking, R. K.; Hambley, T. W., *Chem. Commun.* **2003**, 1516-1517; Cotton, F. A., *Inorg. Chem.* **1964**, 3, 702-711.
78. Cowley, M. J.; Lynam, J. M.; Moneypenny, R. S.; Whitwood, A. C.; Wilson, A. J., *Dalton Trans.* **2009**, 9529-9542.